University of Cincinnati

Date: 2/19/2014

I, Javier A Parrilla , hereby submit this original work as part of the requirements for the degree of Doctor of Philosophy in Aerospace Engineering.

It is entitled:

Hybrid Environmental Control System Integrated Modeling Trade Study Analysis for Commercial Aviation

Student's name: **Javier A Parrilla**

This work and its defense approved by:

Committee chair: Awatef Hamed, Ph.D.

Committee member: Neil Garrigan,

Committee member: Kelly Cohen, Ph.D.

Committee member: San-Mou Jeng, Ph.D.

Committee member: Mark Turner, Sc.D.

9120

Hybrid Environmental Control System Integrated Modeling Trade Study Analysis for Commercial Aviation

A dissertation submitted to the

Division of Research and Advanced Studies

Of the University of Cincinnati

in partial fulfillment of the requirements for the degree of

DOCTORATE OF PHILOSOPHY (Ph.D.)

In the Department of Aerospace Engineering and Engineering Mechanics

Of the College of Engineering and Applied Science

April 2014

By

Javier Parrilla

M.S. Aerospace Engineering, University Of Michigan, 2004

B.S. Mechanical Engineering, University of Puerto Rico, 2001

Committee Chair: Dr. Awatef Hamed

ABSTRACT

Current industry trends demonstrate aircraft electrification will be part of future platforms in order to achieve higher levels of efficiency in various vehicle level sub-systems. However electrification requires a substantial change in aircraft design that is not suitable for re-winged or re-engined applications as some aircraft manufacturers are opting for today. Thermal limits arise as engine cores progressively get smaller and hotter to improve overall engine efficiency[8], while legacy systems still demand a substantial amount of pneumatic, hydraulic and electric power extraction. The environmental control system (ECS) provides pressurization, ventilation and air conditioning in commercial aircraft[7], making it the main heat sink for all aircraft loads with exception of the engine. To mitigate the architecture thermal limits in an efficient manner, the form in which the ECS interacts with the engine will have to be enhanced as to reduce the overall energy consumed and achieve an energy optimized solution. This study examines a tradeoff analysis of an electric ECS by use of a fully integrated Numerical Propulsion Simulation System (NPSS) model that is capable of studying the interaction between the ECS and the engine cycle deck. It was found that a peak solution lays in a hybrid ECS where it utilizes the correct balance between a traditional pneumatic and a fully electric system. This intermediate architecture offers a substantial improvement in aircraft fuel consumptions due to a reduced amount of waste heat and customer bleed in exchange for partial electrification of the air-conditions pack which is a viable option for re-winged applications.

Para Dayana, Isaac y Ofelia

Acknowledgements

I would first like to thank my wife, Dayana, for all her encouragement, support and patience, without her this paper would have not been possible. Her love was ever present, driving me to successfully completing my dissertation, at much sacrifice, because failure was not an option. Gracias!

Furthermore, this dissertation could not have been completed without the help of numerous people. I would like to thank my advisor, Dr. Awatef Hamed, for having trusted in my capabilities and facilitated the opportunity for me to join the Vehicle Energy Systems and Integrations group at GE Aviation, which made this work possible. Thanks to Dr. Kelly Cohen, Dr. San-Mou Jeng, Dr. Mark Turner, and Neil Garrigan for being part of my committee and for all your contributions and direction throughout my work. Additionally, I would like to thank Dr. Hamed for all her motivation and support in the development of this work.

I am indebted to Jesus Garcia who taught me NPSS and helped me a great deal in putting the air cycle machine model together. With his help I was able to form the framework that integrated the various aircraft subsystems in order to support this study. I would also like to thank Rich Goldman for providing his extensive expertise in engine simulation, which contributed to this work.

I would like to thank GE Aviation for providing the sponsorship for my degree and Gary Wendt to who gave me the needed jolt to commence on this seven and half year long trek.

Contents

Figures and Tables

Nomenclature

Acronyms

a_α	-	Solar radiation extinction coefficient
ACM	-	Air Cycle Machine
ACOC	-	Air Cooled Oil Cooler
ACS	-	Air Cycle System
AEA	-	All-Electric Architecture
AGB	-	Accessory Gear Vox
Amb	-	Ambient conditions
AMS	-	Air Management System
APU	-	Auxiliary Power Unit
BPV	-	Bypass Valve
CAC	-	Cabin Air Compressor
C_f	-	Friction Coefficient
Cond	-	Condenser
COP	-	Coefficient of Performance
CPA	-	Conventional - Pneumatic Architecture
CT	-	Cooling Turbine
D	-	Diameter
DISA	-	Deviation from the International Standard Atmosphere
dp	-	Dew Point
ECS	-	Environmental Control System
EMS	-	Energy Management System
EOA	-	Energy Optimized Aircraft
EPS	-	Electrical Power System
Eq.	-	Equation
f	-	Friction Factor
f	-	fin
FAV	-	Fan Air Valve
FCV	-	Flow Control Valve
FTMS	-	Fuel Thermal Management System
GND	-	Ground
H	-	Equivalent height for solar radiation
h	-	See HTC

HBB	-	Hybrid Booster Bleed
HFB	-	Hybrid Fan Bleed
HMB	-	Hybrid MidStage Bleed
HPC	-	High Pressure Compressor
HPSOV	-	High Pressure Shutoff Valve
HTC	-	Convective Heat Transfer Coefficient
Hx	-	Heat exchangers
J	-	Chilton-Colburn Factor
K	-	Kilo
L	-	Length
LPCV	-	Low Pressure Check Valve
$\dot{m}$	-	Mass Flow
MEA	-	More Electric Aircraft
MTBF	-	Mean Time Between Failure
NPSS	-	Numerical Propulsion Simulation System
NTU	-	Number of Transfer Units
Nu	-	Nusselt Number
OEM	-	Original Equipment Manufacturers
P	-	Pressure
PAX	-	Passengers
PHx	-	Primary Heat Exchanger
Pr	-	Prandlt Number
PRV	-	Pressure Regulator Valve
q	-	Precipitation Experimental Constant for Solar Radiation
q″	-	Heat Flux
r	-	Pressure Ratio
R	-	Equivalent Thermal Resistance
Re	-	Reynolds Number
rec	-	Recovery
RH	-	Relative Humidity
RHx	-	Reheat Heat Exchanger
RPM	-	Revenue Passenger Miles
s	-	Entropy
Sc	-	Solar Heat Flux ~ 1367 W/m
Se	-	Solar intensity
SFC	-	Specific Fuel Consumption
SHx	-	Secondary Heat Exchanger
SLS	-	Sea Level Static
T	-	Temperature

TF	-	Turbo Fan
TJ	-	Turbo Jet
TMS	-	Thermal Management Systems
t_w	-	Transmission Coefficient of Water Vapor
V	-	Velocity
VCS	-	Vapor Cycle Systems
W	-	Watts
WE	-	Water Extractor (Water Separator)
Z	-	Zenith Angle

Greek Symbols

α	-	Absorptance of a material surface
β	-	Coefficient of Performance
ε	-	Surface Emittance
κ	-	Material Thermal Conductivity
ν	-	Specific Volume
s	-	Stefan-Boltzmann Constant
τ_{net}	-	Net Thrust
ϵ		Heat Exchanger Effectiveness
η		Efficiency

1 Introduction

The civil air transport business segment in the US alone is responsible for transporting an estimated 793 million passengers over 1,039.3 billion revenue passenger miles (RPM). Overall the industry accounts for an estimated economic impact of $372.2 billion, per 2009 data[9]. Yet due to the high costs of operations, aircraft and engine manufactures as well as commercial airlines have to continually push innovation in all parts of the industry to reduce fuel consumption and maintain profitability. In past years aircraft manufacturers have continually tried to improve the efficiency of their product either through improvements to the aero structure, weight or engine enhancements independently. Today, as vehicle systems become more complex, the need to study interaction between each of the subsystems has become a critical milestone. Suppliers can no longer rely on independent requirements table to obtain the best solution, especially when paring higher efficiency components with legacy systems that are too expensive to upgrade. Compromises that add design complexity will have to be made in order to achieve substantial improvements in fuel consumption and range. This effort will need to start at the preliminary design, PD,

stage where design cost changes are typically low. To this end, an overall architecture model of the main aircraft subsystems must be generated to perform a detailed trade study at this PD level. Once assembled, the integrated performance model becomes the key enabler towards understanding the benefits of a More Electric Aircraft (MEA) and can be used to perform system trade study to uncover new variants that minimize fuel consumption.

In Chapter 1, the concept of aircraft electrification will be discussed. Additionally, it will be shown how electrification has resulted in the latest boost in operation efficiency and what led to the motivation behind this study. The major focus of this investigation will be centered on the ECS and how it integrates with the propulsion engine. The major components of an Environmental Control System (ECS), its operation, and integration on a commercial aircraft are discussed in Chapter 2. The technology will be introduced from its simplest form to the state of the art, an All-Electric ECS. Chapter 3 will continue the discussion by introducing the hybrid ECS concept that combines traits from traditional systems and more electric in an effort to maximize performance. The model needed to analyze the various ECS architectures will be presented in Chapter 4. This chapter outlines the main components of each of the subsystems and how they were integrated together to perform mission analysis. The results generated will then be presented in Chapter 5. This section will provide an overview of the benefits and detriments of each architecture. The final conclusions of this work will then be presented in Chapter 6 along with possible future work in this research area.

1.1 Motivations and Objectives

The aircraft industry has seen a move in recent years to more electric air vehicles, referred to as aircraft subsystem electrification. This represents a shift from the traditional mechanical and pneumatic controls to ones that are operated by electrically powered actuator pumps and motors. The 787, which features electrically driven hydraulic pumps for actuation at peak operational loads[11] is an example of such architecture. A more conventional system would leverage pneumatic power from the engine to drive a hydraulic pump. Substantial savings in fuel consumption can be achieved by moving to an All-Electric architecture. Due to the sizeable reduction in the amount of bleed extracted from the propulsion system.

Aircraft engines use air as the propulsive power by means of a high pressure compressor and combustor. Air extracted from the engines is called customer bleed and it is used to power the various subsystems of an aircraft. This pneumatic power has to be replaced in order to produce the require amount of thrust to propel the airplane. To account for customer bleed, jet engines draw in more air and burn extra fuel to achieve the necessary performance. Air can be bled from various ports on the engine such as the bypass fan exit, a high pressure compressor (HPC), midway port, or the HPC discharge. At each successive stage the air becomes more “expensive” as it robs more thermodynamic energy that has to be replaced by the cycle for a given thrust setting. This accounts for the fuel consumption impact of customer bleed supplied to the aircraft.

There are a several factors that differentiate the operational efficiency between a pneumatic and an electric motor driven system. In pneumatic systems there is static pressure loss through the duct network that delivers bleed air from the engine bay to the subsystem location. There is also an efficiency penalty in converting the pneumatic power to mechanical energy used to operate a pump, compressor or actuator. Lastly, going to a more electric system allows for components to operate on-demand. This means that no energy is wasted by overproduction as components can be controlled to match the required load. In contrast, a pneumatic system depends on the state of the customer bleed dictated by the engine power setting. To account for the discrepancy, pressure regulators decimate the additional pressure resulting in energy being wasted. These are the major factors that make a more electric aircraft (MEA) so attractive for the airline industry.

In an MEA not all benefits come without some costs. A drawback to electrification arises from the increase in power required to operate the subsystems in an aircraft. To keep up with the electric demands, there is an escalation of engine torque extraction to run the onboard generators. In the 787, for example, the electrical power system generates more than double the amount of power compared to legacy systems[11]. Additionally, motors, drives, and electrical distribution complexity needed to run the MEA add weight resulting in an increased fuel burn. Nevertheless, even with these detriments, the benefits of MEA still provide a net improvement to the performance of a large commercial aircraft.

One should therefore study the possibility of combining traditional systems with electrification methods by performing a trade study of the integrated system through the

entire design landscape. This type of architecture is dubbed a “hybrid solution” because it utilizes some portion of pneumatic air obtained from engine customer bleed combined with an electrical architecture to meet subsystem demands. Would there be benefits associated with having hybrid architectures? In essence it was this question that drove the research behind this study and the need for integrated modeling. One potential benefit arises from using a low pressure source of customer bleed that can be augmented on-demand by use of a small motor driven component. This would reduce the amount of torque extracted from the engine, decrease bleed penalty by drawing air from a lower stage port, and reduce the size and weight of the motor needed to drive a given subsystem when compared to an all-electric system.

Complete aircraft systems are extremely complicated and span multiple fields of expertise. A fully integrated aircraft model would require a large team of engineers spanning various disciplines such as aerospace, mechanical, electrical, and controls. As part of this work it will be shown that it is important to assemble a fully integrated model of the system in order to analyze subsystem interaction and find areas of improvement. Although generating a complete synthesis model of an aircraft to fully understand the benefits of a hybrid architecture is outside the scope of this dissertation, one can focus on a few major subsystems to build a case study for the hybrid solution and prove that integrated modeling is key to an Energy Optimized Solution (EOA). To identify the most relevant subsystems, one can view the systems exergy. Exergy is defined as the total available energy in a system to perform useful work. The destruction of exergy, or entropy generation, is a result of inefficiencies in the system. Exergy analysis has shown[18] that nearly 99% of all entropy is generated during cruise.

In the current work a full integrated study of the major contributors to exergy destruction is presented to examine the merits of a hybrid architecture.

This requires an overall air vehicle model assembly that represents the operation of all the relevant subsystems in off-design performance. To enable the evaluation of each architecture in terms of a Specific Fuel Consumption (SFC) impact on engine overall performance.

$$\mathrm{SFC} = \frac{\dot{m}_f}{\tau} \tag{1.1}$$

Where $\dot{m}_f$ is engine fuel flow and τ is net thrust produced by the installed engine.

Reducing fuel consumption increases mission capabilities and reduce operational costs. This has led to a surge in interest on thermal management systems (TMS the major components of an aircraft system are outlined for the benefit of the reader.) onboard civil and military aircraft by the aerospace industry. In the next section the major components of an aircraft system are outlined for the benefit of the reader, as these are the major components that are included in this study.

1.2 Energy Management System

Modern air vehicles have a plethora of subsystems that enable flight in a safe and effective manner. The current investigation focuses on the interactions of a specific of subsystem, namely the Energy Management System (EMS). Figure 1.1 shows that the EMS is composed of the propulsion system, electrical power system, the various heat loads within the aircraft and the ECS or TMS. These subsystems combined, depict

how energy is transferred throughout the aircraft, from generation at the propulsion system to dissipation through the TMS.

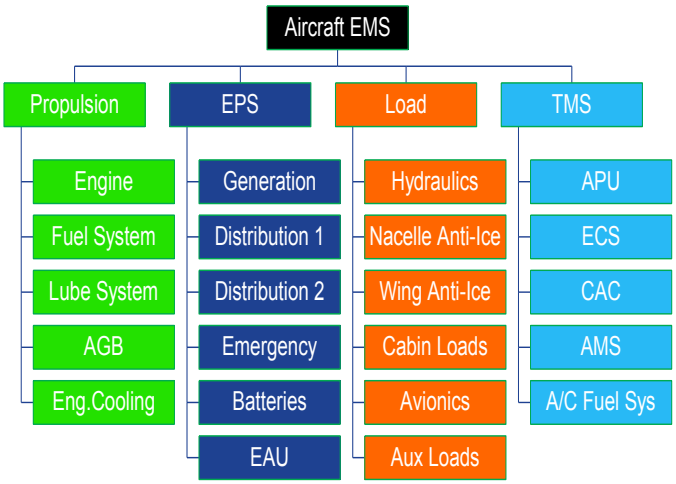

Figure 1.1: Aircraft Energy Management System Components.

1.2.1 Propulsion

The propulsion system for most modern commercial airliners consists of a turbo fan engine to generate thrust, as well as all the support equipment needed for stable operation. Listed here are some of the crucial propulsion subsystems: The engine fuel thermal management system (FTMS) ensures fuel is delivered to the engine nozzle at the appropriate temperature and pressure. The FTMS is highly integrated with the engine lubrication system, which leverages the fuel's heat capacity as well as an air cooled oil cooler (ACOC) to provide oil cooling. The lube subsystem then recirculates cool, clean oil to the various engine bearings, sumps and gears. This leads to the next secondary system on the engine, the accessory gearbox (AGB). The AGB extracts power from the core shaft by use of reduction gears to run a series of pumps and generators for hydraulic and electric power onboard the aircraft. Lastly the secondary flows circuit provides cooling for various components on the engine hot section.

The propulsion system is a highly complex and integrated environment. Yet to model the propulsion system, most of the interactions can be simplified as power extraction, engine bleed, and thrust requirements at a given mission condition. With a 1D performance model one can incorporate enough fidelity to gain insight on parameters that impact fuel consumption. In Chapter 4 the engine model used for this study will be discussed in more detail. Since this thesis focuses on bleed extraction from various locations on a turbofan engine, Figure 1.2 depicts a typical turbo fan engine and highlights the likely locations of customer bleed.

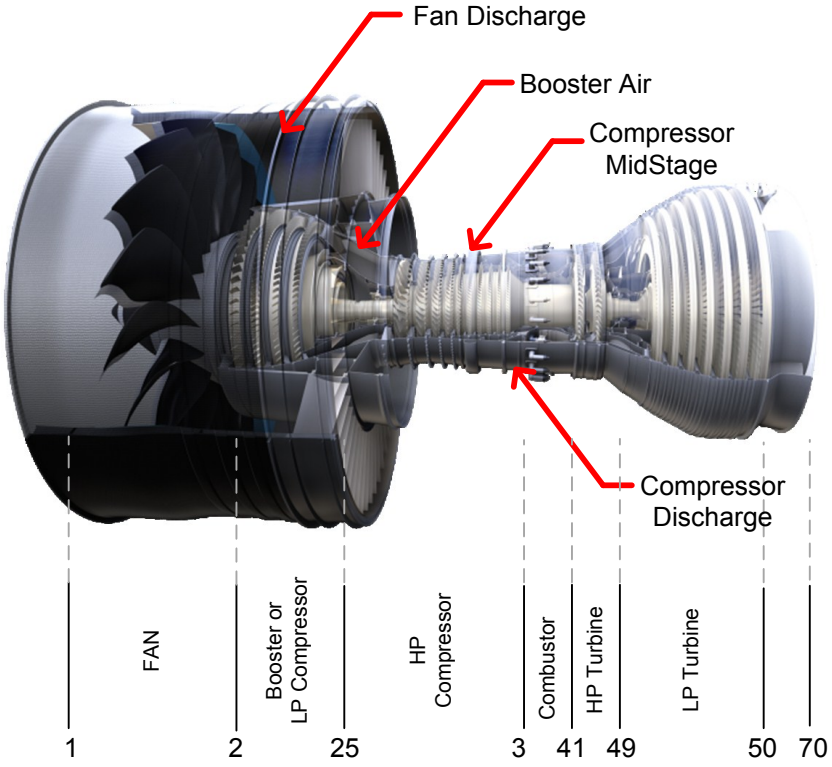

Figure 2.1: Commercial Turbo Fan Engine

1.2.2 Electrical Power System

The electrical power system (EPS) is responsible for the electrical distribution onboard the aircraft, from power generation and storage to delivery at the appropriate voltage. The EPS monitors energy usage for all crucial components such as the avionics' air management computer, electrical motors, subsystem controllers, heating, and lighting. The EPS on most aircraft is divided into two components, the Primary and Secondary Power Distribution. The primary power distribution supplies current from various sources as available. It handles switching between the aircraft engine mounted generator the auxiliary power unit, batteries and ground power when available. In most applications there are subsystems that require different power levels, hence power switching has to be performed. The secondary power distribution system runs all electronics that require a different power level than what the generators are providing. For example, traditional systems use 115VAC for the primary power and 28 VDC for the secondary power distribution system. This allows for greater power generation and less transmission line losses then a legacy system with only 28 VDC.

As part of the study, the complexities of the electrical power system were not examined. This work only focuses on the thermal aspect of the EPS, i.e. the loads generated by inefficiencies on the electric components or power converters. The next section covers the heat load generation within an aircraft cabin.

1.2.3 Heat Load Generation

Aircraft heat loads are generated through a variety of mechanisms that include electrical equipment, passenger and crew body heat generation, and conduction through fuselage. Although there are other sources of heat such as actuators, these

can generally be neglected as they are not handled directly by the environmental control system. Heat loads onboard an aircraft have to be mitigated in order to maintain human comfort and ensure electronics operating within design temperature limits. The TMS maintains the appropriate conditions inside the aircraft.

An additional load that is handled by the propulsion system itself is the wing and nacelle anti-ice. This is a heating load needed to avoid ice formation along the wing and nacelle leading edge. Since this is a transitory load, which is not seen during cruise, it will not be simulated in the analysis.

1.2.4 TMS

The thermal management system is responsible for mitigating all heat loads within an aircraft. For supersonic aircraft applications the TMS integrates with various subsystems in an effort to optimize heat dissipation, maximize capacity and minimize energy use. This type of aircraft have intricate heat management strategies that utilize the jet engine, fuel tanks, lube system and fuel distribution system to handle thermal challenges. Typical thermal management architectures for a fighter application can be found on Figure 1 of Butzin and Johnson[22]. It can be seen that the system utilizes engine bypass air and fuel as its primary and secondary heat sink.

For most revenue share carriers, the TMS is called ECS, which manages heat through air cooling. As opposed to supersonic applications, traditionally the ECS is independent of engine fuel and lube cooling systems. This is mainly because the ECS can use ram air as its main heat sink. This study will focus on the function of a commercial ECS system and how it integrates with the engine.

2 State of the Art Environmental Control Systems

This chapter will describe the main components and operation of an ECS system, also called an air conditioning pack. A large portion of this study is focused on the operation of the ECS because it is one of highest energy consuming subsystems in an aircraft, along with the engine, and necessary for life-support. Once the operation of this subsystem is understood, one can then find ways to improve and optimize the way it interacts with other aircraft systems.

As previously discussed, the main function of the ECS is to provide pressurized ventilation and air conditioning for the aircraft cabin to maintain passenger comfort as well as remove cabin and avionics electric heat loads. At the heart of the ECS is the Air Cycle System (ACS), a reverse Brayton cycle that refrigerates air by intercooling bled air through the use of ram inlet scoops and extracting work from the pressurized air stream. This system is typically pneumatically powered by either the main engine customer bleed, an auxiliary power unit (APU), or an electric motor driven cabin air compressor (CAC) on more electric architectures[11]. The main component of the ACS is the Air Cycle Machine (ACM), a turbo-compressor device that can be assembled in a

variety of ways depending on system demands. Most packs contain 2 or more ACS units that work in unison to deliver the onboard cooling capacity needed as well as provide fail out capability in the event that one ACS is inoperative.

The coefficient of performance (COP) is a parameter commonly used to measure the effectiveness of a refrigeration cycle. It is defined as the total refrigeration capacity over the amount of work put in the cycle:

$$\beta = \frac{\dot{Q}_{duty}}{\dot{W}_{in}} \tag{2.1}$$

The typical COP value for an ACS is close to $\beta \leq 0.5$ which is very low when compared to a vapor cycle systems (VCS) with $\beta \geq 1$. Although the COP of an ACS is very low it still presents various advantages in the field. As will be shown in this chapter, air cycle systems work with pneumatic air, which is readily available on an aircraft, much more so than electrical power on legacy applications. Another advantage is that these systems use air as the working fluid, therefore systems leaks are not a large issue. In fact, ACS can still provide some cooling even with a number of leakages. Compared to a VCS where leaks can cause health and fire issues, as well as render the entire system inoperable. The main advantage that makes the ACS viable for aircraft use is that it can generate large quantities of air at very low temperatures, up to -100°F, in a relatively compact package.

Figure 2.1 shows a typical commercial jet during take-off. From this view one can get some insight on the layout of the major components of an ECS system on a modern aircraft. The jet engine is the source of air during flight, which is transmitted along the wing to the fairing of the aircraft where the pack is located. In Figure 2.1, the

typical NACA inlet scoops can clearly be seen. These are submerged style inlets developed by the National Advisory Committee for Aeronautics (NACA) which offer a reduction in external drag, great pressure recovery, and only diffuse the airflow a small amount[24]. The ram air collected is necessary for the operation of the ACS. In the following discussion the purpose and operation of these components will be discussed.

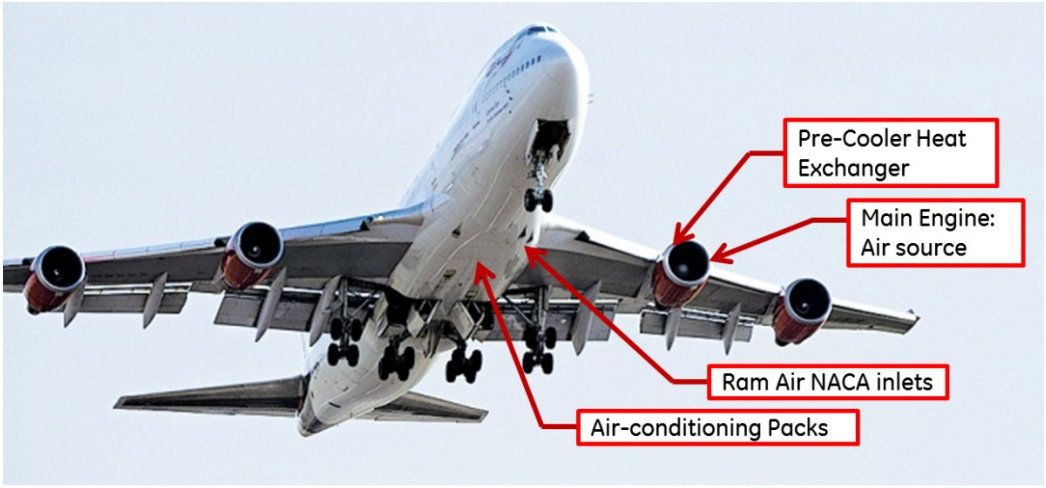

Figure 2.1: Typical ECS External Interface

2.1 Simple Cycle

To understand the underlining principle behind the operation of an environmental control system, let us examine the simplest form of an ACS and walk through the integration with the engine. ECS integration consists of three major components: the engine, Air Management System (AMS) and ACS. Figure 2.2 demonstrates the layout of an ECS consisting of a simple cycle[24], the simplest form of air cooling.

The engine is the power plant of the aircraft, providing thrust, electrical, pneumatic and hydraulic power throughout flight. Pneumatic power is extracted by the AMS and delivered to various subsystems throughout the aircraft including the nacelle

and wing anti-ice, air-conditioning packs, and engine air start systems. The AMS selects the appropriate engine bleed port as a function of engine operating conditions and partially conditions it to be safely delivered throughout the aircraft. Air extracted from the engine and supplied to aircraft subsystems is typically termed customer bleed.

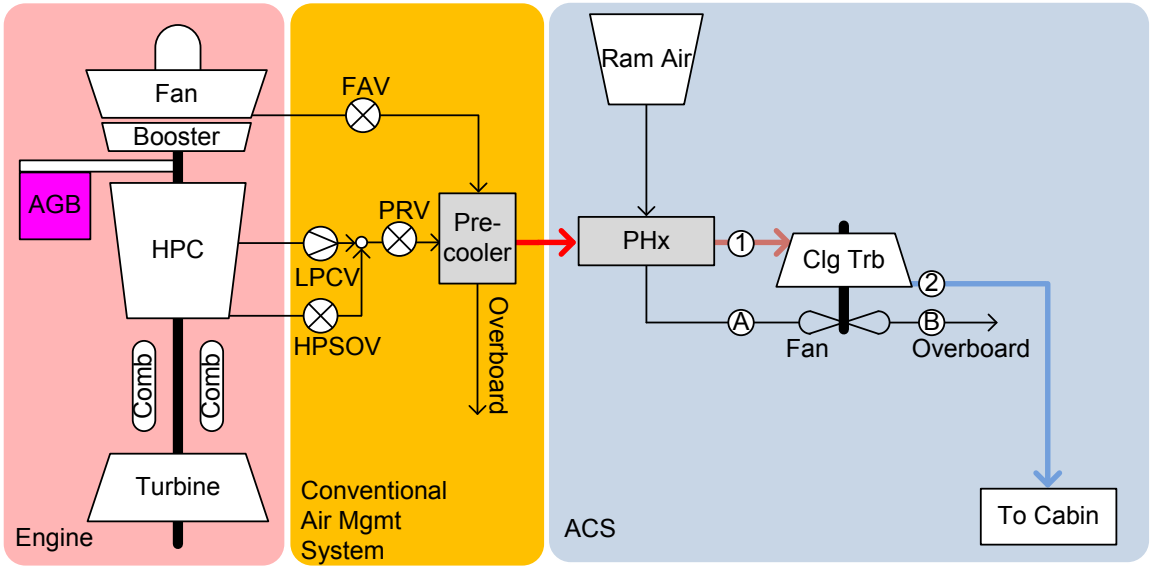

Figure 2.2: Pneumatic ECS with Simple Cycle ACS

A functional AMS has to handle the wide range of pressures and associated temperatures that originate at the propulsion system. The AMS conditions the pneumatic bleed to safely meet ACS requirements needed to deliver conditioned air to the cabin. Most modern ACSs require pressures ranging from 30 to 60 psia depending on the machine's operating state as a function of ambient day or Deviation from the International Standard Atmosphere (DISA), humidity, altitude, aircraft Mach number, and internal loads such as number of passengers and use of electronics.

The operation of a simple cycle will be illustrated with a walkthrough of a sample state. For this example, set the bleed pressure required at the AMS-ACS boundary to

40 psia. In a conventional system, air can be bled from the engine out of one of two ports. One is located at the HPC discharge and the other at a midpoint location along the HPC as previously discussed on Figure 2.1. If the midpoint location pressure is less than the schedule pressure required, then bleed is switched to the more expensive port at the compressor discharge by opening the high pressure shutoff valve (HPSOV) in Figure 2.2. As the HPSOV opens, the added pressure from the compressor discharge locks closed the low pressure check valve (LPCV). Vice versa, if the midstage HPC pressure is sufficient for operation, the HPSOV closes completely and allows the LPCV to open and supply bleed air to the AMS. The amount of flow to actually be bled is controlled by the ECS and will be discussed in section 2.5. The AMS is responsible for both, scheduling the customer bleed flow and precooling it to acceptable temperature outside the engine cowl. As an example, let's say the engine compressor midpoint port currently has a bleed pressure of 100 psia at a temperature of 550°F. Since the pressure is higher than the required amount of 40 psi, this port is selected to supply air [HPSOV is shut off].

The pressure regulator valve (PRV) reduces the pressure from 100 to 40 psia at the outlet by adjusting the valve position setting. However, the temperature is still too hot to be flowed along the wing to the pack location on the fairing, mainly due to flammability concerns associated with the proximity of fuel lines. The purpose of the pre-cooler heat exchanger is to ensure that air leaving the engine bay is below a threshold amount. As seen on Figure 2.1 the precooler is typically located on the engine pylon, where it can use fan discharge air to cool outgoing customer bleed. Cooling air from the fan is regulated by the AMS controls as well. It schedules the Fan

Air Valve (FAV) to flow bleed air from an inlet scoop in the engine bypass duct routed to the cold side of the pre-cooler. The desired customer bleed exit temperature varies with manufacturer due to particular safety practices, level of duct insulation, experience and aircraft design. Since the auto ignition temperature of Jet A fuel is 410°F[20], let's make this the required temperature at the precooler exit for this example. Consequently, the air stream is at the required 40 psia and 410°F, ready to be sent to the air cycle system.

As air is routed to the fairing of the aircraft it reaches the most basic form of ACS, the Simple Cycle. From Figure 2.2, the first component in the cooling system is the primary heat exchanger (PHx). This is a heat exchanger similar to the pre-cooler, but it uses cooler ram air to further chill the bled stream. In this example, the air at location *1* is now close to 35 psia and 150°F as it was cooled by the PHx. So far, the air stream has seen substantial cooling from 550°F to the current state, but it is still too hot to be used as a cooling medium. As the stream enters the cooling turbine (CT), it is adiabatically expanded from 35 psia to 15 psia to be delivered at cabin pressure. As it adiabatically expands, the turbine extracts work from the flow to power the ram air stream fan. The net result is a fresh air stream at an exit temperature of 40°F that is then routed to the cabin. This type of system is typically used for smaller general aviation planes which use 100% fresh air stream or as a supplementary cooling unit.

2.2 Two-Wheel Bootstrap Air Cycle

The previous system, although straightforward, demands a high amount of bleed air from the engine to supply the cabin with an adequate amount of air. With the advent of turbo fan engines, the gas generator has progressively become smaller and thus the

amount of bleed represents an ever larger percent of the core flow[7], resulting in an ever higher penalty on SFC. To reduce the performance drawback, a machine is needed that can cool bleed flows to subfreezing temperatures such that it can mix with partially recirculated cabin air. In fact most large commercial aircraft use a 50/50 split of recirculated to fresh air for maintaining cabin comfort[14]. This greatly reduces the amount of bleed demands from the engine, but can only be done with a more advanced cycle such as the bootstrapped ACM[24], seen in Figure 2.3.

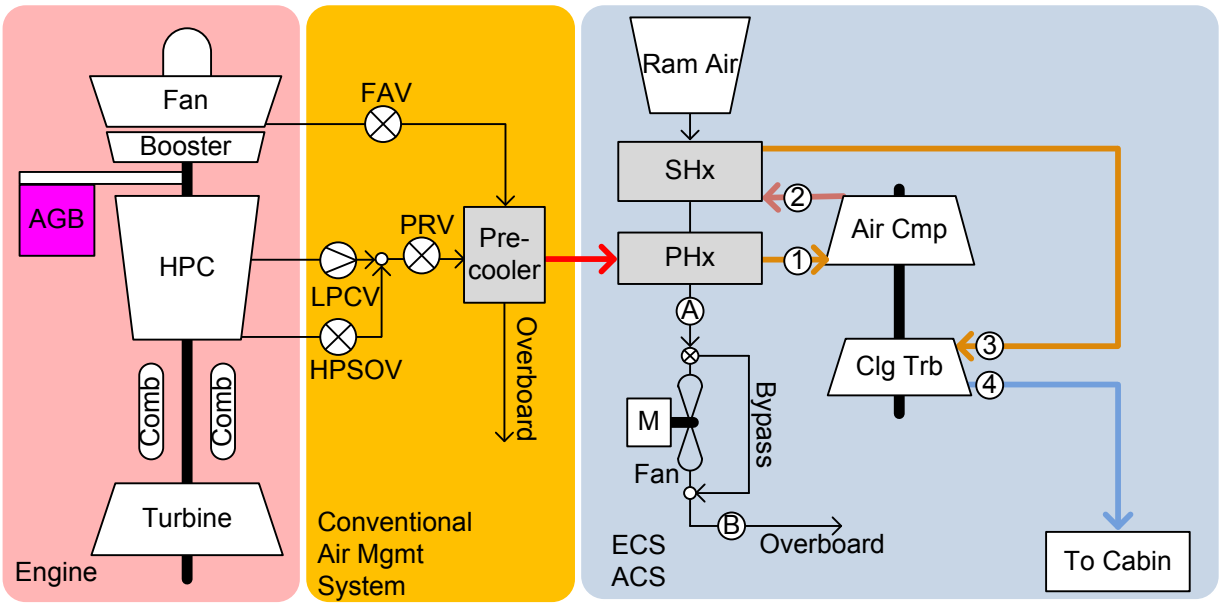

Figure 2.3: Pneumatic Two-Wheel Bootstrap ACS

The principle behind this cycle is to install a compressor that can increase the thermodynamic state of the air stream through a compression process. ACS compressors are typical centrifugal in design and thus can have a pressure ratio (r) as high as 5 in one stage while maintaining good adiabatic efficiency[12] with a simple design. As in the previous scenario, the air at location *1* is at 150°F, 35 psia after exiting the PHx. Nominal operation of an ACS compressor is typically around r = 2.0

with efficiencies from 75 to 85%. Hence at location *2,* the flow has been adiabatically compressed up to 70 psia and a corresponding temperature of 328°F. This boost in temperature enables the flow to be once again flowed through the ram air stream to transfer additional heat to the ram duct. The "bootstrap configuration" refers to this characteristic in which the cycle loops back onto the same ram stream. From Figure 2.3, the SHx is leading the PHx in the ram air duct because air incoming from engine bleed can be a hundred degrees hotter than that coming out of the compressor on location *2*.

At the exit of the secondary heat exchanger (SHx), the flow is cooled to approximately 180°F. Consequently, the fluid is at a very high pressure yet relatively cool temperature at location *3* in Figure 2.3. Similar to the simple cycle, the expansion turbine extracts work from the flow that is needed to power the compressor. At location *4,* fresh air stream is ready to be delivered at a cool -10°F and 15 psi, much cooler than what the simple cycle could provide. This allows the use of a cabin recirculation circuit such as the one seen on Figure 2.4.

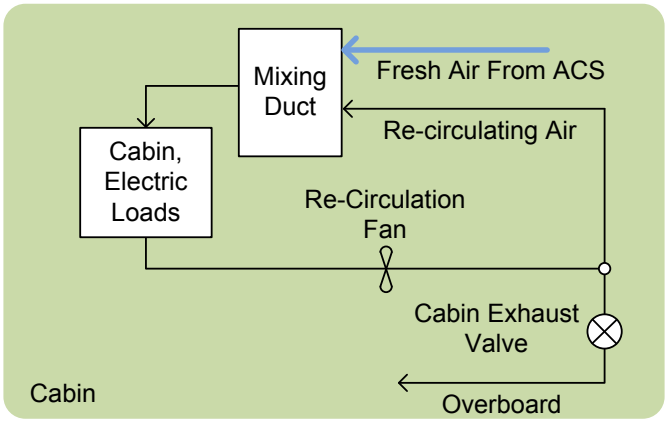

Figure 2.4: Typical Cabin Recirculation System

By recirculating part of the cabin return air the amount of bleed flow required from the engine can be substantially reduced, thus increasing the coefficient of performance of the entire system and reducing fuel consumptions of the aircraft. This is the major advantage of going from a simple cycle to a bootstrap air cycle system.

One thing to note from this cycle is that the ram air duct Fan is powered by an electric motor and is not on the ACM shaft. This allows the electric motor operated fan to be shut off during flight where the cooling circuit has enough ram pressure to induce flow through the PHx and SHx. Another advantage is that it allows for use of the ram air stream independently of the ACM during ground idle. For example, if it is a cool day, the fresh air provided to the cabin from engine bleed could potentially be cooled with the ram air heat exchangers alone, PHx and SHx from Figure 2.3. By having an electric fan, the system can induce flow in the ram air circuit and bypass completely the ACM. This would reduce the required operating pressure and have an impact on ground idle fuel consumption.

2.3 Three-Wheel Bootstrap Machine

A variation to the 2 wheel bootstrap system is the 3 wheel bootstrap. This is a similar thermodynamic cycle, but with the added sophistication of a fan on the same shaft as the compressor and turbine as seen in Figure 2.5. This system has a clear advantage over the previous configuration in that it can be assembled as a highly integrated package and is mostly independent of the electrical power system on the aircraft. This allows for better operation on the ground when the main engines are off and the system has to operate with the aircraft's APU. One challenge is that the ACS is

coupled to the fan and thus has a significant impact on the cycle. This requires the cooling turbine to be oversized for ground idle operation, where the fan might require up to 30hp to force air thought the ram air duct. At the same time, ground idle is one of the most challenging mission points for the cooling system where ambient day condition can be very severe, thus the compressor also is operating at high capacity up to 150hp.

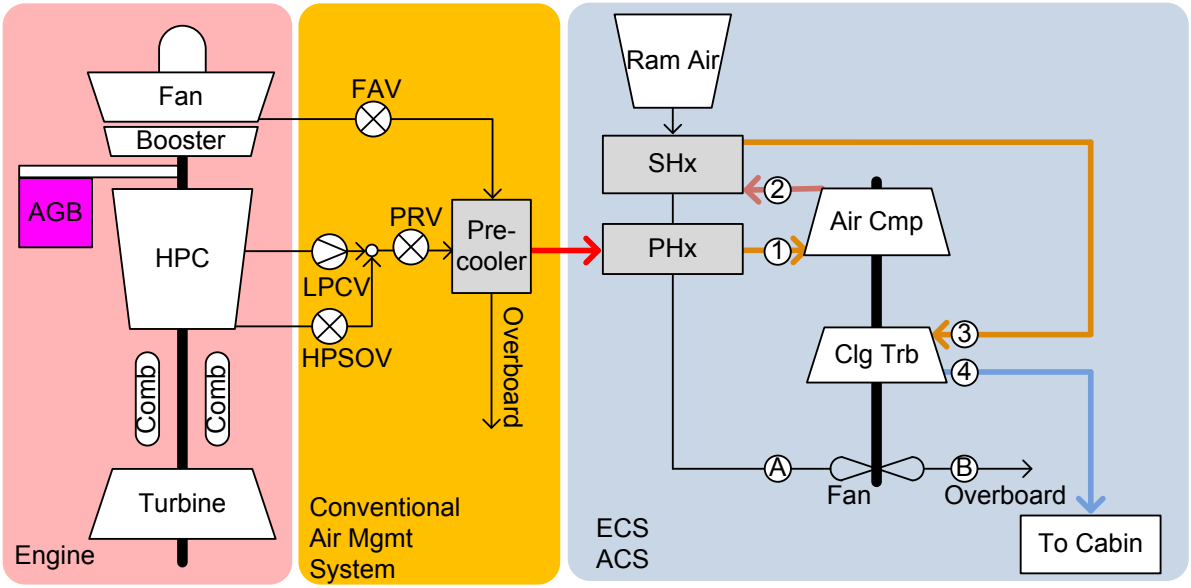

Figure 2.5: Pneumatic Three-Wheel Bootstrap ACS

The cooling turbine must balance the rotational speed and power of the fan along with the compressor at the various operational states. Fortunately at cruise the fan is mainly in a windmill state and does not demand much power from the turbine due to the ram pressure recover at the inlet scoop. In fact, in some cases it can even supply a very small amount of power back to the compressor (~ 1 hp).

2.4 Condensing Air Cycle System

There is a hidden problem in the cycles described so far, one that typically is not reflected on paper, namely water. Water vapor accounts for a significant portion of the

atmosphere in warm/tropical climates and needs to be included in the analysis and design of all refrigeration systems. Removing humidity from the fresh air supply is one of the major functions of any air conditioning system to maintain passenger comfort. On an ACS it also represents a thermodynamic and operational challenge that has to be addressed.

To illustrate the moisture problem, one can use a water phase change diagram[21], as seen on Figure 2.6. This diagram delineates regions of the distinctive states of a material, vapor, liquid or solid as a function of temperature and pressure. Figure 2.6 shows an overlay plot of the thermodynamic states given for the sample ACS run discussed in the previous section. The ACS customer bleed air inlet temperature and pressure was set at 410°F and 40 psia respectively, labeled *ACS Inlet* on the Figure 2.6.

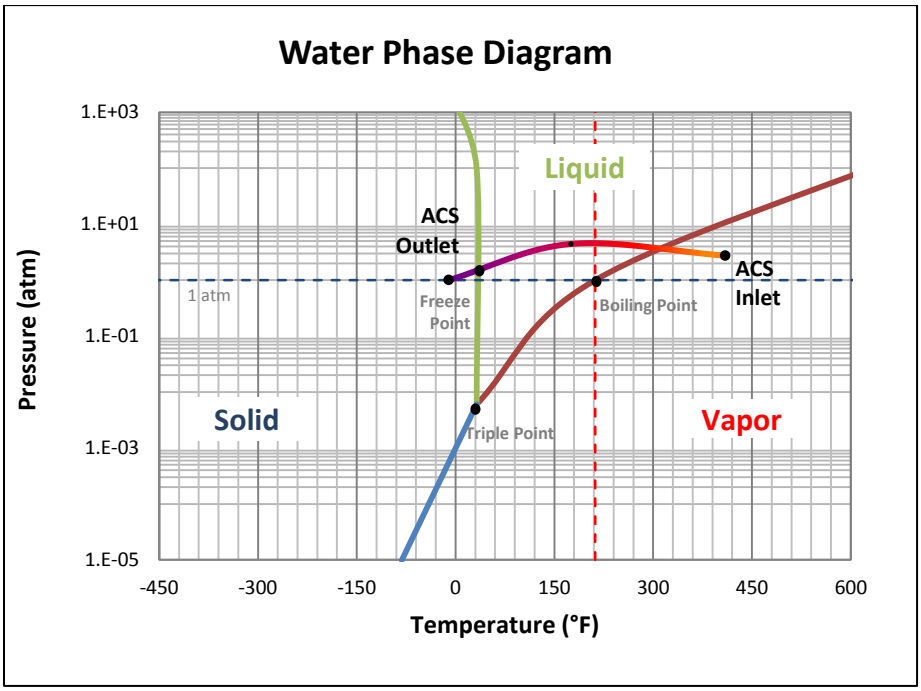

Figure 2.6: Log-Linear Water Phase Change Diagram

It can be seen that at this point there is no moisture present as water is in a vapor state. As the fresh air stream on the ACS gets cooled by the PHx and SHx, it can be seen that there will be condensation forming within the system as the humidity has entered the liquid state of the diagram. Moreover at the *ACS Outlet* it can be seen that the moisture in the fresh air stream has transitioned to a solid. Consequently, one might expect to have icing issues at the turbine exit or on a downstream location of the air cycle machine.

Returning to the ACS schematic on Figure 2.5, air at the CT exit in location *4* is far below the dew point temperature and has entered the solid region of the phase diagram. Water vapor in the ACS stream has condensed into droplets and then frozen, potentially creating havoc on the system. First, it reduces the thermal performance of the machine by adding heat from the latent heat of condensation as water changes phase from gas to liquid. This process reheats the flow due to the energy released from the water vapor as it condenses, reducing the COP of the cycle. Second, freezing temperatures at location *4* can lead to ice accretion downstream of the CT that can clog the system and render the machine inoperable.

This makes moisture a major concern for tropical or humid climate operations where the relative humidity is high. A water extraction mechanism has to be incorporated into the bootstrap system in order to remove moisture from the fresh air stream and avoid problems.

2.4.1 Three-Wheel Condensing ACS

At this point, it is evident that moisture presents a genuine issue for ACS operation. To tackle this challenge and provide dry air for the cabin the ACS has to

evolve once again resulting in the new cycle depicted on Figure 2.7. This architecture contains two additional heat exchangers, namely the Reheat heat exchanger (RHx) or recuperator and the Condenser (Cond). Also new to this architecture is the high pressure water extractor (WE). This device acts as a centrifuge to funnel the incoming airstream in an effort to swing water droplets onto a collector along the walls of the assembly.

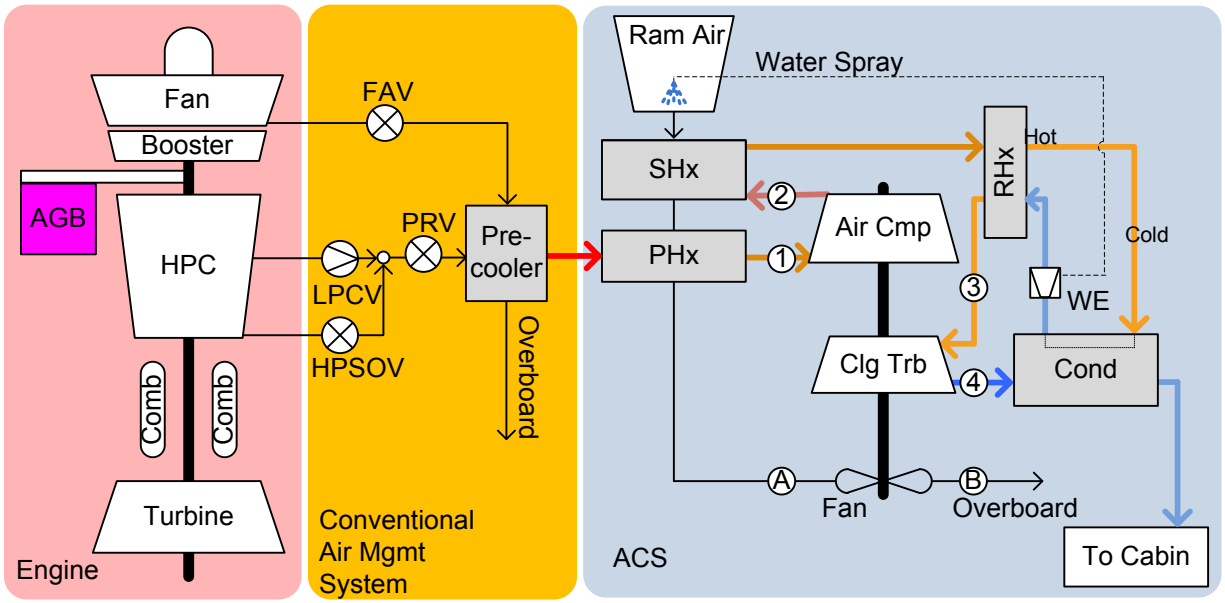

Figure 2.7: Pneumatic Three-Wheel Condensing ACS

The bootstrap scheme on the condensing cycle works in the same fashion as described previously. From the preceding example, air exits the SHx at 175°F and 65 psia and now passes through the RHx, whose function will be explained shortly. Upon exit of the RHx, the stream proceeds to the condenser unit at a cooler 130°F and roughly 60 psi. The condenser is essentially a very cold surface that super-chills the hot flow to incite rapid condensation of water droplets. At the exit of the condenser the fresh air is at 80°F and 55 psi. As seen on the phase change diagram, Figure 2.6, the

air stream has been pushed far into the liquid region. The water separator or extractor is then used to collect and remove the excess moisture from the system. From Figure 2.7 it can be seen that water collected from the system is used to enhance the thermal capacity of the ram air stream, thus recovering some of the heat lost due to condensation as the water evaporates on the surface of the PHx and SHx.

At this point the cycle is mostly dry, however the WE is not 100% efficient, rather 75 - 80%. Consequently, there are still some water droplets left in the airstream, which if not addressed, could damage the operation of the CT. The purpose of the RHx now become evident as it is used to evaporate any remaining moisture left in the stream on the cold side. It also has the dual purpose of enhancing condensation by chilling the airstream before it enters the Condenser on the hot side.

As air exits RHx cold side, location *3* on Figure 2.7, it has been heated back to 130°F with a pressure of 50 psi. At this point the fluid is dry cool air ready to be chilled by the CT expansion process. As detailed in the previous architectures, work is extracted from the stream and is cooled to approximately 10°F and expanded to 18 psi. From location *4*, the stream now enters the cold side of the condenser where it is heated to its final state of 50°F and 15 psi. The fresh airstream is now ready to be delivered to the cabin after being fully conditioned and cooled by the ACS.

As was seen with the simple cycle, section 2.1, 50°F air is not cool enough to be effectively mixed with cabin recirculated air. In order to reduce the amount of fresh air needed to provide the appropriate cooling a new architecture is introduced, the Four-Wheel Condensing ACS.

2.4.2 Four-Wheel Condensing ACS

The final step in the evolution of the ACS is the four wheel machine[24], which represents the Conventional-Pneumatic Architecture (CPA), Figure 2.8. This architecture takes advantage of a second turbine expansion to further cool the dry air to an exit temperature of -2°F which can then be mixed with recirculated air as depicted in Figure 2.4.

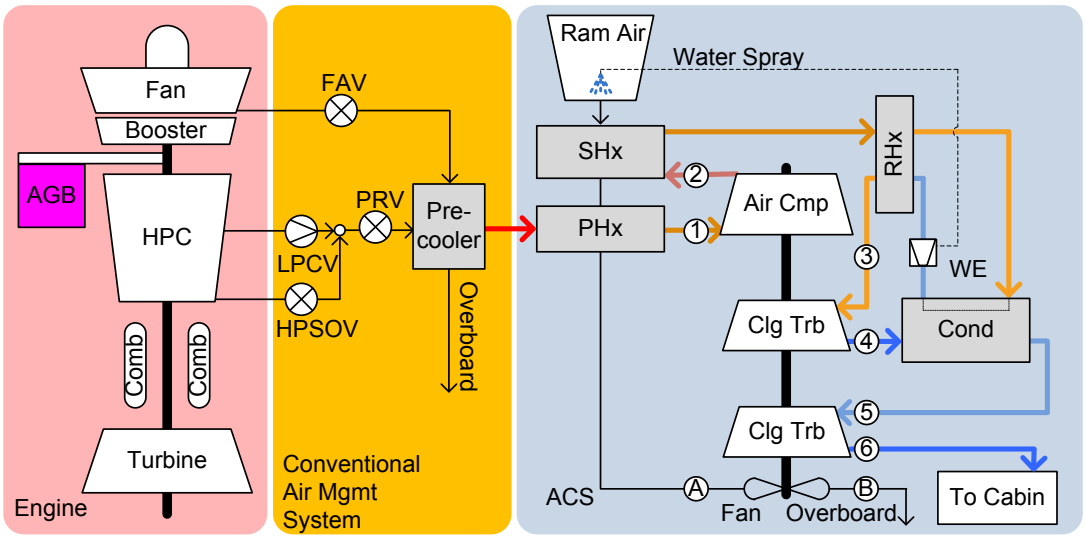

Figure 2.8: Pneumatic Four-Wheel Condensing ACS

This architecture represents the state of the art for pneumatic air cycle systems. The first fully qualified 4-wheel air cycle machine was onboard the 777 pack[13]. In this system there is an additional design parameter that stems from the loading of each turbine. At first glance one might expect that the loading of the cooling turbines might be divided equally to provide power to the compressor and fan. Yet, to ensure proper protection from water and icing at the condenser, stream conditions at location *4* in Figure 2.8 should be designed such that the turbine exit temperature is maintained at or above 35°F. This is accomplished by shifting a larger part of the loading to the second

turbine. For off design operation there are various mechanisms to control the exit conditions of the CT and adjust for cooling capacity.

2.5 Design Point Considerations

In previous sections the discussion has centered around the configuration for different kinds of air conditioning packs employed on modern aircraft. Although each system is very different, the design point conditions are quite similar. Partly the reason is because the pressurization demands at altitude are provided by either the aircraft engine or a CAC. Yet the main reason stems from the way ambient temperature and humidity changes with altitude. Figure 2.9 demonstrates the standard atmospheric temperature model as a function of altitude for a hot day per the MIL-HDBK-310. It can be seen that even in a hot day with a ground temperature of 104°F, at regular cruise altitudes of 30 to 40 thousand feet the temperature drops below 1°F. Right on Figure 2.9, it can be seen that humidity significantly drops with altitude as well. Even in extremely humid climates, at altitudes greater than 22 thousand feet, air is so dry that there are no icing concerns[32].

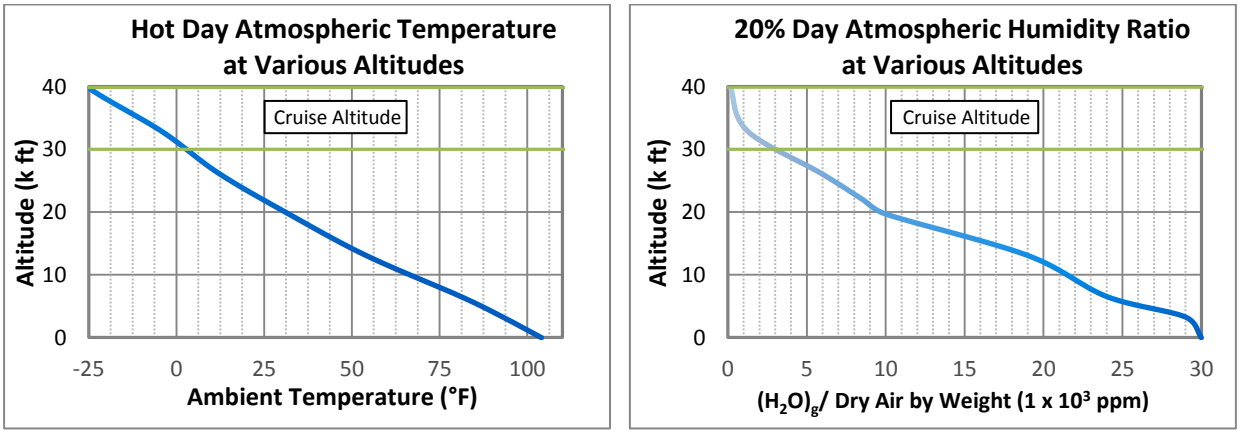

Figure 2.9: Hot Day Temp (Left) 20th% Conditions Humidity Ratio (Right)

Given the temperature and humidity profile, the most demanding operational state of a commercial airliner's air cycle machine is at ground level on a hot day. The high load conditions require a large amount of flow to maintain the cabin at a comfortable temperature. Recalling from Figure 2.2 to 2.8, the ram air stream is the main heat sink for the ECS. Since the ambient air is hot, the compressor has to operate at a higher pressure ratio to obtain the appropriate delta temperature needed for heat transfer. The problem is exacerbated at takeoff when there is resulting rise in total temperature, up to 20°F increase, on the ram air stream. The combination of the high flow rate and additional compressor power makes this the design point for the ACS.

For the trade studies presented in this work, the main point of interest is at cruise, where loads and ram conditions are much more benign. Thus, the analytical models constructed need to perform off-design simulations to accurately predict the benefits of each solution at cruise. From the previous discussion, it becomes evident that there is a substantial variation in thermal loads throughout the mission. In order to maintain the appropriate duty cycle, the ACS has various control mechanisms which will be the topic of the next section.

2.6 ACS Operation & Control

The operation and appropriate control needed to maintain an ACS at stable operation, while providing conditioned air at the appropriate pressure, is not a trivial one. Additionally, there are several protection mechanisms that can be instituted to avoid moisture related icing in the cooling turbine. This section describes the main

control knobs used for ACS control. Figure 2.10 depicts the principal control sensors and valves used in a three-wheel ACS system.

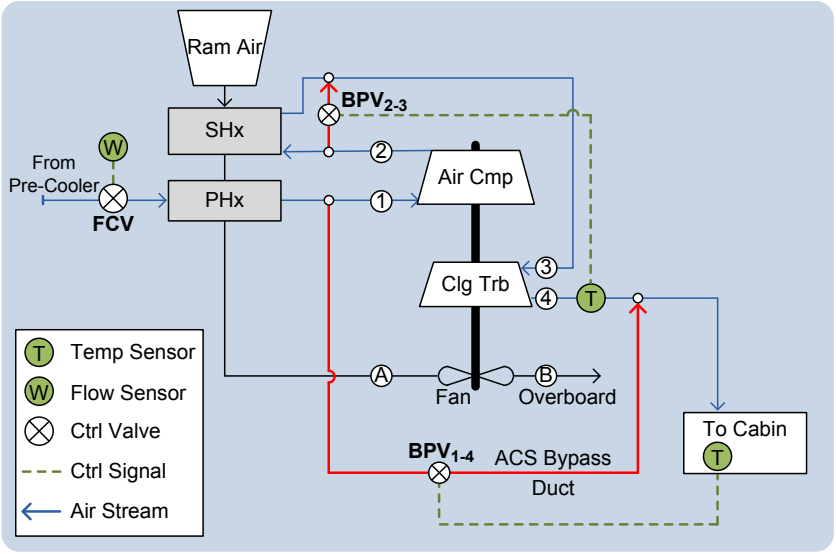

Figure 2.10: Three-Wheel Condensing ACS Control Schematic

2.6.1 ECS Flow Control

The first control mechanism to be discussed is the flow throughput governor. The amount of flow needed for the cabin is dictated by FAA regulation for ventilation per passenger and proper pressurization. Airframe manufacturers require a set flow schedule for various conditions throughout a mission that varies with altitude, heat load and number of passengers. The flow control valve (FCV) is responsible for regulating the amount of fresh airflow through the system[34]. There are various ways the flow through the system can be measured, but the most efficient way is by use of a Venturi nozzle[17]. A converging nozzle, shown in Figure 2.11, measures flow by comparing the static pressure at the inlet of the nozzle to that at the throat.

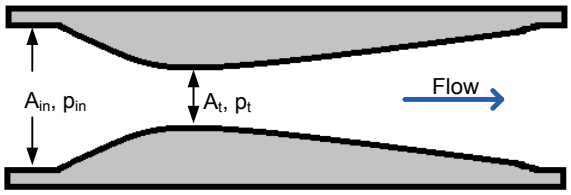

$$\dot{m}_{ECS} = A_t \sqrt{2\rho \frac{(p_{in} - p_t)}{1-(A_t/A_{in})^2}} \qquad (2.2)$$

Figure 2.11: Venturi Nozzle for Flow Measurement

The pressure differential arises from an induced acceleration in fluid velocity due to the decreasing cross sectional area of the duct. To satisfy conservation of momentum, the static pressure at the throat is lowered. This pressure differential can be used to calculate mass flow as shown on equation 1.3. Once the current mass flow is known, the FCV can open and close to allow the correct amount of fresh air enter the system. One thing to note is that the amount of fresh airflow is dictated by the cabin demands. The ACS has to be controlled independently to supply the required mass flow and supply the correct air temperature. In other words, the mass flow though the ACS cannot be varied to control the operation of the of the air conditioning pack. This is because there is a fresh air requirement to maintain the cabin properly ventilated. Two more valves will be discussed that serve as the main controls method for the ACM itself.

2.6.2 Air Cycle Machine Control

In order to provide the right level of cooling at the various mission conditions, the ACM has to spool up or down accordingly to meet demand. From the discussion so far it is evident that the air cycle machine works without an external power source to drive the shaft. The cycle runs through the pressure differential from location *1* to *4* on Figure 2.10. The main mechanism to control the power setting of the ACM is by means of a bypass valve that diverts flow from location *1* to location *4*, as seen in Figure 2.10, labeled $BPV_{1\text{-}4}$. This valve routes a portion of the inlet customer bleed to the ACS exit

duct, where the two flows are mixed to produce the final delivery temperature. Hence by throttling $BPV_{1\text{-}4,}$ the controller can effectively set the ACS to any temperature that is required to meet capacity at a set mass flow.

2.6.3 Cooling Turbine Anti-Ice Control

Icing at the turbine exit can block flow and degrade ACS performance. There are various mechanisms to avoid ice buildup at the exit or downstream of the cooling turbine.

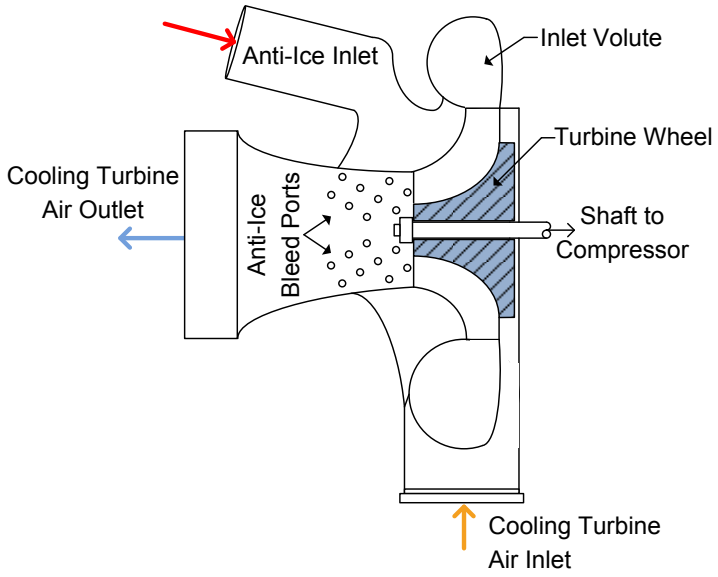

Figure 2.12: ACM Cooling Turbine

A simple way of avoiding ice at the CT exit, on a two or three-wheel ACM, is to add bleed ports that injects hot air directly into the turbine exit as depicted in Figure 2.12. In this architecture, the anti-ice air would be supplied from location *1*.

Although this is a very effective mechanism for controlling exit temperature, it is not very practical for a 4-wheel machine. In a 4-wheel arrangement the system would have to be designed such that the pressurized air for the CT anti-ice bleed originates at

location *2,* Figure 2.8, to ensure there is a positive pressure differential between the anti-ice air and the CT exit. This results in a loss of power in the first CT due to a reduction in chargeable flow. A more effective strategy is displayed on Figure 2.10, where air from location *2* is bled to the inlet of the CT, location *3*, and thus increasing the CT exit temperature to avoid freezing. Recalling the 4-wheel machine of Figure 2.8, this is the mechanism used to keep the condensing loop of the cycle above 35°F and thus avoid icing issues before removing moisture from the airstream.

In the previous sections the main types of air cycle systems were discussed in detail to provide a fundamental understanding on the functions and operation of an ECS. The progression of technology was outlined up to the state of the art architecture, the four-wheel condensing ACS. One can get a sense of how versatile ACS can be to provide cabin cooling from engine bleed at very large flow rates, in excess of 100 ppm, at sub-freezing temperatures. Any other type of refrigeration system would require a substantial amount of power, volume and weight to produce that much airflow at such low temperatures. A big drawback to ACS architectures is that they require fairly expensive air from the engine to operate and have a low COP when compared to other refrigeration systems such as the VCS. In the next section, an All-Electric variant on the ACS will be described.

2.7 All Electric Environmental Control Systems

With the dawn of the more electric aircraft, an increasing number of aircraft manufacturers are riding the electrification wave which has resulted in substantial improvement in operational efficiency and life cycle costs on various aircraft subsystems

such as hydraulic actuation and mechanical linkage systems[11]. Being one of the most energy exhausting systems on the aircraft, the ECS, also sees benefit form electrification. This leads to the full All-Electric Architecture (AEA) depicted on Figure 2.13.

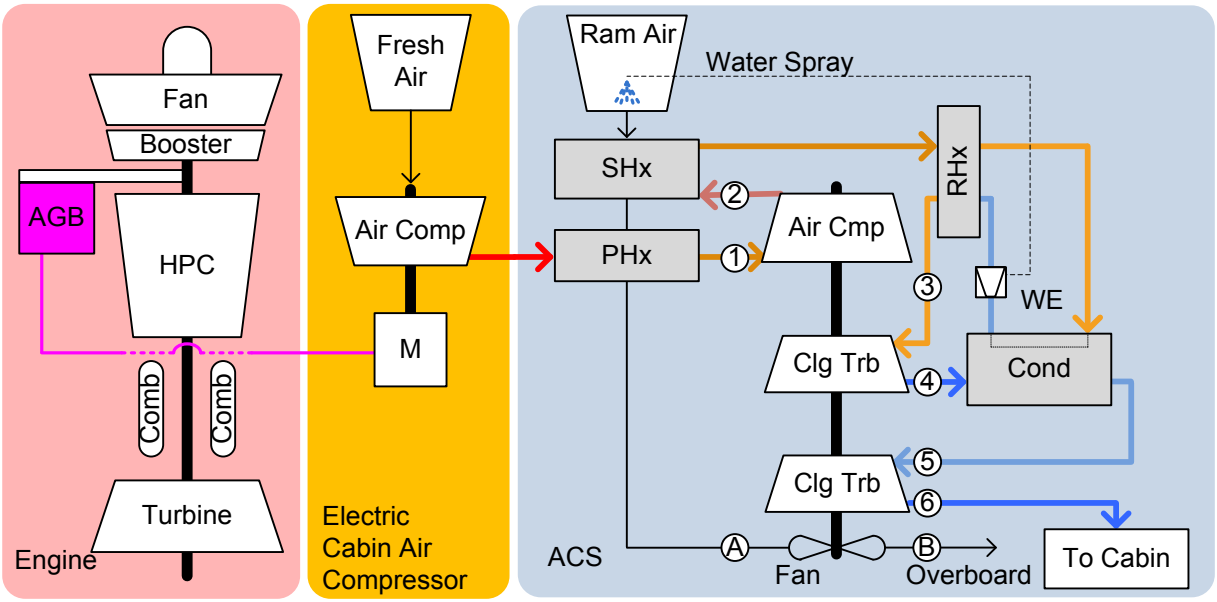

Figure 2.13: All Electric Four-Wheel Condensing ACS

The pack operation on this electrical ECS is the same as the four-wheel ACS described in the previous section, but the air management system is replaced with an electric Cabin Air Compressor (CAC) and a Fresh Air inlet scoop. Figure 2.13 shows the engine customer bleed replaced by power extraction, represented by the purple line from the AGB mounted generator and converter.

Intuitively, one might presume that it would be impossible to have an electric compressor that is equally efficient as the engine HPC and thus electrification would not make sense for this application. Yet the savings imparted by this architecture come from the ability to control the electric compressors exit pressure on-demand to precisely

what is needed by the ACS. Compared to the pneumatic architecture, the savings are evident because the pre-cooler is no longer necessary, hence less entropy generation. By recalling the previous example on the ACS, the engine bleed flow pressure was 100 psi, yet the ACS only required 40 psia to provide sufficient cooling. The PRV was used to regulate the bleed pressure down from 100 to 40 psia. In essence 70% of the work that was performed on the bleed air was wasted. In the All-Electric architecture CAC outlet temperature at sea level static, standard day would be:

$$T_{o1} = T_{oa}\left\{1 + \frac{1}{\eta_{CAC}}\left[r^{\frac{\gamma-1}{\gamma}} - 1\right]\right\} = 265°\text{F} \tag{2.3}$$

Where T_{oa} is the standard ambient temperature (59°F), η_{CAC} is the CAC adiabatic efficiency, typically between 75 – 85%, and r is the CAC pressure ratio. One can immediately see the temperature is much cooler than what the main engine can provide in the form of customer bleed even though the compressor is far less efficient. This mechanism provides the largest amount of savings when switching from customer bleed to the All-Electric architecture. Other savings come from weight reductions associated with the removal of the pre-cooler, air valves (FAV, LPCV, HPSOV & PRV, see Figure 2.2 to 2.8) and ducting from APU and engine to fairing.

One drawback accompanying this architecture is the additional inlet scoop needed to bring in fresh air for the CAC inlet. This scoop imparts an additional source of ram drag for the aircraft that was not present in the conventional architectures. This drag can be quantified as a function of the flow as demonstrated by the equation:

$$D_{Ram} = \frac{\dot{m}_{ECS}V_a}{g} \tag{2.4}$$

where $\dot{m}$ is the fresh air mass flow rate and V_a is the aircraft velocity.

In large commercial planes, the sensitivity on drag can be much more detrimental to fuel burn than weight due to high C_L/C_D ratios[46]. For example, a 200 pound compressor and electrical motor assembly have a much lower impact on fuel burn than an additional scoop with 120 ppm of fresh air flow. Yet this additional penalty is overcome by the decrease in fuel burn observed when moving away from engine customer bleed. This architecture is similar to what is found in the modern commercial aircraft, which estimates savings of approximately 3% by moving to a more electric aircraft[11].

When comparing weights between the conventional system and the All-Electric ECS, there is no clear winner that applies to all applications. While moving to an All-Electric might save weight from the large amount of high pressure ducting that is not necessary, weight is gained back by adding the CAC and the associated electrical motor and controller. The electrical power system weight will also increase to account for the addition power demands of the ECS, which can be quite substantial. For example, legacy aircraft typically had generator capability reaching the 100's of kilowatt range, while the power generation capability for a more electric aircraft increased by an order of magnitude to the megawatt range. Large increases in power demands have serious implications on the preliminary design of the engines. While bleed has to be accounted when designing a high pressure compressor, generally more bleed is beneficial for surge margin. Bleed increases the amount of flow in the compressor and pushes the operating point away from surge. On the other hand, power extraction tends to reduce the operating line surge margin and thus can be very harmful to engine operation if not taken to account in the design process. As aircraft manufacturers

diverge in their preference between bleed based and MEA architectures it is becoming increasingly hard for engine manufacturers to offer the same engine core for different platforms while maximizing SFC. For example, a new aircraft engine was designed with the intent of having the same core for various platforms, but substantial modifications had to be made on the gas generator to account for a the lower bleed and increase torque extraction demands of a MEA aircraft[36].

3 Hybrid ECS Approach

Up to this point the discussion has centered on the state of the art ECS architectures flying today. This background was needed to understand the use and operation of modern packs. From current and new products that will be introduced by major aircraft manufacturer, one can get the sense that there is a divide between the use of fully pneumatic systems and switching to the more novel all electric[37]. In this section a common ground will be found in the hybrid approach between the legacy and new systems. The basis for this architecture is that the aircraft enine has the most efficient compressor onboard an aircraft. Being this the case, then why not tap into available bleed from the engine and use some aspects of the electric architecture to augment the traditional ECS? In order to measure the feasibility of this new architecture there are several items that need be considered.

In this chapter the various modes of operation for a hybrid architecture will be assessed to ensure the design is capable of supporting any commercial aircraft mission. Also, a discussion will be presented on the impact this approach would have on life

cycle cost and mean time between failure (MTBF) in comparison to architectures flying today.

3.1 Description & Benefits of Hybrid Solution

To get a better understanding of the proposed hybrid ECS architecture, it is shown schematically in Figure 3.1. It would have the most modern ACS with a cabin air compressor (CAC), but in this case there is no additional inlet scoop for fresh air. Bleed air from an engine low pressure port would now feed the CAC, which boosts pressure to ECS requirements.

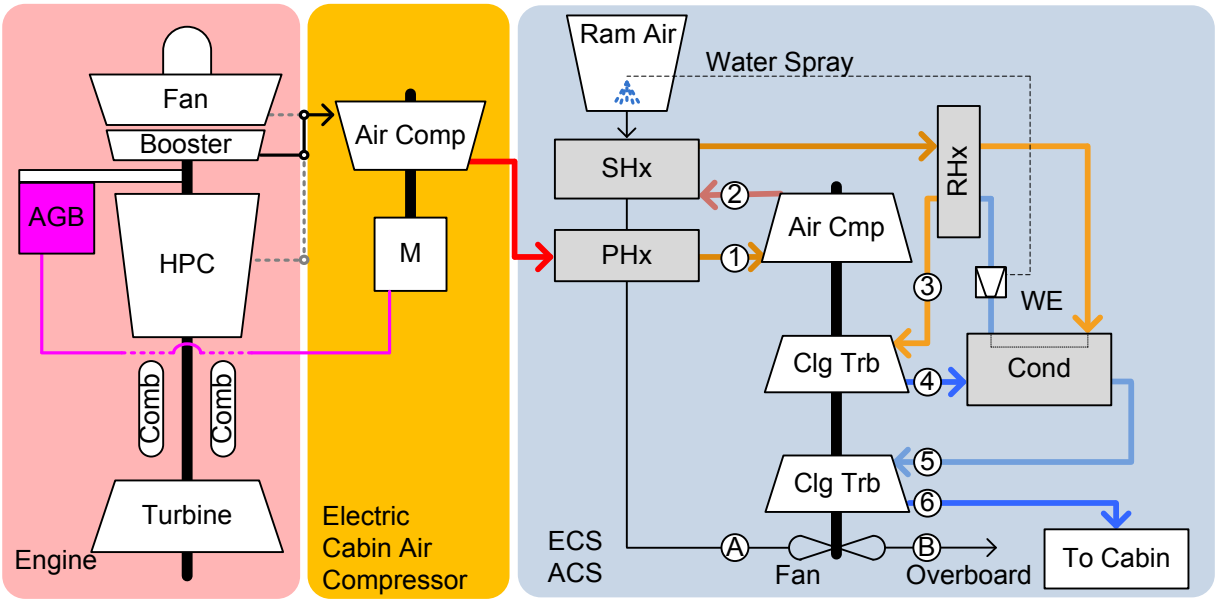

Figure 3.1: Hybrid Electric ECS Scheme

Recalling the discussion on the All-Electric ECS, the fresh air inlet scoop represents a substantial loss on the system. In the hybrid architecture, the system benefits from the engine's high efficiency inlet diffuser and turbo-machinery to boost inlet air. This eliminates the drag count associated with the fresh air scoop and results

in less power being drawn for the CAC during cruise. Although the hybrid ECS will impact engine performance, it will not be as severe as the fully pneumatic systems because the CAC can raise the pressure from a low, less expensive pressure port. The hybrid ECS uses a combination of the two energy extraction methods to provide a true on-demand system that minimizes exergy destruction. The goal is to target a balance between torque and bleed extraction from the engine.

From Figure 3.1, it can be seen that there are various ways this architecture could be setup, at the engine/CAC interface. The CAC can receive supercharged air from the fan discharge, the booster, or a mid-stage HPC location, see Figure 1.2. For this study it was determined that each engine bleed port represents a different architecture. It would be rather complex to have one system choose between the different stages of the compression system. The added weight of valves and ducting needed to accommodate all the different pressures would make it impractical based on the assumptions laid out for this work. For this reason three hybrid architectures will be considered, each one consisting of one bleed port in conjunctions with a CAC to provide fresh air for the cabin.

In order to study the merits of these architectures, a full Engine/ECS model will have to be generated of the hybrid, conventional - pneumatic, and the All-Electric ECS systems. The conventional architecture will be the baseline or control for comparison to estimate the fuel savings against legacy systems. Also, the All-Electric ECS will have to be modeled to determine if the hybrid approach offers a benefit in comparison. In the next section the general assumptions that will be made for such a model will be discussed.

3.2 Integrated Study Approach

Herein the hybrid solution will be studied as a way to improve the operational efficiency of an ECS system, while resulting in minimal impacts on drag and weight. Parasitic drag impacts will be approximated with equation (2.4), for the ram air needed as a heat sink for the PHx, and SHx. Additionally, there will be a drag penalty for the All-Electric architecture inlet diffuser that collects the cabin's fresh air supply. Aside from these effects, the study will assume the aircraft's outer geometry to be constant for all architectures. This assumption implies that all the components for the ECS will fit either on the fairing of the aircraft or within the engine nacelle or pylon structure. Along with this, it should be noted that this study will not include all the details regarding weight differences between the hybrid and other architectures. For a study to include complete effects on aircraft structure and weight, one would need a three or six degree of freedom aircraft performance model. Alternatively, the study could be conducted with industry sensitivity data for fuel consumption impact or coefficient of lift to drag (C_L/C_D) ratio. However this data is rarely found in literature because it is highly protected by aircraft manufacturers.

Although these assumptions would influence the results of this analysis, it can be concluded that the impact would be relatively small. First, from industry published data[29], commercial airliners have very high C_L/C_D ratio averaging ~12 at cruise. With cruise representing the main segment of interest, small differences in weight are not expected to be significant discriminators for the different architectures. Secondly, if there were any major impacts relative to weight and volume they would likely equally influence both the All-Electric as well as the hybrid architecture. Hence, this approach

is acceptable for a comparative study to determine if one demonstrates an improvement over the other,.

The high fidelity components needed to assess the benefits of each architecture reside on the ACS and propulsion system performance model, as well as their interactions. These components are essential because each system produces boundary conditions for the other, at the operating point. For example, the bleed flow temperature entering the ACS changes, impacts the pressure that is required to run the ACM. This in turn affects the engine because less/more power (or torque extraction) will be required to drive the CAC. In addition changes in torque extraction can have an impact on the bleed temperatures and pressures that are being supplied to the ACS. These iterations must go back and forth until a steady state solution is found that represents the total system cost, which in this study is the SFC.

3.3 Modes of Operation

In this section three main operating modes of an ECS will be presented, ground idle, flight operation, and cold day control. It is important to examine each to ascertain their feasibility on a hybrid system even though they were not modeled as part of this study. There are a few rudimentary factors that influence the ECS modes at an overall system level. Modes are set by engine state (on or off), whether the aircraft is on ground idle or in flight and the temperature day (varying from hot to cold). Each of the aforementioned modes presents a challenge for the ECS.

3.3.1 Ground Idle

As many people have experienced, commercial and regional aircraft spend a significant portion of time on the ground, idling. Reasons vary from waiting on passengers or cargo to be brought onboard to servicing ground maintenance issues. Whatever the case may be, the aircraft must be maintained at a comfortable temperature for its passengers and crew. Although the main engines could be on for ground idle, many airlines prefer to turn off all engines and rely on the APU to conserve fuel.

For most wing-mounted-engine aircraft, the APU is located at the tail to provide a good counter weight to the engines. For the hybrid solution to be viable, the dependence on APU to provide pneumatic air has to be eliminated and replaced by electric compressors. This has two benefits, first it eliminates the need for heavy ducting to route bleed air from the rear of the aircraft to the fearing, and secondly, the APU reliability can be substantially improved, up to five times, by going to an All-Electric unit[30]. This means that the cabin air compressor will be responsible for providing all necessary pressure and flow on the ground while the engines are off.

This has two implications that impact the hybrid architecture hardware implementation. First, the compressor needs to be of the same size as the All-Electric architecture discussed previously. As a result there would not be a substantial weight savings between the two options with regards to the compressor assembly and electrical power system. If anything, the hybrid might be heavier to account for ducting from the engine to the fairing. Second, since the aircraft engines would be off to conserve fuel, the surface friction through the ducting from the pylon to the fairing

results in a substantial pressure loss. This would require an oversized compressor to account for the additional pressure drop of 1 to 2 psia. For the hybrid architecture to be viable, an inlet scoop at the fairing would have to open on ground idle to allow for fresh air inlet. This scoop would be closed as soon as the engines are started and would not have a significant drag impact at cruise.

3.3.2 Flight Operation

In flight, the hybrid architecture would operate much like it does during taxi and takeoff, Figure 3.1. The aircraft engine would provide the sufficient pressure boost to supercharge the CAC and allow for it to operate at a lower energy state, when compared to the all-electric. Two hybrid architectures are studied here, one that uses fan bleed air as the fresh air source and the second uses booster bleed air. Although both architectures are expected to present savings over the conventional and All-Electric architectures, the fan bleed air would be more susceptible to engine operating conditions than the booster bleed because of the way turbofan engines operate. The maximum pressure ratio of the fan is approximately 1.5 and it is dependent on the engine operating state. If the engine is at high or part power during Takeoff, Climb, or Cruise the fan pressure ratio will be enough to provide plenty of pressure for the CAC. Yet at low power conditions one would need to examine closely the interaction between the fan bleed and the CAC requirements. This is mainly a problem at top of descend, where the engines are spooled down to flight idle for the descent phase. At these conditions the engine fan pressure ratio is so low that the CAC can experience a higher power setting than its All-Electric counterpart. Fortunately, top of descent is also the most benign mission point as far as heat loads are concerned since the aircraft would

have been substantially cooled throughout the flight and electronic loads are at low settings in the descent phase. More in depth study of this flight segment must be done in order to determine if the CAC design point is shifted to accommodate these conditions in the hybrid system.

3.3.3 Cold Day Conditions

In a cold day, where ground temperatures can be as low as -60°F[32], the ECS functions substantially different. In this scenario the system must to provide warm air for cabin heating. In conventional systems this is not a problem, as hot air is readily available from the engine or APU at all times. For the All-Electric and hybrid architectures, providing hot air is a challenge, especially during flight where temperatures drop to -90°F[32]. Figure 3.2 displays a likely configuration for cold day operation.

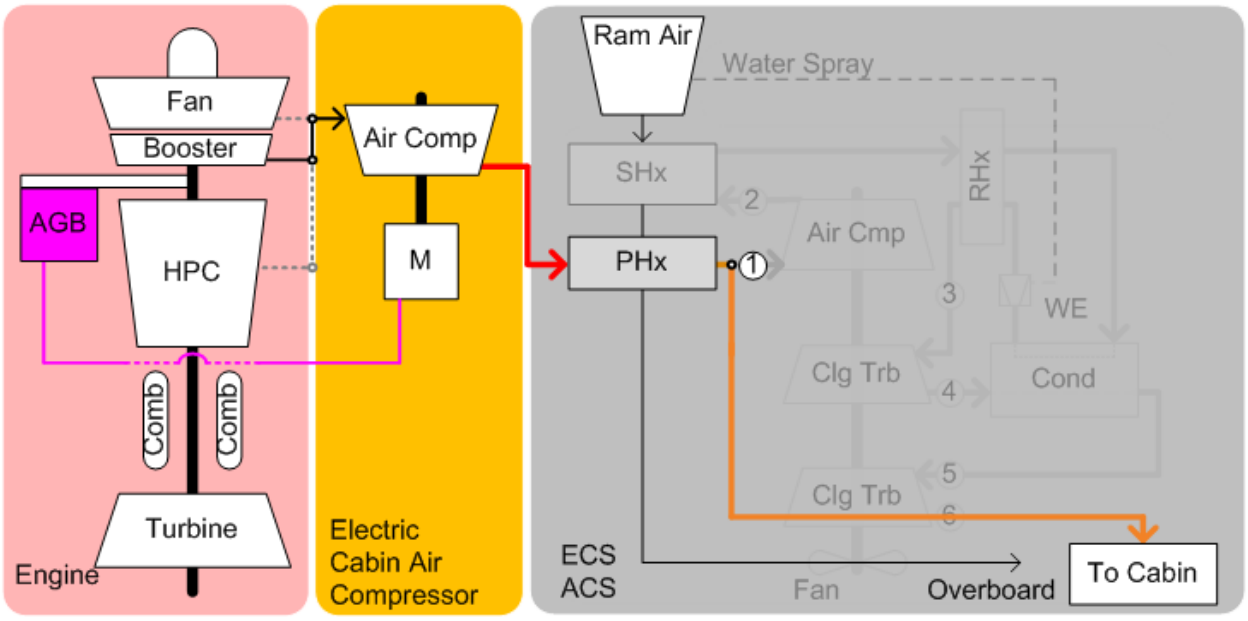

Figure 3.2: ECS Cold Day Operation

Notice that the air cycle machine is completely bypassed, since no cooling is required. In this case the compressor is used at high power to produce warm air for the cabin. If air is hotter than required, the PHx can be used to cool the fresh air stream during flight. If no cooling is required the ram air stream can be controlled though the actuation of the exit or inlet doors[33]. In some cases the CAC might be producing more than the required cabin pressure just to generate enough heat in the system. One way to avoid running the compressor at high power is by installing an electric heater that can provide the required duty more efficiently. This could be accomplished with a resistor element heater that can be added to the ACS bypass duct.

Although cold day operation is important for any ECS architecture, it will not be the focus of this work. The task of optimizing cold day operation would need to be performed as a separate study and compared to conventional systems. It is sufficient for our discussion to state that cold day operation can be accomplished with the hybrid system either by using the CAC to generate hot air or by using an inline electric heater to provide the needed heat.

3.4 Architecture Life Cycle Cost

Going to a more electric aircraft presents substantial improvements, not just in efficiency but also in weight, particularly in the aircraft electrical system. For example, by going from a standard 115 VAC to a 270VDC more power can be transmitted more efficiently. This translates into smaller wires through the aircraft, which reduce the EPS weight significantly. The Auxiliary Power Unit (APU is another system that is greatly impacted by going all electric. A traditional APU needs to provide both pneumatic and

electric power to the aircraft. This would require a machine with an oversized compressor and a gear box to run the various generators. In an All-Electric architecture the APU would only provide electricity. This would allow the machine to be specifically sized for power generation. As a consequence, the generators can be directly integrated onto the gas generator shaft, thus completely eliminating the gear box. This reduces the machine's maintenance significantly and allows it to stay on wing longer[36]. Even if the generator(s) are still operated by use of a gearbox, just by removing all the pneumatic components, the reliability and maintainability of the APU increase by 4 to 5 fold[11][30].

ECS systems must have a substantial mean time between failures (MTBF) in order to be reliable systems that operate for the entire service life of an aircraft, many as long as 30 years. With the advent of foil gas bearing in the 1960s, modern air cycle machines observe an MTBF of up to 100,000 hours[13]. The first commercial application was introduced in 1969 on the DC-10 ECS. In fact, the 4-wheel ACM produced for the 777 surpassed an endurance test of 36,000 cycles that simulated its 30 year service life. It is this type of machine that would be used in the hybrid architecture presented herein.

For the All-Electric and hybrid systems, the cabin air compressor (CAC) is one additional component needed in the ECS. The main impact to life cycle cost from this component is the high power electronics needed for operation. Using the hybrid car industry as a benchmark, the average cost of a CAC driver, ~100kW electric motor is only in the order to $1800 with prices falling exponentially as production rates ramp up[39]. The compressor assembly itself is expected to have similar life to the air cycle

turbo-machinery. The compressor housing and impeller are constructed using existing technology and the device would run on air bearing ensuring a long service life. The electric motor and controller needed to run the compressor are constructed with relatively newer technology. The reasoning to switch between a pneumatic bleed and an electric system has been debated by many in literature, but one thing is clear, Some aircraft manufacturers appears to believes that all electric is the future of aviation[10][11]. One of the strongest arguments in favor of all electric systems is the development trend for performance and cost. Pneumatic system performance improvement trends have been constant since 1995, according to Dornheim[35]. This is a sharp contrast to power electronics, which have a very steep curve of performance improvement. Motors & drives are becoming smaller, lighter and more reliable, for example a major electrical power system manufacturer had developed a 250 kva generator that weighs only 200 lbs. and is reliable enough to be used as the aircraft engine starter[35].

It has been shown by many accounts that going all electric is better for reliability, performance and in some cases weight. This trend is expected to increase as high power electronics such as Silicon Carbide reach maturity in the field. These benefits clearly demonstrate that a hybrid architecture would indeed possess the same or better life cycle costs when compared to a fully pneumatic, conventional, system.

3.5 ECS Transient Operation

In many fields of engineering it is essential to study the transient, or time dependent, behavior of a system. A transient model depicts all the time dependent effects of a system and can be constructed from 1-D to 3-D approximations, by

including the appropriate time dependent derivatives. These effects help validate a design before going into operation and are instrumental in the creation of control algorithms. In order to construct a robust control system, the approximate cycle response time must be understood to set the correct gains and responses on the controller. In an ECS system a transient model can help predict and protect against surge of a compressor or explain variation in heat transfer due to thermal and mechanical lags in the various components. In the following section the major components that contribute to transient behavior will be discussed. Additionally it will be shown that for the trade study analysis presented in this work, a transient model is not required due to the nature of commercial aviation missions.

For modeling of a thermal system such as the ECS, there are five major components that contribute to transient effects. These are: rotor inertia, thermal heat soak of components, valve response lags, sensor uncertainty and volume dynamics. Combined these systems account for the time dependent effects of the AMS and ACS. Rotor mass moment of inertia is the resistance to rotational acceleration about a fixed axis. In the case of the ACS, inertia creates a time lag on ACM shaft due to the mass of turbo machinery. This is not a critical component in a transient model as ACM turbo machinery is typically not very massive. The next transient effect is thermal heat soaks which refers to the transient conduction on the various heat exchanger surfaces and machinery. As the ACS goes from one state of refrigeration to another, thermal gradients arise as the system attempts to reach a new thermal equilibrium. The integral form of Fourier's Law of thermal conduction can be used to estimate the effects of thermal heat soak as follows:

$$\frac{\partial Q}{\partial t} = -\mathrm{k}\oint_s \vec{\nabla} T \cdot \overrightarrow{dA} \tag{3.1}$$

Where $\frac{\partial Q}{\partial t}$ is the heat transfer rate with units of power, k is the thermal conductivity of the material and $\overrightarrow{dA}$ is the heat transfer surface element. The next transient effects are the lags associated with real valves. In a steady state model valves operate instantaneously. Yet in a real systems, as the cycle moves from one point to another there is a maximum rate of change for each particular valve. These effects become important as the system responds to the various loads encountered during flight. Depending on the construction and complexity of the valve, e.g. pneumatic, hydraulic or electrically actuated, valves can be designed to have a fast response time, but fall short of being instantaneous. For modeling purposes a simple rate limiter can be used to control the movement of valve position. The rate limiter constant can be obtained from the particular valve supplier. Another transient effect that is very important for control mechanisms is the sensor uncertainty because data readings will vary with time. This refers to the accuracy of sensors used to detect temperatures, pressures and flows through the ECS system at a given moment. Lastly, one of the most important effects on transient operation is the volume dynamics. This refers to sudden changes in volumetric flow that result in pressure waves through the system. In fluid dynamics this is commonly referred to as 'fluid hammer'. This type of effect can lead to many hazardous conditions such as compressor surge or rotor imbalance. If not well understood and controlled, these effects could potentially damage the ECS system. With the transient factors laid out, it is easy to get a sense of how important it is to understand a system's transient behavior before carrying out a detailed design and construction of an ECS system. To understand why transient modeling was not

performed to ascertain the merits of a hybrid architecture, let's take a look at the way air conditioning packs operate in commercial and transport missions.

Revenue share and transport missions are relatively benign and tend to consist of a similar altitude and Mach number profile such as the one depicted on Figure 3.3.

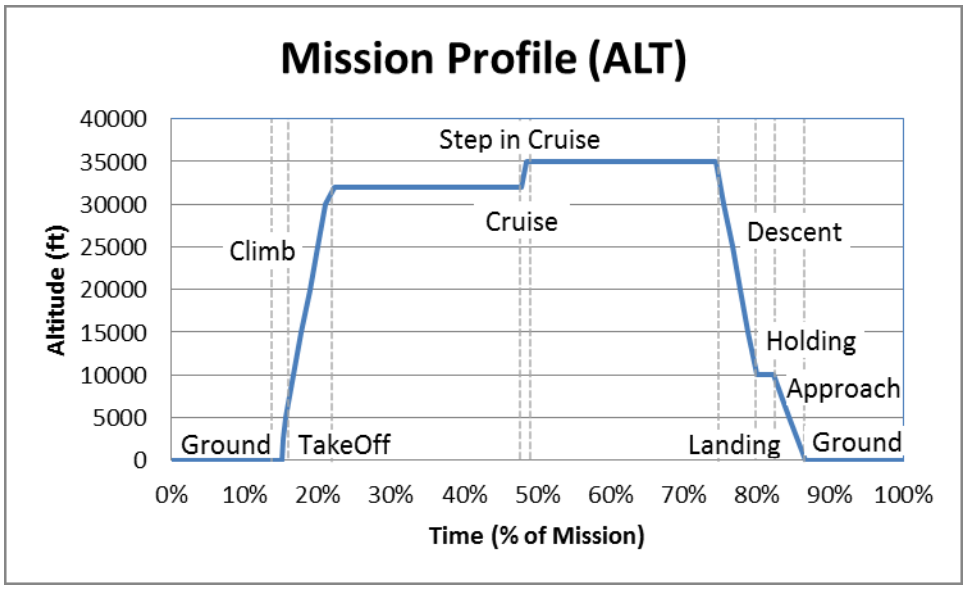

Figure 3.3: Typical Commercial Mission Profile

Typically these missions consist of ten distinct events normal to all carriers:

1) Ground Segment
2) Takeoff
3) Climb
4) Cruise
5) Step in Cruise
6) Descent
7) Descent hold
8) Approach
9) Landing.
10) Post Flight Ground Segment

It is immediately apparent that for large segments of the mission the altitude and Mach number are not changing significantly, i.e. cruise. Cruise represents more than 50% of the flight, where air conditioning packs do not see a significant change in cooling duty. It is this segment that will be used to perform architecture trade study because it also represents the largest portion of most commercial aviation flights. This being said, it would not be worthwhile for this analysis to model the transient behavior of the ECS system when the trade study will be conducted on a portion of the flight that experiences very little transients. It should be noted that the full mission will be run as a series of steady state points, thus approximating an entire commercial flight.

From Figure 3.3 it appears as if the ground segment represents a significant portion of the mission as well. In fact most carriers turn on the aircraft engines just a few minutes before takeoff and turn them off shortly after landing, relying either on APU or ground power for onboard systems. For this reason the ECS is not optimized for ground idle, yet it must be designed to handle the demands of a hot day.

From commercial aviation mission analysis it was shown that to study the merits of a hybrid architecture the modeling details of the time dependent effects do not necessarily have to be fully captured. If the architecture were to be tested, to improve the technology readiness level, then a full transient model would likely be constructed to implement the design and control of the system. Some of the major aspects of transient operation are discussed in the following section.

3.6 Hybrid Architecture Trade Study

An architecture trade study is developed by building physics based models of the individual subsystems that can accurately represent their design and off-design performance. Once the individual models are verified, they are linked together in a common integration framework, built on NPSS. With an integrated model one can capture the components interactions. It is important to note that for this case study all models developed are steady-state in nature. This being said, for typical commercial missions, most of these systems operate in steady state due to the extended duration of each flight segment (e.g. Ground Idle, Climb, Cruise, etc.).

The trade study to be outlined includes two cost functions for the discrete architectures being studied. The first and most important is the engine SFC, which is affected by any change in the engine's operating state. The second parameter is the amount of airflow entering the ram scoops, as shown in Figure 2.13, used by the ACS. This parameter impacts the amount of ram drag imparted by each system and is directly correlated to SFC because the aircraft engine has to compensate for the added drag.

Lastly since the main purpose of this study is to gain insight into the benefits of this new hybrid architecture, it is desirable to maximize the performance of an ECS system by understanding the way subsystems interact with the engine. Finally, real benefits can be achieved by having the capability of putting together complex integrated models at the preliminary design stage and allowing for a trade study of the various architectures considered.

3.6.1 Hybrid Fan Bleed ECS Architecture

The first ECS architecture to be presented is the Hybrid Fan Bleed (HFB), shown schematically in Figure 3.4. This setup utilizes an electric compressor much like the All-Electric architecture, Figure 2.13, yet fresh airflow is turbo charged by engine fan air. This allows the CAC to utilize less electric power at cruise by bleeding a small percentage of partially compressed air from the fan flow.

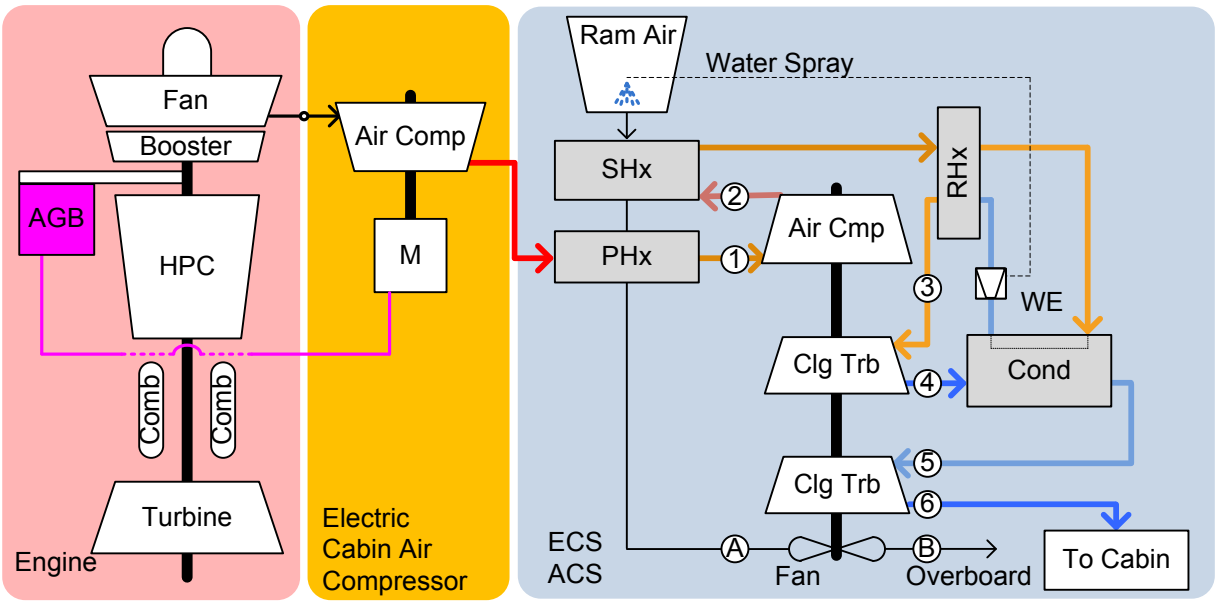

Figure 3.4: Hybrid Fan Bleed ECS

Looking at Figure 2.1, one can see that the partially compressed air from the fan has to be piped along the wing to the ECS bay, where the electric compressor is assumed to reside. This produces a slight pressure drop in the system, especially at low engine power conditions such as ground idle and descent. At this power condition the engine fan pressure ratio is very close to one, so any slight pressure drop in the system can be significant. In order to alleviate this problem the next architecture is introduced that provides a few percent of engine booster flow.

3.6.2 Hybrid Booster Bleed ECS Architecture

The second architecture to be traded upon is the Hybrid Booster Bleed (HBB), shown schematically in Figure 3.5. This architecture benefits from using engine booster bleed air as a means to super charge the electric cabin air compressor. The higher pressure ratio results in a reduction in electric power extraction at cruise, but when compared to the HFB system, this one uses more expensive engine bleed. It will be interesting to see how this trade in air bleed vs. power extraction affects engine performance and thus fuel burn.

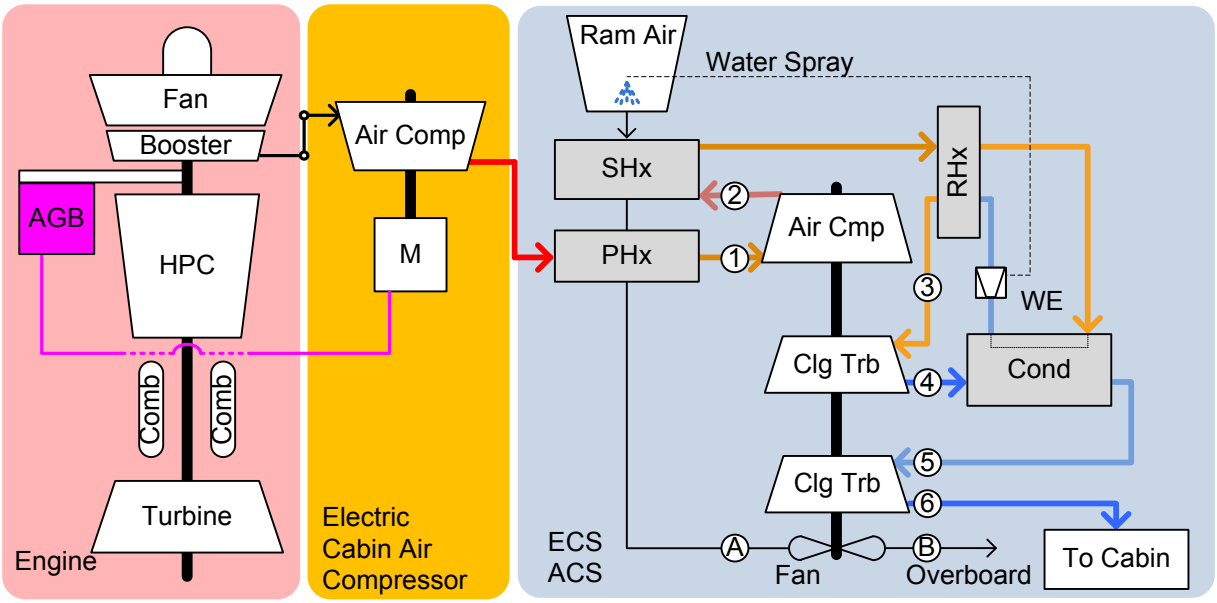

Figure 3.5: Hybrid Booster Bleed ECS

There is an additional architecture that is worth considering for completeness. In addition to the HFB and HBB main architectures, the Hybrid Mid Stage Bleed ECS is examined and compared to the baseline Conventional/Pneumatic Architecture (CPA), and the All-Electric Architecture (AEA).

3.6.3 Hybrid Mid-Stage Bleed ECS Architecture

The last hybrid ECS to be presented in this work is the Mid-Stage Hybrid Architecture (MHA), Figure 3.6. This architecture is somewhat more complex than the HFB and HBB systems previously discussed. In this case, the ECS uses mid-stage high pressure compressor bleed. Since this air is too hot to flow along the wing in some portions of the mission, such as takeoff. This scheme requires a PHx to maintain air below 410°F as discussed in Section 2.1. Additionally, this mid stage bleed port could potentially have the required, or excess, pressure for the ACS at cruise, hence a pressure regulator valve is needed to avoid over pressurizing the system.

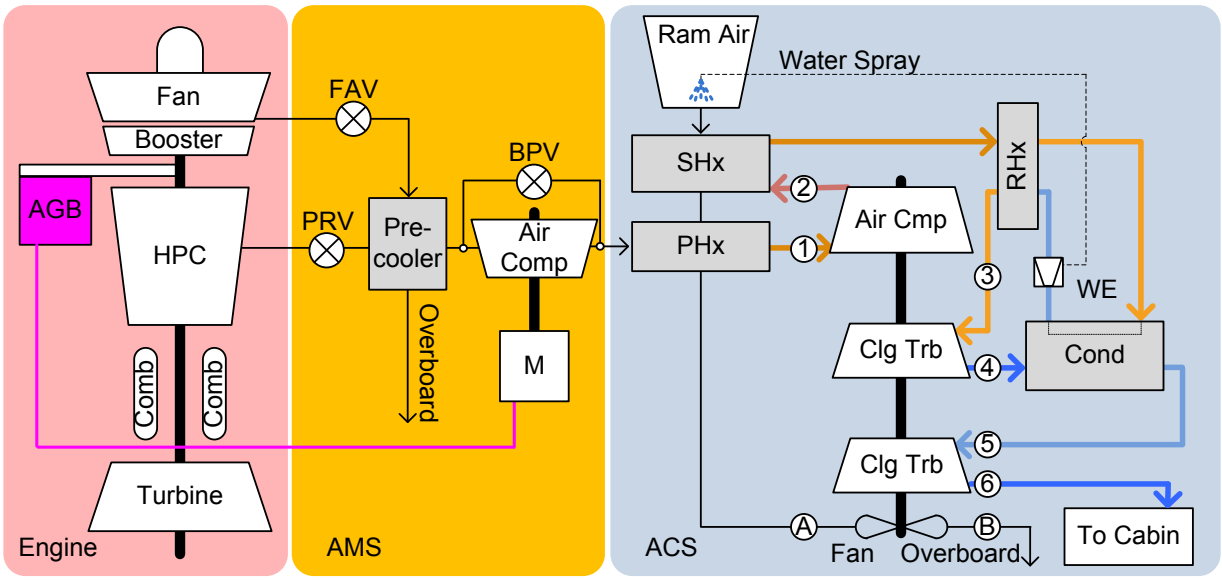

Figure 3.6: Hybrid Mid-Stage Bleed ECS

Refering to Figure 3.6, a compressor bypass duct would be needed with an additional bypass valve (BPV) to circumvent the CAC when there is enough pressure at the mid-stage port. The additional weight and volume have to be accounted for when considering this architecture. The advantage of this system is that it would work well for

aircraft manufacturer that want to replace legacy aircraft with hotter cores engines. The CAC in that case could boost the customer bleed pressure and alleviate design requirements on the engine that are detrimental to performance.

In the next chapter the techniques used and model fidelity level of each component are discussed. The discussion includes the assumptions for each component model, the integration framework developed, the boundary conditions used, and the requirements for each mission point.

4 Aircraft Subsystem Modeling Methodology

An architecture trade study is developed by building physics based models of individual subsystems that represent their design and off-design performance with sufficient fidelity. Once verified, the individual models are linked together in a common integration framework, which in this case was built on NPSS. With this toolset one can begin to evaluate the model to model interactions of the entire system. In Chapter 3 the importance of transient effects were laid out in detail. Nevertheless, it was concluded that, for this system trade study, the short time dependent interactions do not play a significant role. This is because the longest segment of a commercial mission consists of cruise, where the subsystems studied herein all reach steady state. The subsystems considered in this work are discussed in this chapter. Additionally, the methods used to model the aircraft subsystems, including important assumptions are outlined. The developed modeling platform and the integration framework put together to combine the different subsystem in this system of systems are discussed first.

4.1 Modeling Framework

To remain competitive in the market, engine designers try to reach higher levels of thermal efficiency by increasing core temperatures and higher bypass ratios to improve propulsive efficiency. These design decisions drive hotter operational temperatures in the HPC and smaller core mass flow. Although good for fuel consumptions, the advances in turbomachinery have adversely impacted some of the aircraft subsystems that interact with the engine. If not studied early in the design process, these interactions might drive the engine to operate far from its optimal setting. For this reason, an integration framework linking various independent models in a runtime environment, shown schematically in Figure 4.1, is developed. This design tool is used at the preliminary design stage to achieve a higher level of product efficiency.

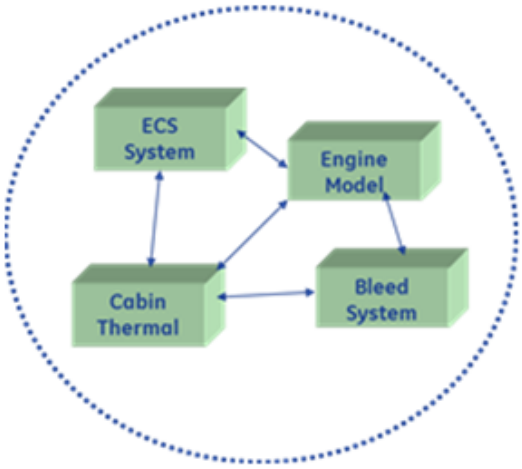

Figure 4.1: NPSS Integration Framework

The integration framework relies heavily on the Numerical Propulsion System Simulation (NPSS), a programming language developed in an aerospace industry initiative led by NASA Glenn Research Center[48]. The goal of the NPSS developers was to create a versatile aero-thermo modeling tool that the entire global aerospace

community would share. The object oriented language, NPSS, is used to model physical interactions between the components of a complex system. Due to the flexible nature of NPSS, the concept-to-production time can be reduced by running steady state analysis and off-design transient performance predictions on various architectures. NPSS has been utilized successfully as an engine design and analysis tool by various propulsion manufacturers, thus its immense capability can now be leveraged to model other aircraft subsystems.

For example, engine manufactures have been modeling in NPSS since 1996, building the first full native model in June of 2001[23]. Today all engine cycle decks are developed exclusively in NPSS, using common components that are tailored to the specific needs of each application. Building upon this vast experience the ECS architecture simulations were built using components with proven algorithms that have been implemented in production aircraft engines. This resulted in a robust model that can be tailored to a specific application and fully integrated with other components at an air vehicle level.

In this chapter, the aircraft components modeled and integrated in this preliminary design trade study are discussed in more detail. The subsystems included in the integrated framework are the Cabin thermal loads, ACS, AMS and Engine for a single aisle, 80 passenger (pax) plane with wing mounted engines. Since an aircraft aerodynamic performance simulation was not available, thrust requirements for a mission run was obtained from scaled tables found in literature[42]. Added drag penalties associated with increase in nacelle or fairing size and additional weight were assumed to be negligible due to the similar nature of the architectures traded.

4.2 Cabin Thermal Model

Various sources of heat are imparted upon the aircraft's cabin, which have to be mitigated through the ECS. In this section an approximation is made to substantiate the total heat load (duty) of the ECS that is used in this trade study. Three main heat sources are fundamental to this heat transfer problem, namely: internal heat generation, solar radiation, and kinetic heating through conduction/convection across the aircraft skin, see Figure 4.2.

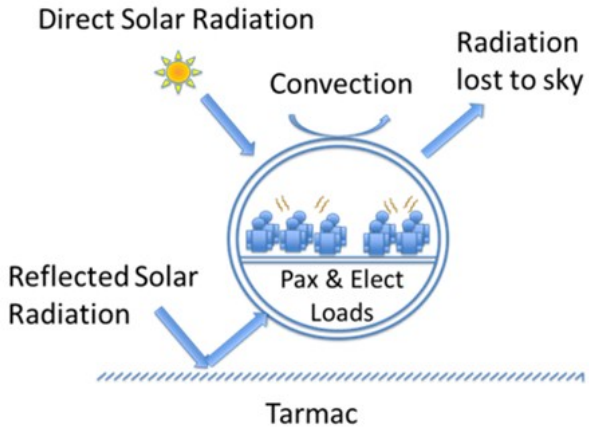

Figure 4.2: Sources of heat present in a commercial aircraft cabin

4.2.1 Internal Heat Generation

The main sources of heat within an aircraft are the electronics and the passengers plus crew members. Although the aircraft engine produces a substantial amount of heat, it is assumed that this heat is mitigated by the secondary flow circuit, fuel and lube systems within the engine. These effects are catalogued as a performance detriment on the engine cycle model itself. Heat generated by the flight surface actuators and motors is not considered directly as most of those systems are ambient/ram air cooled.

Electronic loads represent a big portion of the internal heat generated within the cabin. The main sources for heat generation are the inefficiencies in avionics and galley electronics within the aircraft. These can be lumped together into one bulk efficiency to account for all the losses in the electrical power system:

$$q_{elect} = \eta_{elect} \cdot \mathrm{Pwr}_{\mathrm{elect}} \tag{4.1}$$

Where q_{elect} is the heat load generated due to the bulk inefficiency, η_{elect}. The value of 85% was selected as a conservative bulk efficiency. The $\mathrm{Pwr}_{\mathrm{elect}}$ parameter is a function of the flight phase, and varies from the maximum value of bus power at takeoff, to a nominal value at cruise and a minimum at descent. As an approximation, the amount of power consumed by electronics can be estimated by using the total capacity of the engine mounted generator as follows:

$$Pwr_{elect} = \kappa_{segment} \cdot \mathrm{MaxPwr}_{\mathrm{gen}} \tag{4.2}$$

Where $\kappa_{segment}$ is a usage factor as a percent of MaxPwr_{gen}, the maximum capacity of a generator. The heat generated by the electronic power system during a particular flight segment can be approximated from the summation of Eq. 4.1 and 4.2.

For commercial aviation, passengers are the second major sources of heat within the cabin. Even when a person is at rest, he or she generates heat that has to be mitigated by the air conditioning pack. The ASHRAE standards[1] can be used to approximate the latent heat gain for the passenger and crew. For a person seated and doing very light work, such as in an aircraft cabin, the ASHRAE standard estimates an average of 120 watts per person. For an 80 passenger flight with 5 crew members this represents a constant heat load of approximately 10.2 kW.

4.2.2 Solar Radiation

The sun radiates vast amounts of energy towards the planet. Although in outer space the solar heat flux constant is Sc = 1367 W/m[2], part of that energy is absorbed and diffused by the various constituents of the atmosphere as it travels down to the ground. The main culprits are ozone and water vapor, which diffuse the solar radiation substantially. Therefore, solar irradiance is a function of altitude and will vary with the mission segment. As the aircraft climbs in altitude the irradiance increases exponentially, this is especially a problem in high altitude supersonic applications. For commercial transport applications, simplified expression for the solar irradiance can be derived from Beer's law as follows[3]:

$$q''_{solar} = S_e \, e^{(-a_\alpha \cdot H \cdot \sec(Z))} \cdot t_w^{(W \cdot \sec(Z))^q} \tag{4.3}$$

Where S_e is the solar intensity above the troposphere, a_α is the extinction coefficient, H is an equivalent height, Z is the zenith angle, t_w is the transmission coefficient of water vapor, W is the precipitable water vapor and q is a precipitation experimental constant as outlined by Majumdar et. al[3]. Using Eq. 4.3, the solar heat flux can be plotted as a function of altitude as seen in Figure 4.3. The figure shows a 15% increase in solar heat flux as the aircraft climbs from ground to its cruising altitude of 37,000 ft. The radiation heat transfer is the product of surface material absorptance (α), the total surface of the fuselage exposed to the radiation , and the solar irradiance. In most commercial aircrafts, the outer skin is bare aluminum with α = 0.09. The dimensions of various aircraft are readily available from sales brochures found in OEM websites. Typical 80 passenger aircraft dimension in such a brochure[40] were used in this study.

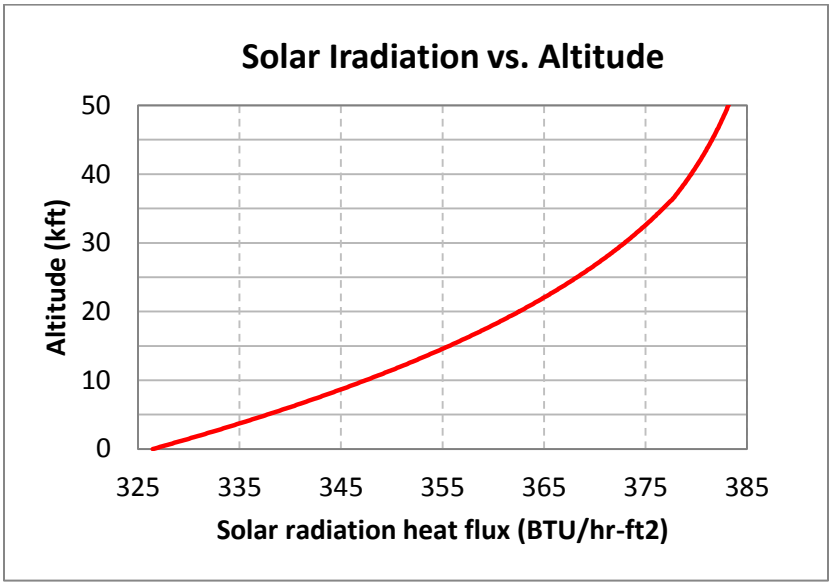

Figure 4.3: Solar Irradiation as a function of altitude

Radiation lost to the sky and ground can be accounted for by using the gray body approximation[2] with the appropriate sky and ground temperatures:

$$q''_{sky} = \epsilon\sigma\left[{T_{surface}}^4 - {T_{sky}}^4\right] \tag{4.4}$$

Where T_{sky} can be obtained as follows[2]:

$$T_{sky} = T_{amb}[0.711 + 0.0056T_{dp} + 7.3 \times 10^{-5}{T_{dp}}^2 + 0.013\cos\left({}^{2\pi t}/_{24}\right)]^{1/4} \tag{4.5}$$

Where T_{amb} is the local ambient temperature, T_{dp} is the dew point temperature, and t is the hours past midnight. For this correlation T_{sky} and T_{amb} are in Kelvin and T_{dp} is in degrees Celsius. Similarly the radiation lost to the ground can be given by:

$$q''_{gnd} = \epsilon\sigma\left[{T_{surface}}^4 - {T_{ground}}^4\right] \tag{4.6}$$

In both equations (4.4) and (4.6) σ is the Stefan-Boltzmann Constant and ε is the surface emittance. Using these three equations (4.3, 4.4, 4.6) the major components of radiation that influence cabin temperature can be calculated.

4.2.3 Heat Conduction through Fuselage

The aircraft's outer surface temperature is influenced by the environment through friction between air molecules and the outer skin. This forced convection can heat up the aircraft surface at high Mach and/or low altitude conditions. In more benign portions of the envelope it can actually cool the aircraft and reduce the internal refrigeration duty. The local heat flux due to convection, q''_{conv}, at the external surface of the fuselage can be expressed as follows:

$$q''_{conv} = \overline{h_L}\left[T_{surface} - T_{rec}\right] \tag{4.7}$$

The average convective heat transfer coefficient (HTC), $\overline{h_L}$, along the exterior surface of the aircraft can be obtained by using the average Nusselt number, $\overline{Nu_L}$, along the surface length of the fuselage as follows:

$$\overline{h} = \frac{\overline{Nu_L}\, k_f}{L} \tag{4.8}$$

The average Nusselt number is obtained using a flat plate turbulent boundary layer approximation[41][2]:

$$\overline{Nu_L} = 0.036 Re_L^{0.8} Pr^{\,0.6} \tag{4.9}$$

Where Re is the Reynolds number, based on the fuselage length:

$$Re_L = \frac{\rho\, U_\infty\, L}{\mu} \tag{4.10}$$

Using the local density, ρ, viscosity, μ, and the aircraft velocity, U_∞, for the length of the fuselage, L. The Prandlt number, Pr, used in Eq. 4.9 is defined as:

$$\mathrm{Pr} = \frac{\mathrm{Cp}\,\mu}{\mathrm{k_{air}}} \tag{4.11}$$

Where Cp is the specific heat and k is the thermal conductivity of the fluid.

As opposed to the adiabatic wall temperature, which would closely approximate the total temperature along the leading edge surfaces, most downstream surfaces experience what is termed the recovery air temperature[28]. Where the recovery air temperature, T_{rec}, can be approximated as[4]:

$$\frac{T_{rec}}{T_\infty} = 1 + \frac{1}{2} r_c (\gamma - 1) M^2, \quad r_c \approx Pr^{\frac{1}{2}} \tag{4.12}$$

The corresponding aircraft skin can experience harsh temperature conditions at high Mach numbers. As shown in Figure 4.4, Eq. 4.12 can be used to compute a contour plot of recovery air temperatures on a standard day.

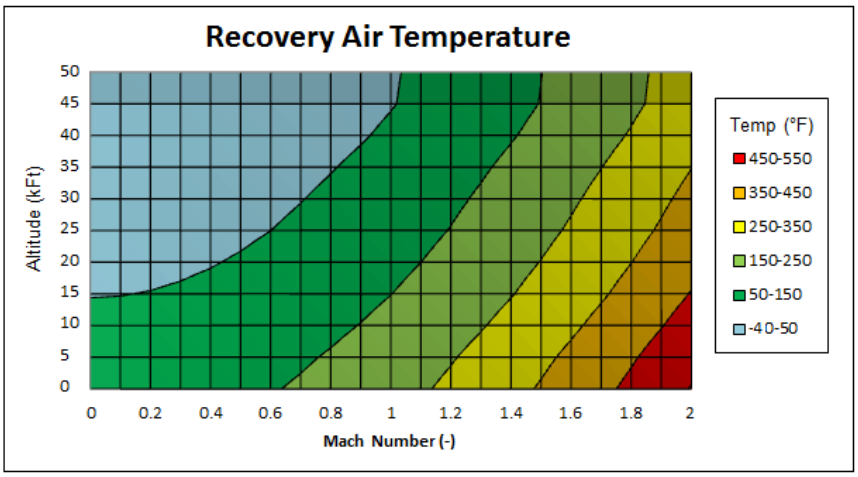

Figure 4.4: Hot Day Aircraft Recovery Air Temperature in Flight Envelope

A conservative approximation is used to evaluate the convective HTC by natural convection. When the aircraft is not moving on ground idle, the effects of natural convection can be simplified by assuming a small amount of flow to be induced over the skin surfaces and then applying Eq. 4.7 to obtain the appropriate heat flux.

On the inside of the cabin, convective heat transfer can be approximated using a similar method. This is due to the controlled air circulation patterns that are meant to maximize human comfort. A key feature of cabin recirculation is to avoid cross contamination between passenger rows and cabin classes. To accomplish this, fresh air is supplied by overhead diffusers and is vented at floor level. This pattern induces an up-down local flow minimizing row cross contamination. Additionally, in order to avoid draftiness, airflow has to be closely controlled. In a simplified cabin model the internal convective HTC can be calculated assuming an induced flow that does not exceed 10m/s inside the cabin. With this assumed velocity the internal heat transfer coefficient can be approximated from Eq. 4.7.

In order to calculate the heat transfer through the aircraft skin, from the interior cabin to the atmosphere, a conductive heat transfer analysis must be performed. A partitioned circuit of thermal resistances is formulated by approximating the fuselage wall to be composed of insulation foam and an aluminum layer as shown in Figure 4.5.

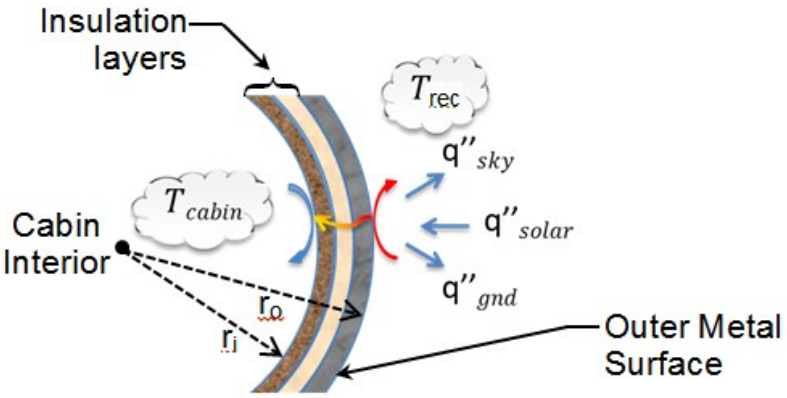

Figure 4.5: Insulation layers assumed for cabin wall

Where r_i is the internal radius or the fuselage and r_o is the external radius.

At this point all the thermal resistances can be calculated using equations (4.3, 4.4 and 4.7). To get the equivalent resistance from the inside of the cabin to the ambient conditions outside a thermal circuit is constructed about the aircraft's skin as shown on Figure 4.6:

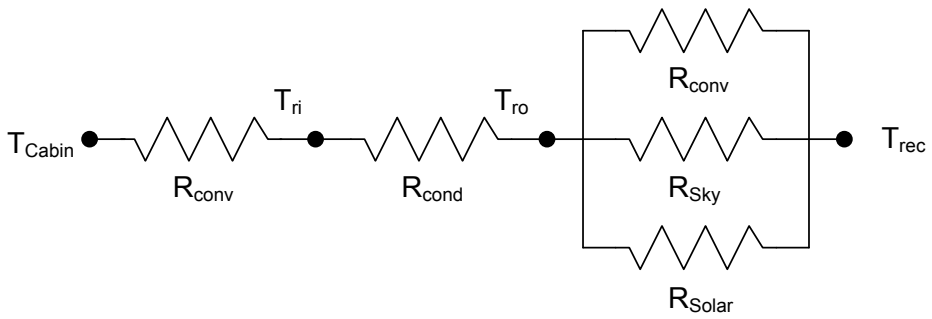

Figure 4.6: Equivalent thermal circuit diagram of heat transfer across skin

Referring to Figure 4.6 the equivalent resistance is:

$$\mathrm{R}_{equiv} = R_{\mathrm{conv}_{\mathrm{cabin}}} + R_{cond} + \frac{R_{conv}*R_{rad}*R_{solar}}{R_{conv}*R_{rad}*+R_{conv}*R_{solar}+R_{rad}*R_{solar}} \tag{4.13}$$

Therefore the heat flux per unit area of the cabin surface is given by:

$$q''_{cabin} = \frac{(T_{cabin}-T_{rec})}{R_{equiv}} \tag{4.14}$$

Eq. 4.14 is used to calculate the heat flux into the cabin at the various mission conditions within a commercial flight. Using the methods presented in this section, it can be seen that the heat transfer across the skin of the aircraft varies greatly from ground idle to cruise. At ground idle on a 20% hot day (104°F ambient temperature) q_{cabin} = 7.2kW, heating the cabin interior, whereas at cruise the load shifts to q_{cabin} = -5.2kW of cooling. Hence at cruise the heat transfer through the skin helps reduce the overall duty on the aircraft cabin. On a cold day the cabin might need some heating

rather than cooling because of the skin heat transfer. The full derivation of the cabin model with a sample calculation can be found in Appendix A.1.

4.3 ECS Modeling

As mentioned in Section 4.1, the modeling platform chosen for the ECS is NPSS, since many of the components needed for ECS simulation are already available as NPSS objects. Since the NPSS objects have been fully validated for production aircraft engines by the NPSS Consortium, this work will only introduce the components and their main features. The modeling assumptions and methods used for the Air Management System (AMS) and Air Cycle System (ACS) are discussed in the following sections.

4.3.1 AMS Modeling

The main components of the AMS were reduced to ducting, valves, heat exchanger and in the case of more electric architectures an electric compressor. The compressor will be discussed in more detailed with the ACS. It is important to note that the pressure drops resulting from bends, pipe couplings and fittings were not considered in this model because the specific details of a design are not public domain. This being said, the only duct that results in a significant pressure drop is the pipe carrying flow between the engine pylon and the fairing where the ECS packs reside. This pipe length was estimated at 10 ft from published wing span data found on an aircraft manufacturers site[40]. The duct diameter was chosen to obtain a reasonable pressure drop of less than half a psi in the system, with the pressure drop is given by:

$$\Delta P = 4c_f \frac{(\rho V^2 L)}{2D} \tag{4.15}$$

Where V is the flow velocity, D is the duct diameter and L is the pipe length. c_f is the friction coefficient approximated using the Karman-Nikuradse correlation for a turbulent flows as follow[41]:

$$c_f/_2 = 0.023\ Re_D{}^{-0.2} \tag{4.16}$$

For simplicity the valve models were chosen to simulate the fundamental physics behind a valve, without having the specific complexities of a particular arrangement. Therefore, system valves were approximated as a duct with an orifice, in which the flow rate changes with the pressure drop across the pipe.

The heat transferred through all heat exchangers (Hx) in the ECS models have been calculated using the ε - NTU method[4][6]. This is an industry standard for plate fin configurations, where NTU is the number of transfer units and ε is the effectiveness of the heat exchanger.

$$\epsilon = \frac{\mathrm{q}}{\mathrm{q}_{max}} = \frac{1 - \mathrm{e}^{-NTU\left(1 - C_{\min}/C_{max}\right)}}{1 - \left(\frac{C_{min}}{C_{max}}\right) e^{NTU(1 - C_{min}/C\_max)}} \tag{4.17}$$

Where C is the heat capacity of the cold and hot fluids (minimum and maximum) and the NTUs can be calculated from:

$$NTU = \frac{\mathrm{UA}}{\mathrm{Cmin}} \tag{4.18}$$

Where *A* is the total heat transfer area and *U* is the overall heat transfer coefficient for

the heat exchanger surface. This parameter is a function of the fin effectiveness, η_f, and an experimentally obtain Chilton–Colburn *J*-factor analogy[4][6] as demonstrated by Eq. 4.19:

$$U = \mathrm{J}\,\frac{\mathrm{C_p}\rho\,\mathrm{V}}{Pr^{\frac{2}{3}}}\left(1 - \frac{\mathrm{A_f}}{\mathrm{A}}\left(1 - \eta_f\right)\right) \tag{4.19}$$

Where A_f is the total fin surface area. The Chilton-Colburn factor can be found in textbooks such as by Kays and London[6] or Kakac and Liu[4] for various heat exchanger types.

The pressure drop for each stream, which is computed from its friction coefficient, Eq. 4.15, is critical for estimating the performance of an ECS system. Because of the complicated geometry of plate-fin heat exchangers, this coefficient is also obtained experimentally and provided in published sources[4][6].

Using Eq. 4.15 and 4.17 along with the corresponding J-Factor and friction coefficient, a heat exchanger can be sized to a given target effectiveness and pressure drop. Once sized, the heat exchanger off-design performance was approximated using the methods outlined references [4] and [6].

4.3.2 ACS Modeling

Figure 4.7 displays an NPSS representation of how all the components are linked together to model the ACS. One can take advantage of the object oriented nature of NPSS and recycle the same components developed for the AMS such as the ducts, valve and Hxs. The same concept applies for the turbomachinery found in the ACM.

Borrowing proven and validated algorithms from aircraft engines, the ACM was assembled using the following components:

Compressor

Turbine

Shaft

Nozzle

These components are linked together in NPSS in order to satisfy continuity in all streams of the system, as shown schematically in Figure 4.7.

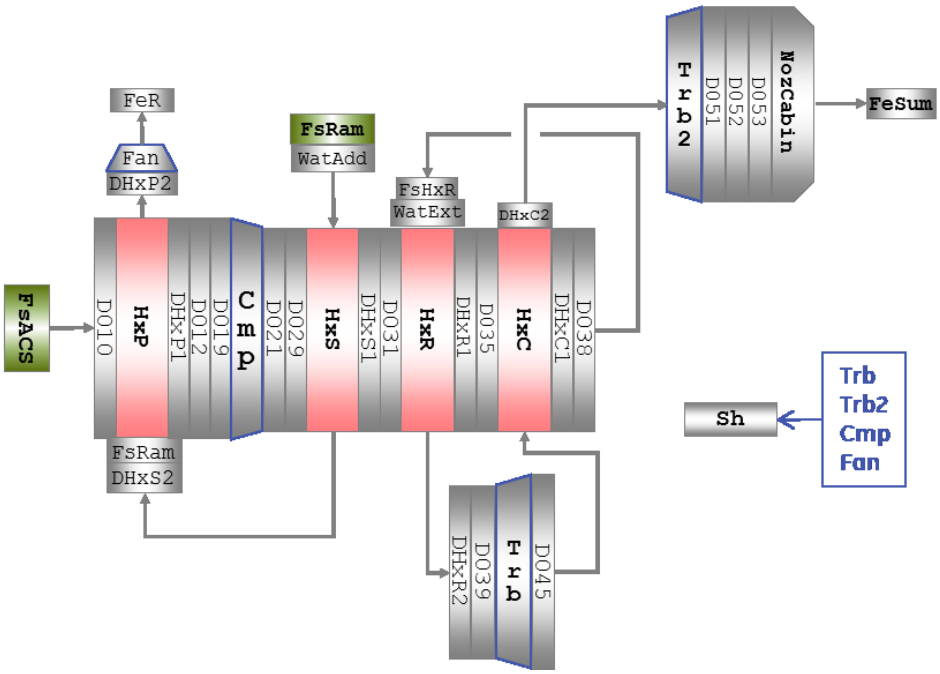

Figure 4.7: ACS NPSS Representation of Model

Referring to Figure 4.7, two streams are represented, the fresh air supply (FsACS) and the cooling RAM air supply (FsRam), labeled in green. The rotating components are identified by a blue border and are connected to the same shaft element, labeled *Sh.*

While the heat exchangers are depicted in a red shade. Figure 4.7 depicts a standalone ACS, yet it is common for all architectures studied.

The design mode ACS model, sizes the components to meet a specification, e.g. ground idle heat load. In off-design mode it relies on physics based modeling and parametric maps to predict the component's performance. One of the strongest features of the NPSS is its capability to scale the performance maps of rotating machinery. For example, the compressor module utilizes the design point specified to scale parametric maps based on industry experience and stall margin calculations. The result is a new map centered on the machine's design point that can then be used to predict off-design operation. Figure 4.8 shows a compressor map that has been scaled from the TJ Native model (an NPSS Consortium Turbo-Jet model) to an ACM application. The cartoon on Figure 4.8 is only for demonstration purposes and has been exaggerated to enhance scaling effects.

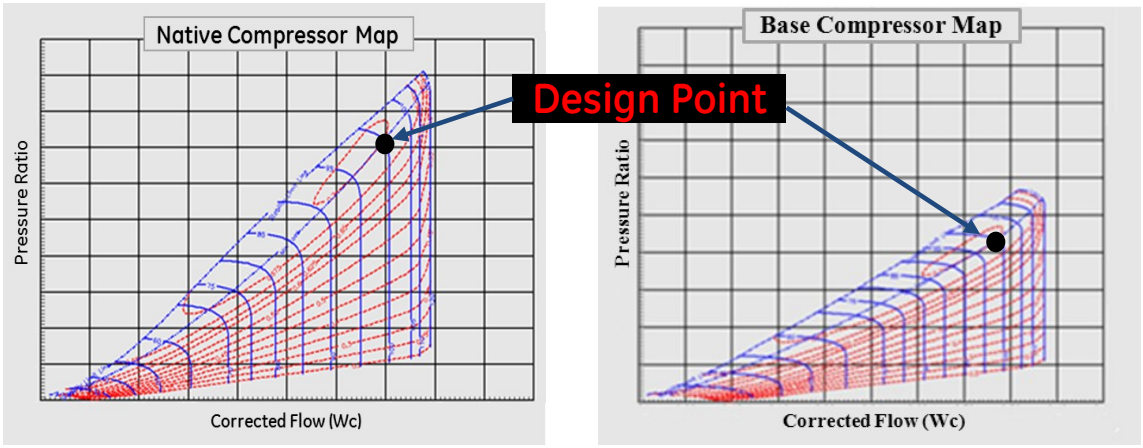

Figure 4.8: Original Compressor Map (Left) and Scaled Map (Right)

From the discussions in Chapter 2, it was concluded that the presence of water vapor should greatly influence the performance of an ACS. In order to study this

phenomenon, the same algorithms employed in production aircraft engine models to assess thrust impact due to changing humidity conditions are utilized in the model, using psychrometric data for air and the thermodynamic state of water droplets. This allows for the simulation to predict the amount of water condensed in the ACS for a given relative humidity (RH), pressure and temperature, and subsequently the increase in ram air thermal capacity as the extracted water is sprayed on the PHx and SHx, as shown in Figure 2.8.

Lastly, to implement the system control and ensure the appropriate operation, independent variables are set up for NPSS in order to iteratively solve for values that satisfy the dependent conditions in the system. For example, in an ACS the compressor pressure ratio is independently varied in order to match the required exit temperature, while other constraints ensure that the exit flow is at the correct pressure, while continuity of mass, momentum and energy are enforced throughout the model.

4.4 Engine 1-D Performance Model

The cycle model that was used for this analysis is 1-D NPSS simulation that represents the major components and processes that occur in a modern turbo fan (TF) engine. This TF Native model was developed by the NPSS Consortium and distributed to its various members. Although this model is generic in nature, not pertaining to a fielded engine, it has been validated through the use of components and scaled compressor maps that are common in support of many engine programs. The model is highly sophisticated, as it models losses due to parasitic bleed, domestic cooling, combustor pressure losses, and horsepower extraction due to gearbox accessories, etc.

To model the engine operation at off design specialized maps that have been scaled from years of industry experience were used for the fan, booster, compressor and turbines. This arbitrary model was sized for a typical regional jet according to the parameters listed in Table 4.9:

Design Parameter	Value
SLS Net Thrust	20,000 lbf
Overall pressure ratio at max. power	30.0
Bypass Ratio	6:1
Power-to-weight ratio	[-]

Table 4.9: NPSS Native Engine Model Sized for this study

For this application the typical engine size is set at 20,000 lbf of net thrust at sea level static (SLS) conditions. The overall pressure ration (OPR) was set to 30.0 with a bypass ratio of 6:1 to maximize efficiency. Because this is an arbitrary engine model with no production equivalent, the power to weight ratio set in this work. For a modern regional jet engine the power to weight ratio is in the range of 5.5[49].

In order to predict the thrust requirements at cruise, a literature search was conducted for similar applications throughout which a typical regional jet mission was selected[42]. In order to fit the thrust to the engine class selected, the mission thrust by Tona[42] was scaled by the factor of π to attain a thrust of approximately 20klb$_f$ at takeoff. The Mach numbers were increased by a factor of 1.1 for a 0.85 Mach at cruise. This resulted in a good fit while maintaining a realistic profile for each of the flight segments. The resulting mission, in which the flight phase, duration, and altitude of each segment

was matched to the work from Tona[42], is summarized in Table 4.10. Referring to Table 4.10, the focus of interest for this work is the longest segment of the mission, consequently where efficiency is maximized, is at cruise conditions of 37kft, 0.85 Mach and 5.4 klb_f thrust.

Flight Phase	Altitude	Mach
[-]	[ft]	[-]
Ground Idle	0	0
Takeoff	0	-
Climb	-	-
Cruise	37000	0.85
Descent	-	-
Holding	-	-
Ground Idle	0	0

Table 4.10: Mission used in Study, see Tona[42]

One thing to note is that although ground idle is tallied at half an hour, most commercial carriers actually turn both engines off approximately 5 to 10 minutes after landing and switch to ground or APU power.

4.5 Overall Integrated Model

The overall integrated model is constructed using the NPSS integration framework that allows the solver element of each model structure to be independent. In NPSS each component is transformed into a 'black box' by using NPSS structures known as assemblies. The system then uses communication links between connecting subsystems as boundary conditions. Interactions continue with each iteration until the system as a whole converges to a steady state solution.

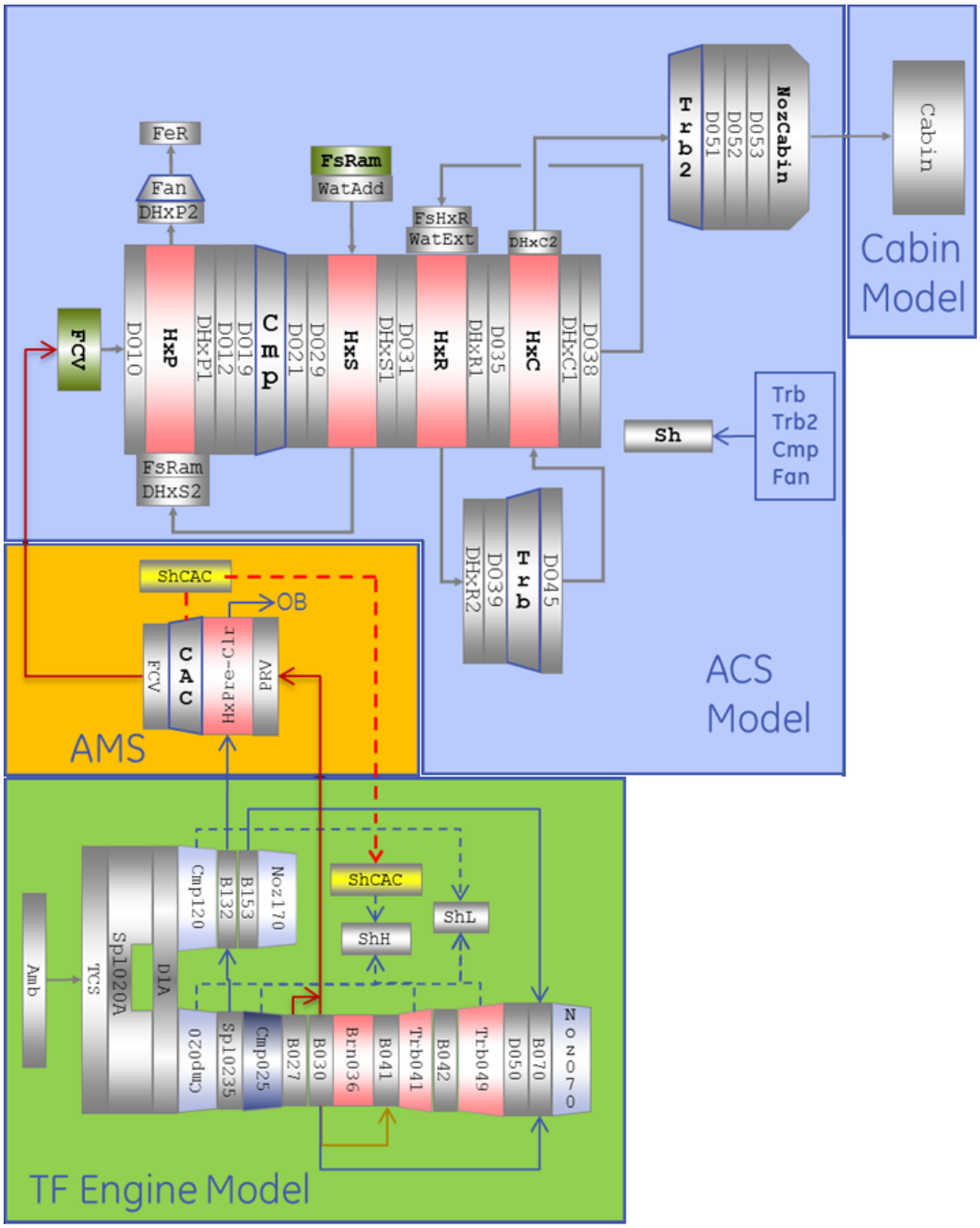

Figure 4.11: Integrated ECS Model with Assembly Boundaries

Figure 4.11 presents a simplified ECS version of the NPSS structure, where each boxed element represents an assembly and thus has an isolated execution. Arrows seen crossing assemblies are the only allowable interface between the subsystems

while each runs as an independent model. This allows each subsytem of the integrated model to reach at a converged solution at each intermediate step before receiving new instructions from its adjacent subsystem. In essence this reduces the convergence time and greatly improves the stability of the model as errors from one subsystem can be filtered before being propagated throughout the entire system model.

Referring to Figure 4.11, flow from the engine cycle model is passed to the AMS, ACS model and is subsequently delivered to the cabin. The AMS pictured in this schematic belongs to the hybrid architecture depicted in Figure 3.6, with the precooler heat exchanger model included. The MHB model is seen to receive pressure and temperature information from the engine model and sends flow and power extraction back to the TF cycle model. It also delivers flow conditions from the ACS to iterate to a required heat load at the cabin. Although this heat exchanger is not needed for several of the hybrid architectures it is still present because it is used when modeling a hybrid architecture that uses 4^{th} stage air as its cabin bleed source.

4.6 Integrated Model Verification

The turbo-fan model used for this research is a generic model in NPSS commonly used for training purposes. This cycle model includes the same level of fidelity found in many production cycle decks. Being that NPSS is an object oriented language it shares the same components with models that have been validated with full rig data in the propulsion industry.

Given that this engine model was not created for this study, only a simple verification of the engine model was performed to ensure continuity within the flow path

at the design point, as can be seen on the P-ν and T-s diagrams of Figure 4.12. Note that station numbers used in Figure 4.12 have been outlined in Figure 2.1. The model was observed to be operating within the expected performance, all cooling flows were accounted for in the core flow path, bypass ratio and overall pressure ratio resulted in the expected performance and fuel flows seemed reasonable for the given thrust.

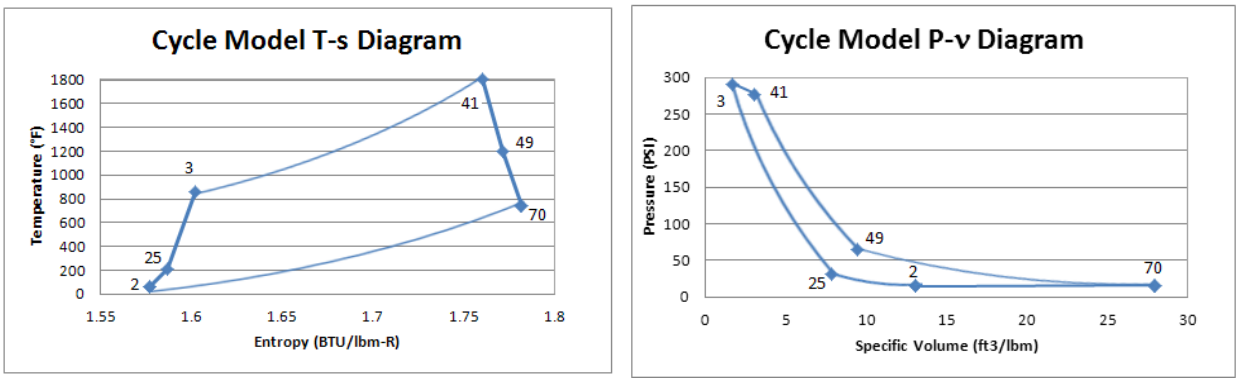

Figure 4.12: Cycle Model P-ν (left) and T-s (right) Diagrams

A three step approach was used to validate the ACS developed for this work, Figures 2.8, 2.13, 3.4-3.6. In the first step each component was verified independently. The heat exchanger algorithms were thoroughly checked out to ensure heat was flowing from the cold to the hot side and that the pressure drops varied properly with increasing flow. Secondly, it was compared with existing code provide by an industrial research center and even vendor heat exchanger data to ensure the elements were operating as expected. For the turbo-machinery components, such as the inlet scoops, compressor, turbines and nozzle there was a less rigorous verification process since these are the same components used in industry engine cycle models. As stated before, these

components have been validated outside of this work and are in use on production engines.

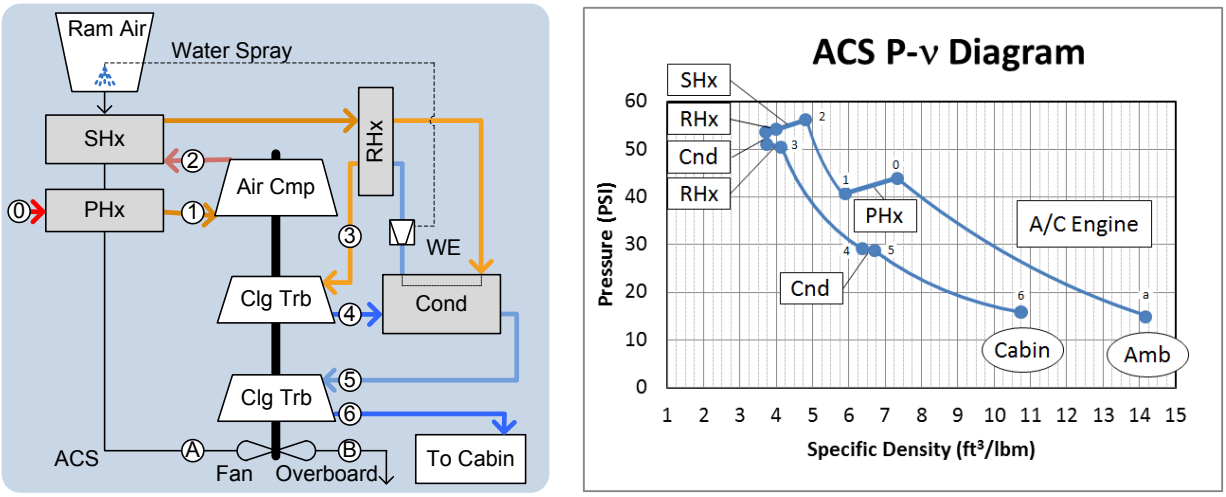

Figure 4.13: ACS Model Pressure Specific Density Diagram

Once the components had been verified and some validated, the full ACS model was assembled as depicted in Figure 4.13 (Left). Note the station numbers used for the ACS from station 0 at the inlet to 6 at the exit to the cabin. The first step in verifying the integrated model is to plot a pressure specific volume (P-ν) diagram to ensure the cycle is operating as expected. Referring to Figure 4.13 (Right) one can see the continuity in the model starting at the aircraft engine compression process from ambient (location a) to station 0 on the ACS. From 0-1 there is a pressure and volume reduction as air passes through the PHx. From station 1-2 there is another compression process through the ACM compressor, depicted as a pressure increase. Next, the condensing process removes moisture from the air flow via the re-heater, condenser and water separator. The water separation process involves a high penalty in pressure drop on the system, as the air is forced through a mechanical water extractor. This can be observed on Figure 4.13 (Right) as a step pressure drop attributed to the condenser.

Subsequently, the air flow is expanded twice as it exits the ACS on station 6. The P-ν diagram demonstrates that the cycle as a whole is operating as expected with no discontinuities in pressure or volume.

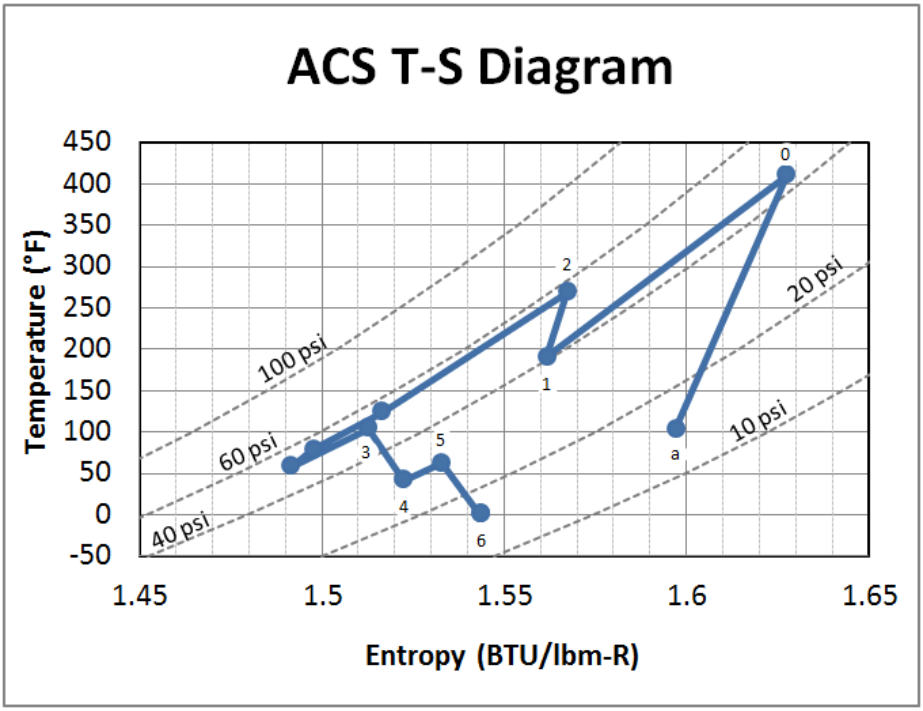

Figure 4.14: ACS Model Temperature Entropy Diagram

To further verify the model, a temperature entropy (T-S) diagram is presented in Figure 4.14, to visualize changes to temperature and specific entropy throughout the ACS. The T-S diagram indicates that the cycle conserve based on the 2nd Law of thermodynamics, which states that the entropy of an isolated system will only increase to a higher state of disorder, and only by means of external effects will entropy decrease. From Figure 4.14, it can be seen that entropy increases in the compression processes a-0 and 1-2. Also on the irreversible process of expansion entropy increase as depicted by process 3-4 and 5-6, corresponding to turbine cooling in the ACS. The

reduction in entropy on this cycle, provided by the heat exchanges, use the external ram air cooling sources.

In this chapter the model used for this study was described in detail, outlining the main assumptions and formulations used to obtained system results. Attempts were made at explaining the details of the Cabin, Air Management System, Air Cycle System and Engine Cycle model to properly document operation. Lastly the verification made on the model to ensure proper operation was conducted by thoroughly examining the output data, ensuring continuity of mass, momentum and energy and where possible comparing it to expected vendor or test data. In order to protect third party or proprietary information, validation runs are not presented as part of this paper, as a normalized or sanitized plot would add little value to our discussion. The next chapter presents results obtained from running the various architectures.

5 System Performance Results

The integrated model presented in Chapter 4 is used to assess the relative performance of the various ECS architectures described in Section 3.6. The results from these model runs are presented and discussed for the five architectures studied, namely the conventional ECS (Figure 2.8), the All-Electric ECS (Figure 2.13), the hybrid fan-bleed ECS (Figure 3.4), the hybrid booster bleed ECS (Figure 3.5) and the hybrid mid-stage bleed ECS (Figure 3.6). All scenarios were run with the same operational and thrust requirements for an 80 PAX regional jet to ensure that results represent a one to one comparison of performance. First, the mission profile used for comparison is presented in detail from pre-flight ground idle to shut down. Secondly, the study focuses in on the cruise segment, as it is the longest portion of the mission and can be used as the differentiator. Lastly, full mission results are presented to demonstrate how conditions change from one flight phase to the next. Finally the results are discussed and compared for the different architectures in terms of comparative savings for each system.

5.1 Mission Profile

The main purpose of the mission profile is to provide the boundary conditions and thrust requirement for the engine cycle model, since a regional jet aircraft performance model was not developed. Figure 5.1 demonstrates the mission altitude and Mach number profiles applied to the engine cycle deck with a thrust profile outlined in Table 4.10 to ascertain the performance for each of the architectures

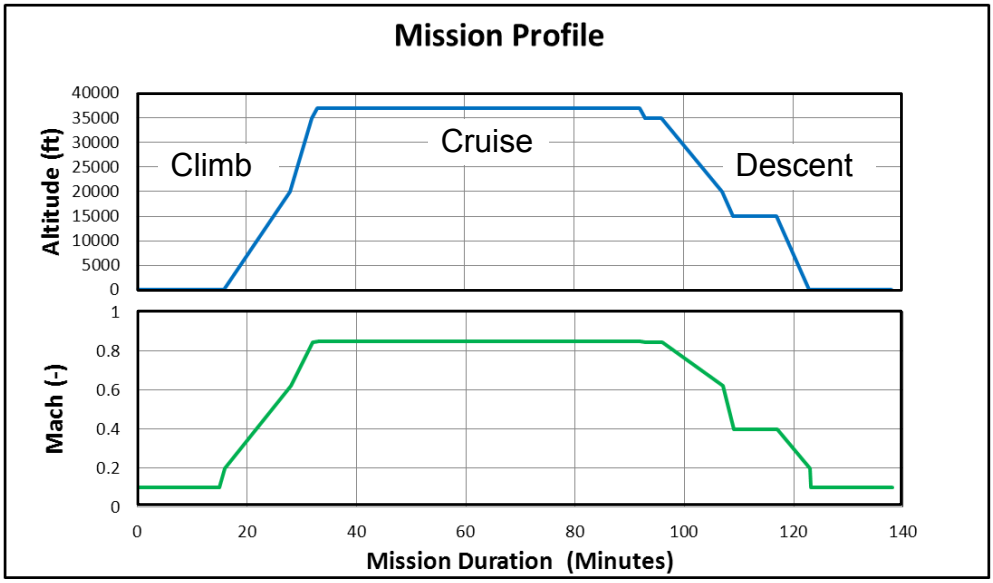

Figure 5.1: Mission Profile: Altitude and Mach Number

The mission profile is also used as a boundary condition for cabin thermal performance model, outlined in Chapter 4.2. For every given mission point the cabin model has the same set of requirements needed to maintain passenger comfort. The requirements include maintaining a set temperature within the fuselage, while providing the recommended fresh air volumetric flow rate per passenger at the correct pressure. For this analysis the requirements were set for a cabin temperature of 72°F, providing 20 CFM per passenger at the pressure profile depicted in Figure 5.2. From Figure 5.2,

it can be seen that as the aircraft gains altitude the pressure within the cabin drops from 14.7 psia to 11.3 psia. This shift in pressure is necessary to reduce the pressure differential between the internal cabin and the atmospheric conditions at 37,000 ft. The corresponding change in air density results in a variation of the fresh air mass flow rate as seen in the bottom part of Figure 5.2.

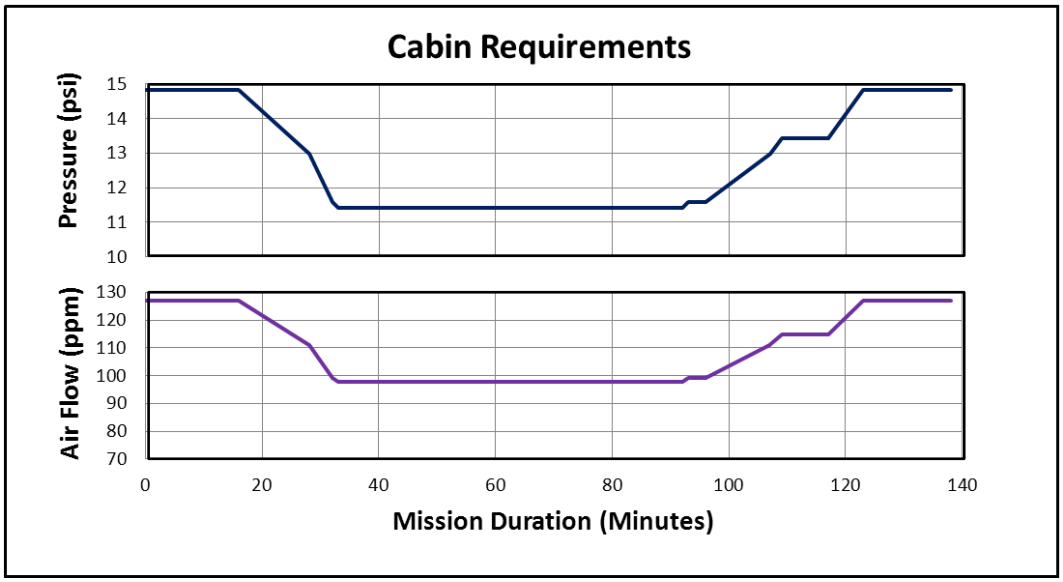

Figure 5.2: Mission Profile: Altitude and Mach number

The estimated cooling duty required within the aircraft for each mission point can be seen in Figure 5.3, where duty is normalized to the maximum (design) heat load at ground idle. For this study a 20% hot day, or 104°F at SLS, was used to compute cabin heat load. This assumes one of the harshest conditions experienced by this type of aircraft. The ambient conditions for a 20% hot day seen on the mission profile on Table 4.10 were computed by the Atmospheric Element provided by the NPSS Consortium. Figure 5.3 depicts how the cabin duty drops considerably with altitude, where the cruise heat load is only 31% of the total ECS capacity. This decline is due to the swift reduction in ambient temperature as the aircraft gains altitude.

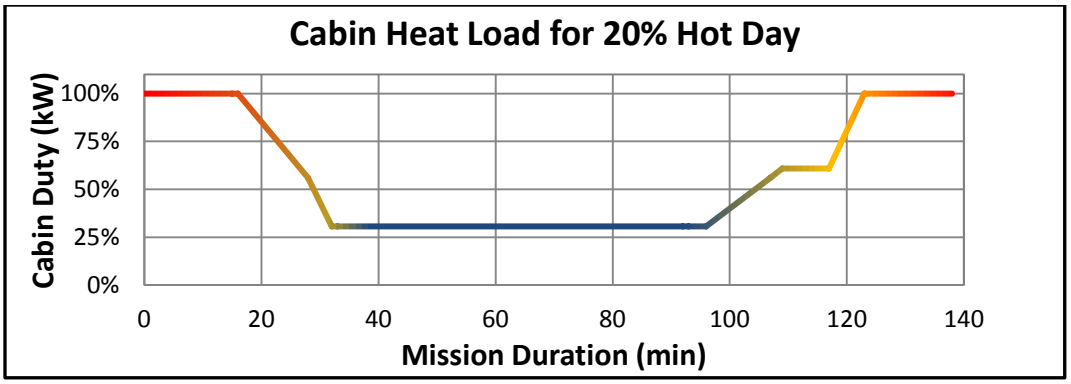

Figure 5.3: Normalized Cabin Duty for 20% hot day

According to Figures 5.1 to 5.3, the altitude profile influences the cabin pressure, temperature and required flow, which are all maintained at appropriate levels by the ECS. The same figures demonstrate that the cruise segment represents the longest portion of the flight and where the highest fuel savings can be achieved. Although, one might argue that ground idle seems to be the longest duration of a flight, most of the time the main engines are off and aircraft use ground connections to provide power to all systems. Therefore most of the design optimization of an aircraft is done at the cruise conditions to reduce fuel consumption.

5.1 Cruise Flight Segment

For this study the parameter that was mainly used to compare the various architectures was the engine Specific Fuel Consumption, SFC (Equation 1.1). To get a basic understanding on SFC, one can picture it as a measure of gallons of fuel to amount of thrust needed to propel an aircraft. For this reason, a lower SFC indicates that the vehicle is consuming less gasoline for the same thrust.

For any given cruise condition, in this case 37,000 ft & 0.85 Mach, the SFC corresponding to the various engine thrust settings can be plotted to understand how this performance parameter varies as a function of net thrust.

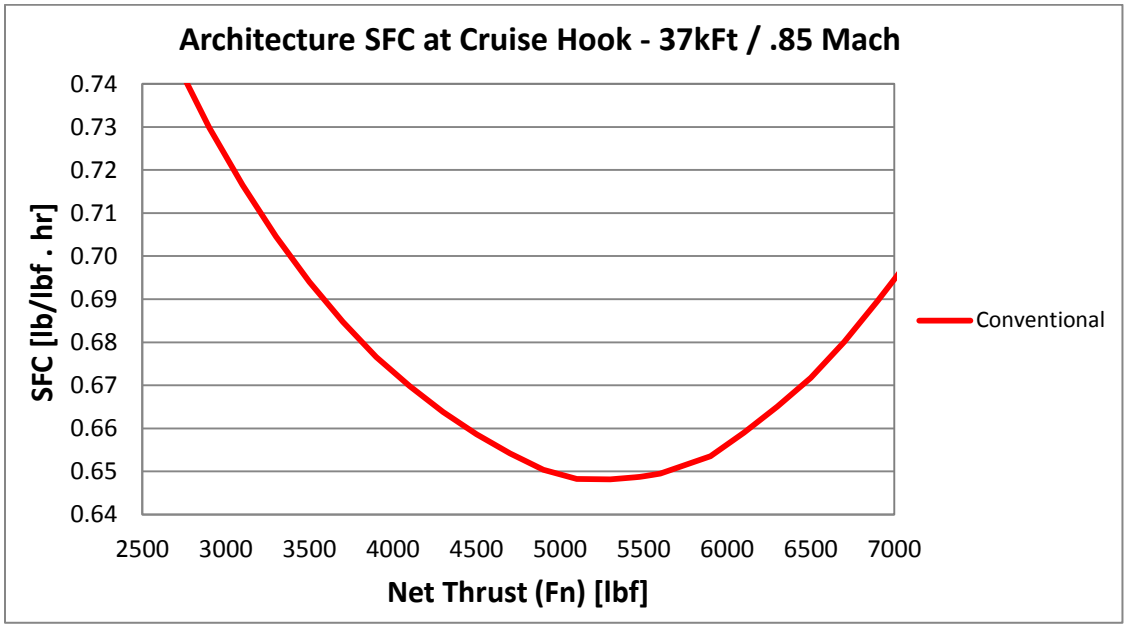

Figure 5.4: Conventional Architecture Thrust Hook

In the industry, this is termed a thrust hook and it shows a summarized representation of how the engine will operate when installed with varying cruise thrust levels. Because the engine is most efficient at its operating line or design point, the resulting SFC forms a “hook” or “bucket” as seen in Figure 5.4. To the right or left of the design point the aircraft is less efficient and thus burns additional fuel, resulting in a higher SFC.

The variation in thrust results from parameters such as takeoff gross weight, fuel consumption during flight duration, wind conditions, and aircraft structure modification, all of which can lead to an increase or decrease in drag. These plots are useful because they illustrate the contrast between the top of climb, entry to cruise, mid-cruise,

and min-cruise. Since most fuel is burned in the cruise leg of the mission, it is a quick way to estimate the overall impact of architecture changes. An average SFC was obtained for the typical variation in net thrust of F_{net} = 300 lbf. This can be obtained by measuring the weight of fuel consumed during cruise and using the C_D/C_L ratio for a regional jet such as the one being studied herein.

Figure 5.4 depicts the performance of the Conventional ECS architecture (Figure 2.8). The Conventional ECS architecture thrust hook can be overlaid with the other systems studied to determine the relative SFC improvement and thus aircraft fuel consumption. Figure 5.5 depicts the system performance run for the Electric, Hybrid Booster and Hybrid Fan systems overlaid on the conventional ECS.

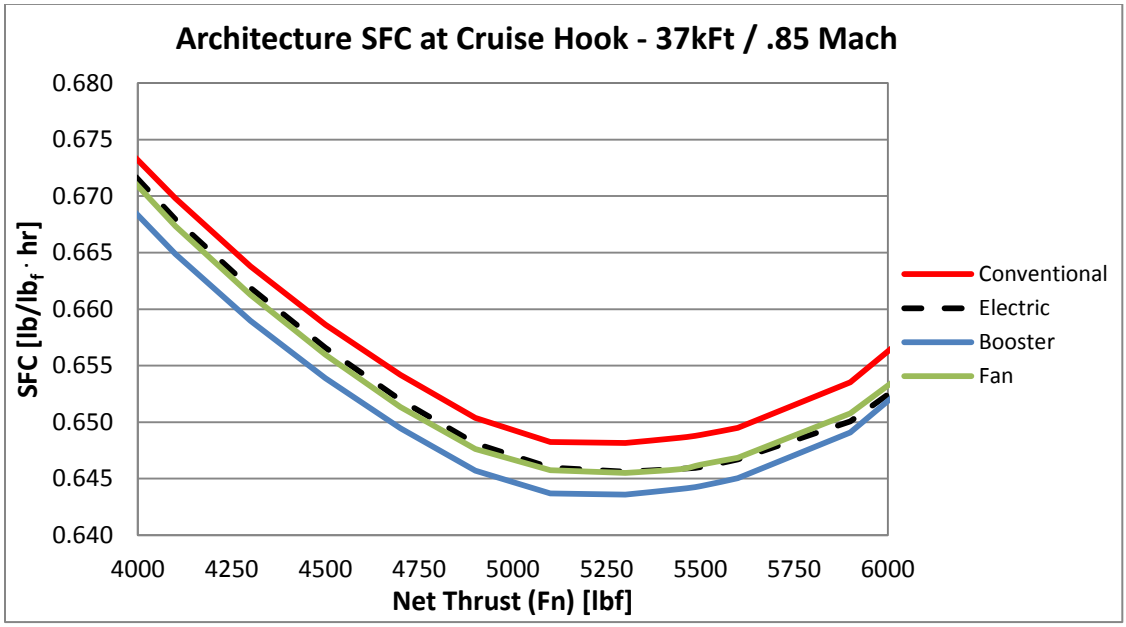

Figure 5.5: Thrust Hook Comparison between the Different Architectures

From Figure 5.5 it can be seen that all architectures perform better than the conventional pneumatic system. Although the improvement in SFC is relatively small, savings could reach millions of dollars due to the price of fuel and the high volume fleet

operation of commercial carriers. To get a better understanding of the relative improvement, Figure 5.6 shows the percent improvement in SFC when using the Conventional pneumatic ECS as a baseline. Since the nominal cruise thrust was set at $F_n = 5447lb_f$ (Table 4.10), this value will be used as the main point of comparison. See Figures 2.13 & 3.4 for the All-Electric and Hybrid Fan architecture respectively.

At the nominal cruise thrust selected the average percent improvement in SFC is 0.42% for both All-Electric and Hybrid Fan. From Figure 5.6, it can be seen that the Fan architecture shows an improvement that is very similar to the All-Electric ECS. This improvement is largely due to reduction in drag, because air is pulled from engine Fan bleed rather than using a dedicated ram air scoop. Yet as thrust increases, electric power extraction becomes a smaller percentage of the engine's overall shaft power. As such, its influence on the cycle diminishes and thus leading to better performance than the Fan Hybrid.

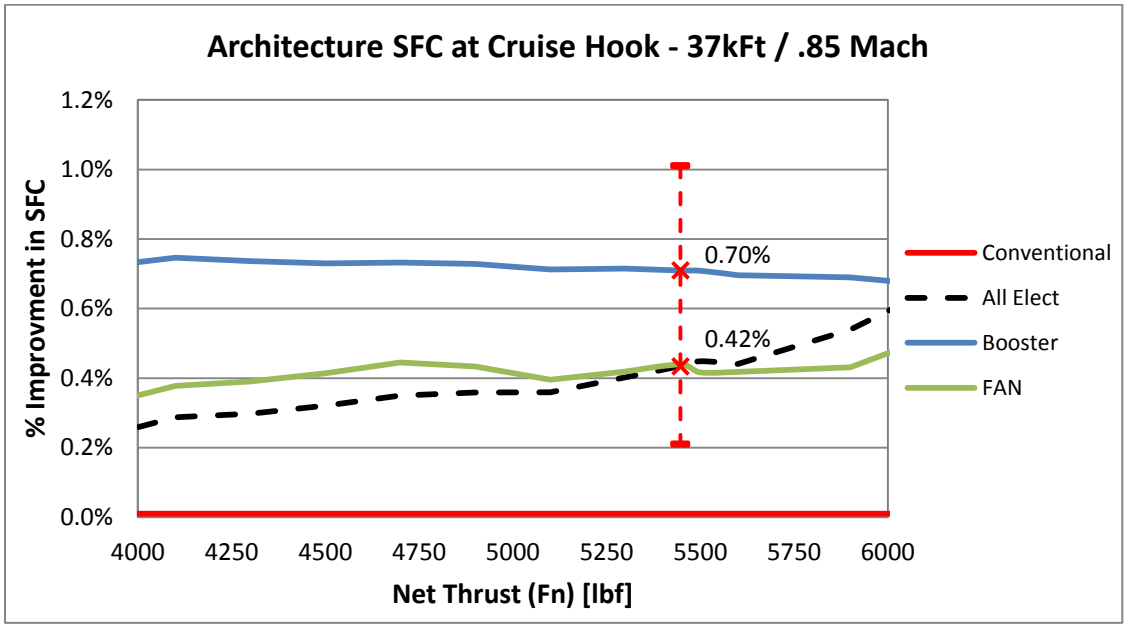

Figure 5.6: Thrust Hook Percent Improvement Comparison

It should be noted that the Hybrid Fan pulls a very small percentage, 0.25%, of the total fan flow, that will not have a significant impact on cycle performance with increasing thrust. For this reason the SFC % improvement for the Hybrid Fan architecture remains relatively flat. The Hybrid Fan architecture is a better choice at lower thrust, but is overpassed by the electric architecture at the higher engine power settings.

It is clear from Figure 5.6 that the Hybrid Booster ECS offers the biggest advantage at cruise thrust, with a 0.7% improvement in SFC. This is because if offers a good combination of engine pneumatic boost and torque extraction, see Figure 3.5 for a schematic of the architecture. With the Hybrid Booster the improvement in SFC is seen to decrease slightly by 0.08% with increasing thrust. This drop is associated with engine core bleed needed for ECS, in cruise it amounts to 1.3% of the core flow, and engine performance is very sensitive to SFC. Looking once again at Figure 5.5, one can appreciate that all three architectures show a tangible improvement over the conventional pneumatic ECS. The Fan and All-Electric are relatively equal in improvements of approximately 0.42%, yet the Hybrid Booster can be seen as the clear winner on a relative basis, with the highest improvement in SFC.

To understand the impact of each ECS on the main engine, the stall margin of the high pressure compressor and booster were examined using the NPSS model. Stall indicates a point where the compressor airfoils lose their ability to provide a pressure rise, causing a flow reversal within the turbo-machinery. These are violent events that can cause great damage to the engine and should be avoided. The stall margin is a measure of how far the operating point of a compressor is from stall conditions. Figure 5.7 depicts the computed HPC stall margin at cruise for each ECS studied.

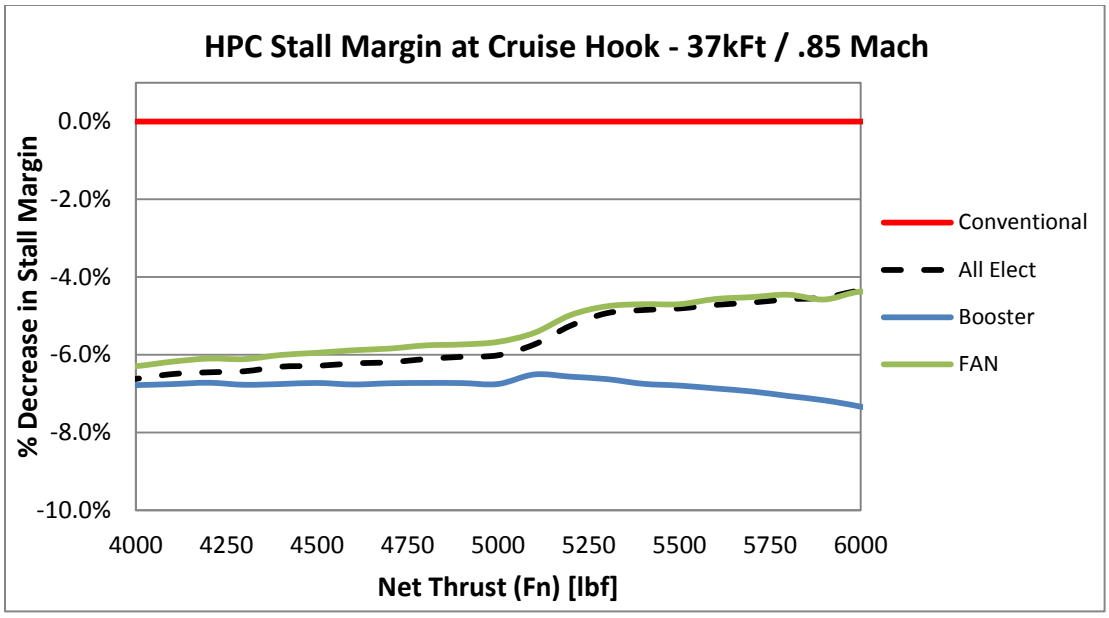

Figure 5.7: HPC Stall Margin Comparison at Cruise

All three systems are seen to reduce the stall margin between 4.0% and 8.0%. This reduction is attributed to the added power extraction demand on the engine by the All-Electric and Hybrid systems. This is consistent with the results outlined in the work by Slingerland and Zandstra[27]. The Booster Hybrid ECS was found to result in the highest reduction in HPC stall margin, even though it draws 36% less power than the All-Electric architecture at cruise (Figure 5.8).

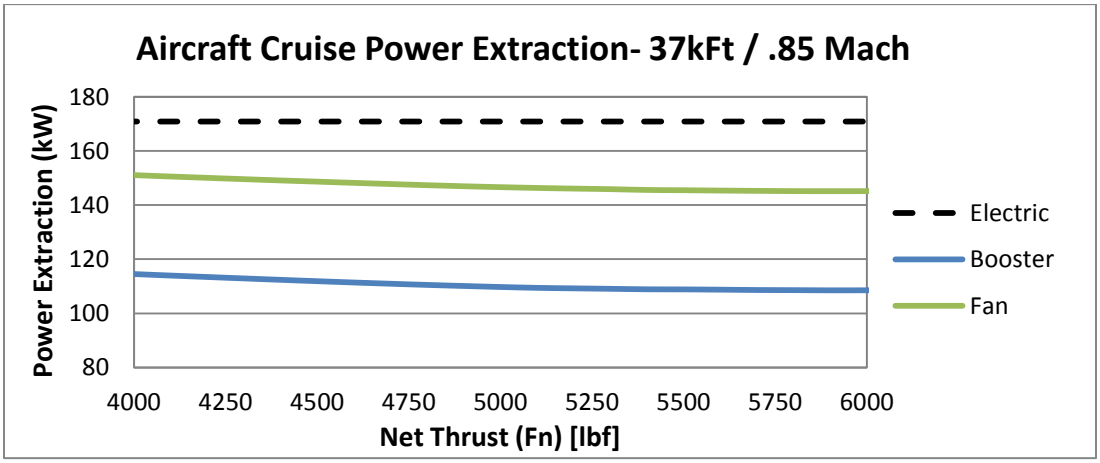

Figure 5.8: Aircraft Cruise Power Extraction

The decreased stall margin in the case of the Hybrid Booster is a result of having both power and bleed extraction on the engine core stream to supply the needed fresh air for the ECS. This hits the HPC in the two main ways that could drive to stall, too much power extraction and starving the compressor of air.

It is important to note that the slight variation in power extraction of the hybrid architectures in Figure 5.8 is due to changing the inlet conditions imposed on the CAC as the engine ramps up in thrust. This variation is not seen on the All-Electric Systems because the ECS inlet conditions are only a function of the ambient conditions, which are unchanged for the cruise point.

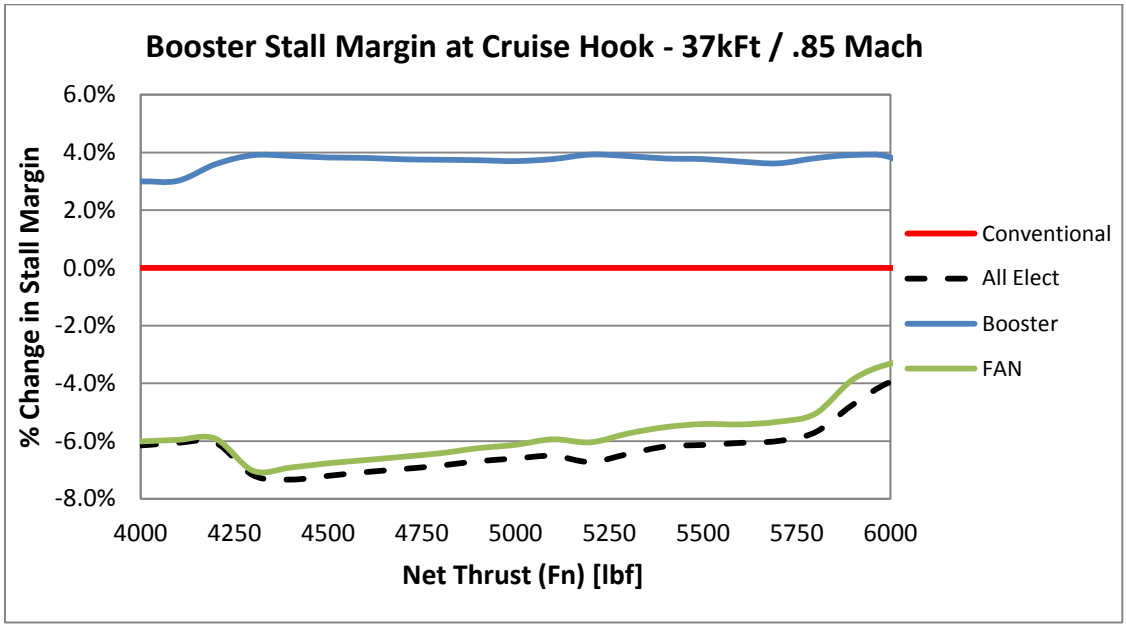

Figure 5.9: Booster Compressor Stall Margin Comparison at Cruise

Looking at the stall margin in the engine booster (or low pressure compressor) in Figure 5.9, it can be seen that the Hybrid Booster improves the stall margin on the booster compressor by approximately 4%. This added margin is a result of the increased flow going through the low pressure compressor for the ECS system. The

All-Electric and Hybrid Fan again result in a reduction in the stall margin for the booster compressor. This reduction can be attributed to the same effects of power extraction as discussed for the HPC. As power is extracted from the core there is a resulting 0.2% reduction in core speed, accounting for the additional torque. On the low pressure spool there is a corresponding 0.2% increase in speed due to the additional core mass flow. This results in the booster spinning at a higher RPM while maintaining the same corrected flow. This effect tends to drive the operating point of a compressor towards stall, and this is what is seen on Figure 5.9.

It is clear that the Hybrid Booster bleed offers a substantial benefit of 0.7% in SFC over the Conventional Pneumatic system and is 0.28% better than the Hybrid Fan and All-Electric system. Yet the improvement comes with a detriment to the compressor stall margin, indicating that the compressor would have to be redesigned specifically for this type of ECS system. Lastly, it was seen that the booster compressor is greatly enhanced by the Hybrid Booster due to the additional mass flow that is pushed through the low pressure compressor.

5.3 Mission Level Benefit

In this section the discussion will be focused on the overall mission level benefit provided by each of the architectures studied, as compared to the Conventional Pneumatic system (Figure 2.8). To perform a comparison at the mission level the fuel consumption for the entire flight was observed as well as a per segment comparison. Additionally, the differences between architectures were substantiated to understand where the benefits lie in each system.

As discussed in Section 5.1, all architectures were exercised using the mission profile on Table 4.10. The resulting overall mission fuel consumption improvements are presented in Figure 5.10. It can be seen that all hybrid and electric architectures provide substantial improvement in fuel consumption, ranging between 0.35% and 1.27%. This could save commercial carriers millions of dollars in fuel savings of the lifetime of the aircraft. For example, a typical regional jet can use approximately 2000 gallons of fuel per flight. With jet fuel prices close to $6/gallon, each flight has a fuel cost of $12,000. By assuming that a typical airline has 3 flights per day, the total cost of fuel is then $360 thousand for a fleet of 10 aircraft. On a yearly basis this translates to $131MM in fuel costs. Hence, a 1.27% improvement in performance could potentially provide a yearly savings of $1.6MM for commercial carriers.

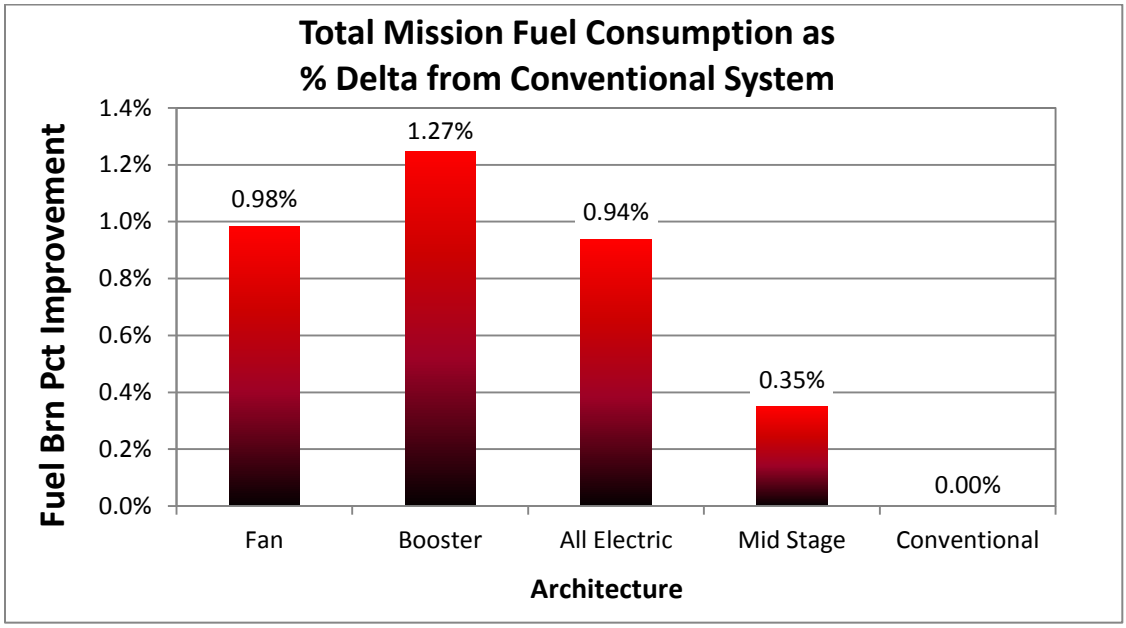

Figure 5.10: Overall Mission Fuel Consumption

Again, the clear victor in this analysis is the Hybrid Booster architecture, Figure 3.5, followed by the Hybrid Fan and All-Electric. The Mid-Stage Hybrid system, Figure

3.6, shows some improvement as well, but is not as good as the All-Electric, HFB and HBB systems. Most of that improvement is attributed to the ground idle segment of the flight, as will be presented in Section 5.3.3. It is important to note that the total fuel burn improvement was calculated using an average SFC at cruise to take into account the variation in thrust that occurs as a result of fuel burn. Yet, since all SFC curves on Figure 5.5 trend in the same fashion, averaging SFC with thrust does not alter the result significantly.

5.3.1 Flight Segments

In order to understand how these savings are generated, the relative improvements are presented in Figure 5.11 for all the individual flight phases as depicted on Figure 3.3. The comparative performance of the different systems through the Ground Idle portion is presented separately in Section 5.3.2. The ordinate axis in Figure 5.11 displays the percent improvement in fuel consumption relative to the conventional system. In other words, a positive delta indicates less fuel consumed. The first thing to notice in Figure 5.11 is that not all flight segments depict an improvement, for example the Top of Climb (TOC), Descent and Approach & Landing depict an -0.18% to -0.37% detriment to fuel consumption for the Hybrid Fan and All-Electric ECS. These particular segments represent locations where the engine tends to operate at or close to flight idle. For these conditions the engine mid-stage bleed port (see Figure 2.8) provides pressures that are very close to what is needed for the ECS, thus exergy loss is minimized even for the Conventional ECS. In contrast, the high and part power conditions all show significant improvements in fuel consumption with the Hybrid and All-Electric ECS because at those conditions the conventional system loses a substantial amount of

energy between the pre-cooler and PRSOV (Figure 2.8). Using more expensive air, to charge the ECS, results in a significant performance drop in the engine.

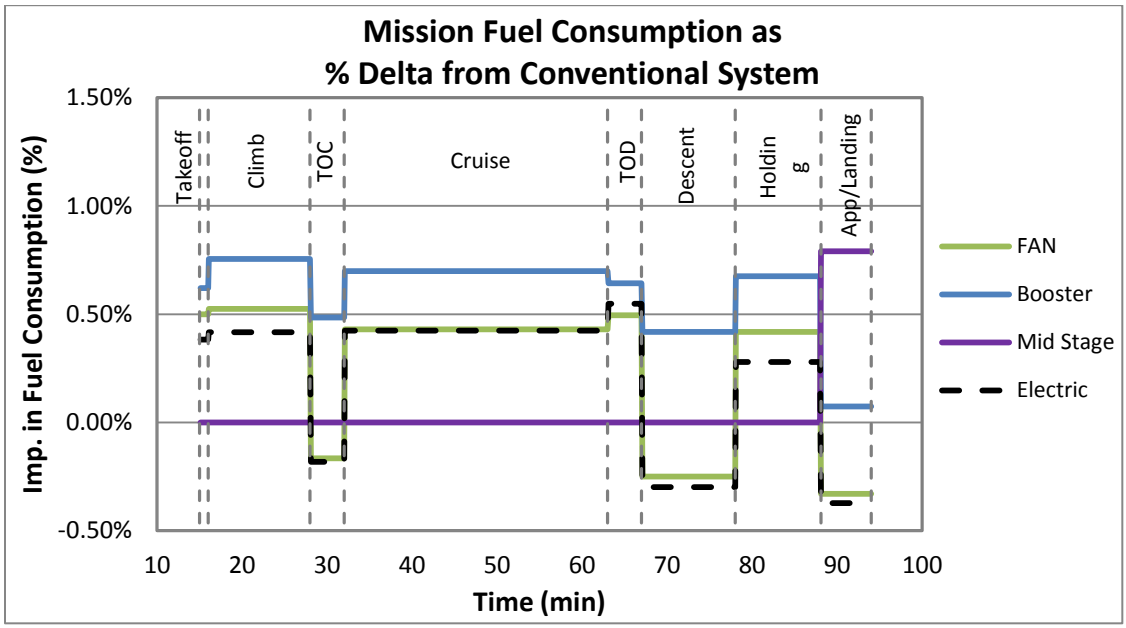

Figure 5.11: Mission Segment Fuel Consumption

The Mid-Stage Hybrid architecture can be seen to provide the same level of benefit as the conventional except for the approach and landing segment, seen at the 90 minute mark. This is because for that flight segment the conventional system switches from the mid stage bleed port to the compressor discharge as outlined in Section 2.1. This is evident when looking at the CAC pressure ratio over the flight profile (Figure 5.12). Notice how the CAC is at PR = 1, which corresponds to a bypass state, when it is not in use. In comparison, it can be seen that the CAC pressure ratio for the other architectures progressively increases, up to PR = 5.5 for the All-Electric ECS. The hybrid systems simply turn on the CAC to provide the required ECS pressure and only draw less electric power.

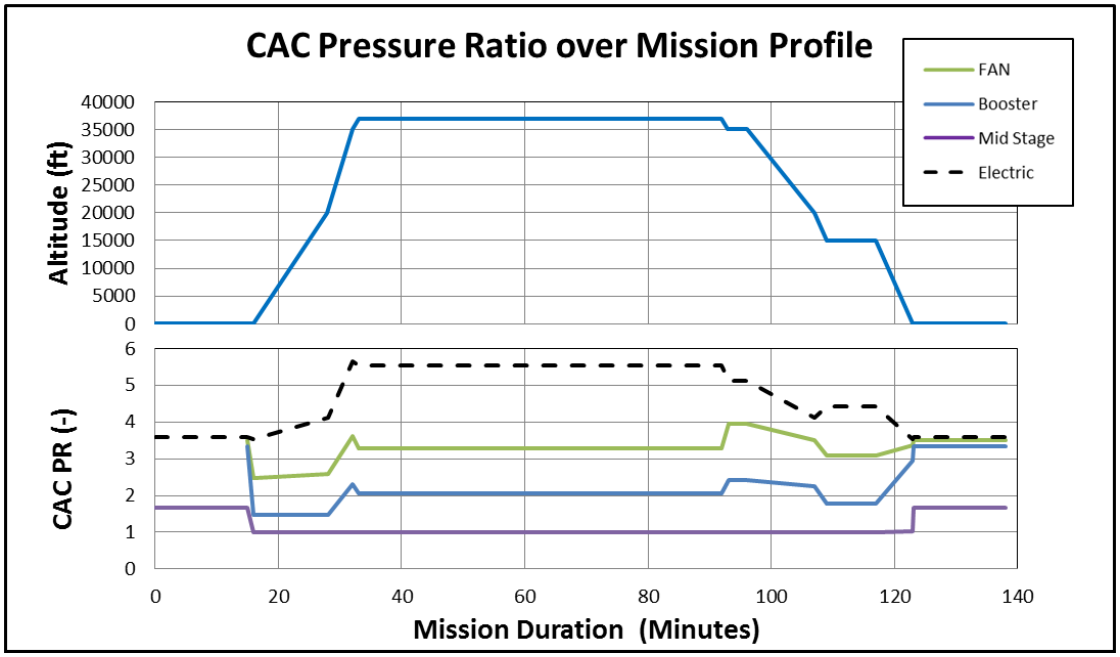

Figure 5.12: CAC Pressure Ratio Variation with Altitude

Referring to Figure 5.11, the Hybrid Booster is the strongest performer, consistently providing benefit over the entire mission. This is the main reason why it provides the highest benefit over the other systems studied.

5.3.2 Ram Drag Implications

Ahead of moving on towards analyzing the ground idle segment, the variation in performance between the Fan Hybrid and the All-Electric ECS will be discussed. From Figure 5.11 it can be seen that the Hybrid Fan system is better performing than the All-Electric for most segments of the mission, save for cruise which was discussed in Section 5.3.1. The additional loss in the All-Electric ECS arises as a result of the ram drag generated at the fresh air inlet scoops. This is a necessary feature in the All-Electric ECS (Figure 2.13). The Hybrid systems do not incur this penalty because these architectures pull engine bleed. The ACS itself has a drag penalty due to the NACA inlet scoops used for cooling as depicted in Figure 2.1. Figure 5.13 presents the ram

drag associated with each ECS for a given flight segment. It can be seen that the All-Electric architecture has more than 2.5 times the amount of ram drag than what is typically seen on a conventional ECS system. This additional drag consumes some of the potential benefits because the engine has to produce extra thrust to compensate.

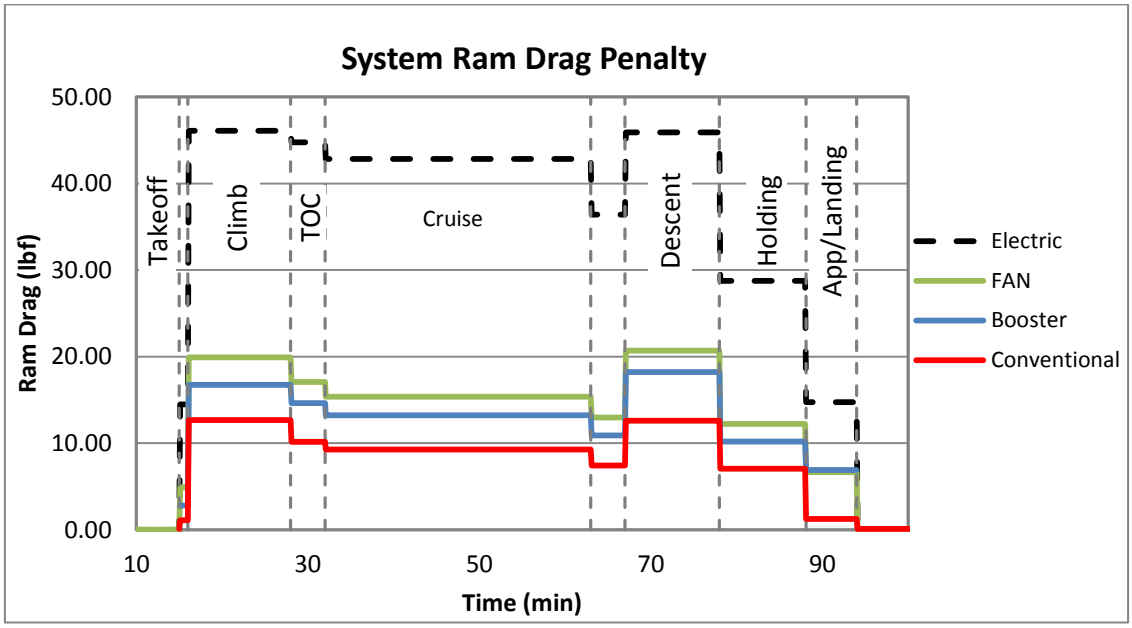

Figure 5.13: System Ram Drag Penalty per Engine

When compared to the conventional system, the Hybrid Fan and Booster ECS experience an additional ram drag because of the removal of the pre-cooler (Figure 2.8). In the hybrid systems air is compressed via the CAC and delivered directly to the ECS, this results in inlet temperatures that are hotter than a Conventional ECS. Still this only results in an additional 7lbf of drag on the overall system. For the ground idle segment the fresh air inlet scoops do not create any losses and serve as a means to compare the systems without the impact of drag on the model.

5.3.2 Ground Idle Segment

Although the fuel savings of the nonconventional systems over the various flight segments presented in Figure 5.10 seem very attractive considering the vast number of flight flown per day by commercial airlines, they dwarf in comparison to the savings at ground idle. Figure 5.14 depicts the percent improvements in fuel consumption for the nonconventional systems when compared to the conventional ECS architecture.

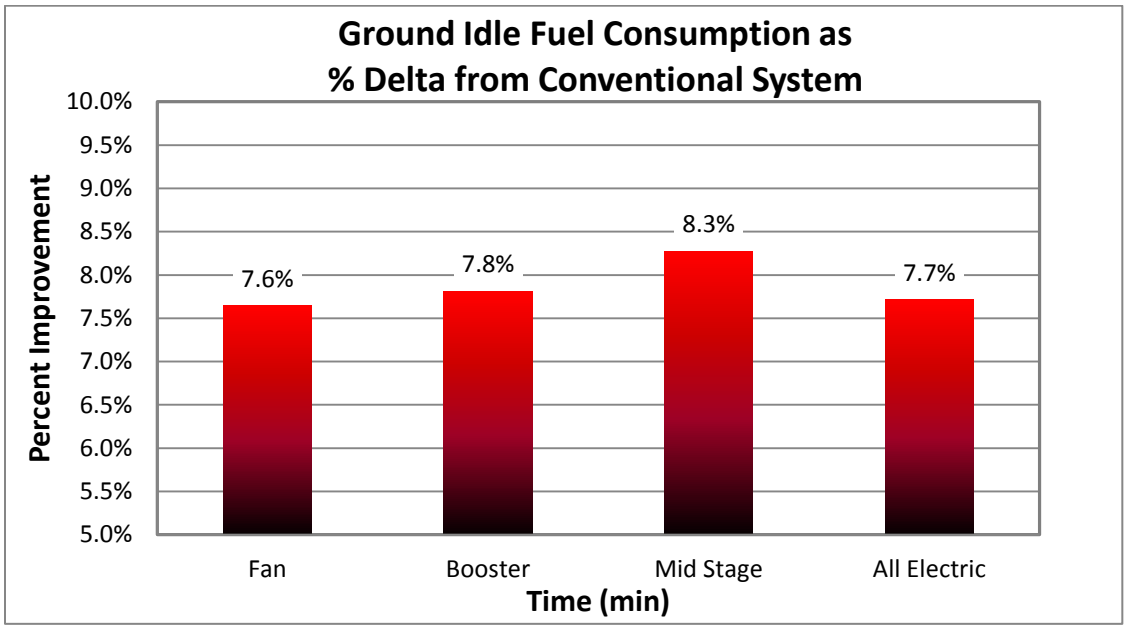

Figure 5.14: Ground Idle Segment Fuel Consumption

The savings are seen to range from between 7.6% and 8.3%. This would result in phenomenal savings for airlines, because many flights have approximately 15 minutes of ground idle. In this segment it can be seen that the Mid Stage Hybrid systems presents the highest savings with an 8.3% improvement over the conventional system. Keep in mind that the conventional system operates with the CDP bleed port at ground idle. The Fan, Booster Hybrid and All-Electric ECS can be seen to have almost the same amount of savings, with 7.6%, 7.8% and 7.7% respectively. For the case of

ground idle the Fan Hybrid behaves in the same manner as the All-Electric. The main engine fan cannot provide sufficient pressure to push air along the wing duct that connects the bleed port on the engine cowl to the ECS bay in the fairing of the aircraft, as depicted in Figure 2.1. A special access door must open to allow the CAC to draw in fresh air directly into the fairing. The Hybrid Booster system shows some benefit, but it so close to the other architectures that it can be considered to be equally beneficial to the All-Electric architecture.

It is clear that a more electric architecture would provide a substantial improvement over the traditional pneumatic air system. Whether it is the All-Electric or the Hybrid, there is a true benefit to be had with aircraft electrification. The results obtained from the integrated model demonstrated that in this relative study, the Hybrid Booster ECS provides the most benefit by establishing a balance of engine power to bleed extraction.

6 Conclusions and Continuation

This study has examined various aircraft level ECS architectures for the purposes of performing a trade study in the design space of an 80 passenger regional jet over a standard commercial mission. In this chapter the discussion will focus on the main drivers that contributed toward an architecture being superior to another. It is important to note that the results observed herein should not be generalized as they are very dependent on the assumptions and have conceptual design traits to details that would be defined later in the design process of an aircraft system. It is important to note how system level modeling can present benefits by allowing rapid prototyping and full scale trades studies at the preliminary design stage of the aircraft and engine systems.

Subsequently, an introduction will be presented on the effects of scaling an aircraft to a different passenger count. This is an area of importance for aircraft manufacturers as they decide on direction for future applications. The next step in designing systems that minimize exergy destruction is to perform a vehicle level optimization. This is one of the newest trends in the aerospace industry used to maximize design efficiency and approximate an EOA solution. Subsequently, various

system level improvements, which could enhance this work by tuning the fidelity of the solution, are documented. Lastly, future work that could be continued in this same area of study is discussed, whether the focus is placed on the ECS or the actual power extraction and some areas worth studying in the military arena.

6.1 Conclusions

As mentioned in Section 1.1, most aircraft manufacturers are trending towards a more electric aircraft in an effort to maximize overall system efficiency, while maintaining or improving life cycle costs. Understanding the overall systems impacts of ECS electrification was the main motivation for this work. The impact of electrification was assessed in a trade study consisting of five different ECS architectures. Each architecture drew power from the aircraft engine in different methods, going from full torque extraction to full pneumatic bleed. The maximum payback points to a hybrid architecture that balances the torque off take with pneumatic bleed.

The trade study conducted involved a Conventional ECS, Figure 2.8, All-Electric, Figure 2.13 and three hybrid ECS: Fan, Figure 3.4, Booster, Figure 3.5 and Mid-Stage. These last three represent different torque to pneumatic extraction ratios in an effort to maximize performance. The Conventional and All-Electric ECS serve as the bounds in the trade study and are currently fielded systems. The Conventional is full pneumatic extraction, while the opposite extreme, with fully electric operation, is represented by the All-Electric ECS.

The five ECS presented where modeled using an integrated NPSS model, composed of 4 subsystems, namely the Engine, Air Management System (AMS), Air

Cycle System (ACS) and lastly the Cabin Thermal model. For each of the trade studies the interface between the AMS and the engine was reconfigured to resemble a new architecture. The model was independently verified by thoroughly examining the output data, ensuring continuity of mass, momentum and energy. Furthermore some parts of the model were validated by comparing results with vendor data, but these results were not presented herein. The fully integrated model was then run with the mission presented in Table 4.11 to obtain the expected total fuel consumption for that aircraft ECS configuration.

Results obtained from the integrated ECS model show significant differences in performance. Using the Conventional ECS as a baseline, the Hybrid Mid-Stage system provides a 0.38% improvement in fuel burn over the entire mission. This is the smallest saving provided by any of the systems presented. This is because the Hybrid Mid-Stage is only a slight variation from the Conventional, only switching to a CAC if there is not enough pressure at the mid stage port of the engine. This behavior is only seen at ground idle or when there is a pull back to flight idle, see Figure 5.10.

In this study, it was found that both the Fan and the All-Electric system provide on average the same benefit over the flight segment. The All-Electric resulted in a 0.94% improvement, while the Fan bleed provided just a small benefit above that, with a 0.98% enhancement over the Conventional ECS. This is mainly because the Hybrid Fan has to extract almost as much power from the engine as the All-Electric. Figure 5.8 depicts the total power required to provide the correct pressure and flow for the ACS. It was noted that the Fan architecture is only 25kW below the All-Electric during the cruise segment. Additionally, the Fan Hybrid is extracting 0.25% of the total fan flow, which

translates into a detriment on SFC. The Fan system also has a pressure drop along the ducting from the engine cowl to the fairing of the aircraft, which results in an additional loss to the system. These are the main factors which bring the All-Electric system to almost match the performance of the Hybrid Fan. For this type of aircraft it would be recommended to use the All-Electric architecture since it offers reduced complexity in the mechanical sense and similar electrical challenges.

Moving to the Booster Hybrid system, substantial improvements over the All-Electric are seen to merit further study and consideration. This architecture pulls less expensive engine air as a trade for electric power in CAC, when compared to the conventional system. From results presented in Chapter 5, it is clear that this system provides the biggest benefit in fuel savings. The low pressure compressor provides a charged flow that can easily be piped to the fairing with low pressure drop along the wing duct.

From the description of the Hybrid Booster system, it might not appear to be the best option because one is replacing a highly efficient compressor with a small radial machine. Yet the savings come in the matching that can be performed on the airflow needed. In other words, in a conventional system the main engine is over compressing bled air in most cases for what the ECS requires. As such, a lot of energy is discarded by way of the precooler and the pressure regulation valve (Figure 2.2). With this Hybrid system air is supercharged and then perfectly matched to the ECS by the CAC. It is no surprise that the Hybrid Booster system fared better than Hybrid Fan because the engine does most of the work. From Figure 5.12, it was shown that for any point in the mission the Booster system has a relatively low CAC pressure ratio of approximately 2.

This results in less power extraction from the engine, while maximizing the use of pneumatic power. Notice that the All-Electric has a pressure ratio of PR = 5 at cruise, while the Fan Hybrid has a PR = 3.4.

The purpose of this work was to perform a full system trade study in an effort to maximize design performance, while providing equal functionality. Through this analysis it was shown that by combining the merits of the electric and pneumatic systems one can attain an architecture that provides substantial benefit over either. The Hybrid Booster was shown to be approximately 1.3% better than the conventional system and 0.33% better than the fully electric ECS. It is clear in this case that the All-Electric architecture is not best option for electrification due in part to the ram drag generated by the fresh air inlet scoop and the higher efficiency of the main engine low pressure compressor.

6.2 Scaling for Different Aircraft Applications

The trade study conducted targeted an 80 passenger regional jet. This is a smaller craft, but it is widely used by many airlines in the industry. In this passenger class there are various players vying to enter or obtain a higher share of the market. This is the main reason trades studies are so crucial early in the preliminary design. Integrated models such as the one constructed are increasingly important for system engineers to make the appropriate decision and ultimately enter the market with a viable product.

One trend that is not touched upon in this work is the impact of aircraft size on electrification. As aircraft scale in size the ECS requirements also change to

accommodate the larger passenger count. Cabin airflow increases substantially to handle the fresh air requirements for the additional passenger count. Recalling from Section 5.1, as an industry standard 20 CFM is allocated per passenger, going from an 80 pax plane to a 130 pax, airflow requirements jump by 63%. Additionally, the cabin heat load will be greater due to human heat load. Larger cabin jets also have much longer missions that could impact the outcome of a study. From the results, it was clear that Ground Idle played a strong role in producing a clear winner. As the Cruise leg is extended, this will reduce the influence of other flight segments and alter results.

The models developed for this work can be scaled to accommodate various aircraft sizes in fuel economy tradeoff studies. The main challenge would be to scale the engine model with the appropriate parameters for the targeted thrust class. It is important to get as much information as possible on the engine to increase the fidelity of results, since it ultimately determines the savings expected. Next, the ACS would have to be redesign to handle the additional loading. Heat exchangers would have to be resized to have an appropriate effectiveness and pressure drop at the design conditions. The cabin model will have to be updated to take into account the additional cabin size and electric heat loads present. Once the integrated system has been scaled, the Air Management System (AMS) will have to be designed with an appropriate Pre-cooler and/or CAC for each of the ECS being traded on.

The scaling procedure could be done for larger wide-body jets aircrafts, ranging from large single aisle to twin aisle. The study would provide an in depth understanding on the way electrification trends from one application to the next. It would convey insight into the following questions: Will the Hybrid Booster ECS system provide the

same level of benefit for a twin aisle aircraft as it did for the smaller regional jet? Can the engine handle the additional torque and/or power extraction? Will the CAC mass and volume eventually outweigh the benefits of electrification? The answer to these questions will likely shape the architecture of future air vehicle and can only be achieved with very close collaboration between aircraft manufactures, engine and ECS suppliers.

6.3 Vehicle Level Optimization

Although the work presented herein is a trade study between 5 competing architectures, it can lead to the next apparent phase, optimization. Various cost function would have to be added to constrain the optimization and achieve a viable solution. In this section the various steps needed to perform an integrated optimization will be delineated. This would transform the current trade study to a more complex multi-disciplinary optimization problem. In this type of effort, the integrated model will need to have 'zooming' capabilities for each of the various components in order to size according to the current iteration. One thing to keep in mind is that the optimizer will only have a set of choices depending on the available technology, but will not be converging to any new architecture based on the design space. A discrete level optimizer (DLO) will have to be implemented, followed by a continuous optimizer acting on the current architecture being iterated. An optimization can be defined as[44]:

$$Maximize\ f(x): x\ in\ S, g(x) \leq 0, h(x) = 0, \tag{6.1}$$

Where S is a subset or real numbers and is within the scope of f, g, and h which result in a real space. Additionally, the problem is bound by some constraints $g(x)$ and $h(x)$. The function f is typically called the objective function that is being maximized or minimized. To setup an optimization of this scale the first step is to identify the

technologies available for each of the subsystems. In our case we have 5 different AMS scenarios, more can be added as technology improves, see Section 6.4. There are many documented techniques for DLO that can be weighted on given the bounds of this system. Since DLO is the premise of the overall system optimization it can be said that the answer is not truly optimal. True optimization would require an intelligent system that could effectively unearth new subsystems. As one can imagine the computational cost of such a system would be immense. For this reason DLO is done and often trade studies are conducted to study various options. The work by Chepko et al.[43] outline the implantation of this type of optimization using a Genetic Algorithm applied to an in-situ resource utilization system model with nine primary architectures. Using a Genetic algorithm the architecture optimization can be formalized.

Once a particular architecture has been selected a continuous optimization problem arises. In order to tackle the optimization of an integrated system the problem would have to be setup heuristically by independently optimizing each subsystem and subsequently iterate on boundary conditions. This presents a problem because the initial state for the optimization has to be relatively close to a valid solution in order to perform the first iteration. For each subsystem a different cost function would have to be implemented. A lot of work has been done on ACS optimization such as the work by Vargas and Bejan[45]. In that case the cost function is exergy destruction with weight and volume setup as constraints. For the ACS the various heat exchangers can be optimized in isolation and then iterated upon on the higher level system. This tier level optimization would have to take place in all subsystems of the aircraft such as the engines, cabin, air management system, etc.

For the subsystem optimization a plausible technique could be Particle Swarm Optimization[47]. This algorithm finds the optimum design by iteratively trying to improve a candidate solution with regard to a given cost function, in our case exergy destruction. The way this method operates is by labeling each solution as a 'particle' with position and relative velocity. Each particle knows its relative location and is influenced by the local best known position. As the iterations run the particle updates to a better position until the swarm coalesces on the optimal answer. This method can be applied to each of the subsystems in conjunction with the higher level genetic algorithm that iterates on the best possible architecture.

With all this being said, it is understood that an overall system optimization can be very complex with many decision variables. Given this complexity, it could be possible that a solution with all the given constraints does not exist. The method implemented for optimization has to be robust enough to be able to handle these cases and explore elsewhere in the design space to find a suboptimal answer.

6.4 Improvements and Future Work

In this dissertation the interaction that occurs between the engine and the ECS were studied to determine what configuration would yield the biggest savings at the air vehicle level. Although great care was taken to add the necessary fidelity to obtain a valid result in the trade space, there are still some elements that could be implemented to refine the granularity of the solution. This section will outline improvements that can be added to this work and briefly touch on future work needed in this area of Aerospace Engineering.

The model generated for this study includes the needed aircraft subsystems to adequately assess the impact of the ECS on the engine. There are many details that were assumed or obtained from limited literature data, see Chapter 4, in order to make the study possible. One example is the ducting that routes air from the engine cowl to the fairing of the vehicle. This parameter has the potential to impact results. This is especially true in a comparison between the All-Electric and Hybrid Fan, where their performance was found to be comparable. To truly determine the benefits one would have to partner with both an aircraft manufacturer and an engine company to get the accurate boundary conditions and design parameters. This would be the simplest way to increase the fidelity of the model presented herein.

Geometric factors were not included in this analysis, such as the component weight and volume deltas of each particular system. There are a few reasons for which this study did not include this level of detail and still has validity. As mentioned in Section 2.7, large commercial aircrafts have a very low sensitivity to additional weight due to large lift to drag coefficient ratios. Additionally, when comparing weights between architectures many components have to be removed from the legacy system, and replaced by new components such as motors and controllers in the All-Electric System. There is still some room for improvement if these factors are taken into consideration, although it is not expected to heavily influence the outcome. Volume changes would only impact the solution if parts of the plane would need to bulge out in order to fit the new equipment. This is critical in the engine nacelle, where subsystems are tightly fit and real estate is limited for new hardware. A nacelle bulge could cause substantial drag in the more electrical system and reduce their overall improvement.

In this system trade study, most of the modifications were made in the AMS. The ACS did see some slight variation in design due to delivery temperatures, but overall the Coefficient of Performance (COP) was constant. For future studies it would be beneficial to resize the engine design point to account for the SFC differences and correct the stall margin shortfalls. This would be in line with a true aircraft design process. In some cases the core would have to increase to accommodate the additional torque extraction, while in other cases the compressor map would have to be modified to retain the required stall margin. This engine resizing exercise would certainly impact the solution of each system since the SFC and fuel burn would change as the engine is scaled. Since this work was centered on the ECS, the engine size and design parameters were not altered. This would be the case for an aircraft block upgrade, where the engine is not changed, but some internal subsystems are replaced for more advanced ones. These types of projects are seen often in the military side of aviation.

An important function of the ECS that was not touched upon in the work is the cold day or cooling requirements. Often aircraft cabins have heating requirements either on the ground for a cold day or at cruise depending on the number of passengers onboard. This mode of operation is easily accomplished with the conventional ECS, which has readily available hot air from engine bleed. In the more electric systems fresh air heating might have to be accomplished by the CAC and/or the addition of an electric element heater in the delivery ducting. This system could potentially be heavy and create an additional pressure drop in the system. More so, it will be a higher energy demand on the aircraft electrical generator, mounted on the engine accessory

gear box. As power demands on the ECS increase, the overall system will see decrease in savings when compared to Conventional. A future study could look into these conditions and determine if the conclusions obtained in this work would differ for cold day operation.

The models developed in this work could easily be applied to study dual spool power extraction, an industry trend in military applications. In current generation aircraft accessory and electrical power is only extracted from the high pressure spool, on the gas generator. The low pressure spool, which operates the Fan and LPC, does not support any onboard system. A study such as this could be complemented by incorporating the impacts of load sharing between the high and low pressure spools of the engine. As a result, one could gage the benefits of various power split for the different architectures. This approach would offset some of the compressor stall margin concerns, but might introduce losses in the low pressure compressor or fan operation. Understanding the major implications of dual spool extraction is an important topic for future applications.

Overall this study focused on the interaction between various aircraft subsystems as a way to influence the design process of future air vehicles. It was demonstrated that by shifting the way energy is extracted from the main engines, one can have a positive impact on fuel consumption. This is primarily achieved by limiting exergy destruction where possible. For the five different architectures studies it was shown that the Hybrid Booster provided the best balance between pneumatic and torque extraction. Yet as mentioned in this section there is still a large space to explore if one is to find the true optimum solution for an aerospace application.

References

[1] American Society of Heating, Refrigerating and Air-Conditioning Engineers, “ASHRAE standards & guidelines: The complete collection of ASHRAE standards and guidelines,” ASHRAE, 2008

[2] Lienhard IV, J. H., and Lienhard V, J.H., *A Heat Transfer Text Book*, Phlogiston Press, Cambridge, MA, 2011.

[3] Majumdar, N. C., Mathur, B. L., and Kaushik, S. B., “Prediction of Direct Solar Radiation for Low Atmospheric Turbidity,” *Solar Energy*, Vol. 13, No. 4, 1972, pp. 383-394.

[4] Kakac, S., and Liu H., *Heat Exchangers Selection, Rating and Thermal Design*, 2nd ed., CRC Press, Boca Raton, FL, 2002.

[5] Incropera, F. P., and DeWitt, D.P., *Fundamentals of Heat and Mass Transfer*, 5th ed., J. Wiley, New York, NY, 2002.

[6] Kays, W. M., and London A. L., *Compact Heat Exchangers*, Repr. ed., Krieger Pub. Co., Malabar, FL, 1998.

[7] Hunt, E. H., Reid D. H., Space D. R., and Tilton, F. E., “Commercial Airliner Environmental Control System - Engineering Aspects of Cabin Air Quality” , *Aerospace Medical Association Annual Meeting*, Anaheim, AsMA, CA, May 1995.

[8] Gerstler, W. D., *“*Aircraft Engine Thermal Management: The Impact of Aviation Electric Power Demands (*GLOBAL Gas Turbine News)*,” *Mechanical Engineering-CIME,* ASME, December 1, 2008.

[9] Grizzle, D., “The Economic Impact of Civil Aviation on the U.S. Economy,” Federal Aviation Administration, AJG-6, Washington, DC, Aug. 2011.

[10] Butterworth-Hayes, and P. Brighton, “All-Electric Aircraft Research Speeds Up (International Beat),” *Aerospace America*, Vol. Jan. 2009, pp. 4-7.

[11] Sinnett, M., “787 No-Bleed Systems: Saving Fuel and Enhancing Operational Efficiencies,” *Aero Quarterly*, QTR_04|07, Dec. 2007, pp. 6-11.

[12] Hill, P. G., and Peterson, C. R., Mechanics and Thermodynamics of Propulsion, 2nd ed., Addison-Wesley, Reading, MA, 1992.

[13] Agrawal, G. L., “Foil Air/Gas Bearing Technology ~ An Overview,” *International Gas Turbine & Aeroengine Congress & Exhibition*, ASME, Orlando, FL, 1997.

[14] Nassauer, S. “Up in the Air: New Worries about 'Fume Events' on Planes,” *The Wall Street Journal*, July 2009.

[15] Lunau, K., “A New Meaning to ‘Cabin Fever’,” *Macleans*, Vol. 122, No. 28, 2009, pp. 41-42.

[16] Bejan, A., *Advanced Engineering Thermodynamics*, 2nd ed., John Wiley & Sons Inc., New York, NY, 1997.

[17] Fox, R. W., McDonald, A. T., and Pritchard P. J., “Internal Incompressible Viscous Flow,” *Introduction to Fluid Mechanics*, 6th ed., John Wiley & Sons, Inc., New York, NY, 2004, pp. 370-376.

[18] Gandolfi, R., Pellegrini, L. F., Lima da Silva, G. A., and Oliveira, S., “Exergy Analysis Applied to a Complete Flight Mission of a Commercial Aircraft,” *46th AIAA Aerospace Sciences Meeting & Exhibit*, AIAA, Nevada, 2008, pp. 2-11.

[19] Frick, C. W., Davis, W. F., Randal, L. M. and Mossman, E. A., “An experimental Investigation of NACA Submerged-Duct Entrances,” NACA ACR-5120, Oct. 1945.

[20] Standard Specification for Aviation Turbine Fuels, *Vol. D1655-09a*, ASTM International, West Conshohocken, Pennsylvania, 2010.

[21] Rukes, B., "Guideline on the Use of Fundamental Physical Constants and Basic Constants of Water," IAPWS, Sept. 2001.

[22] Butzin, E. L., Johnson, P. K., and Creekmore, R.E., “Airframe Thermal Management System Modeling in NPSS,” *43rd AIAA/ASME/SAE/ASEE Joint Propulsion Conference & Exhibit*, AIAA, Cincinnati, OH, 2007, pp. 1-11.

[23] Sampath, R., Irani, R., Plybon, R. C., and Meyers, C., “High Fidelity System Simulation of Aerospace Vehicles Using NPSS,” *42nd AIAA Aerospace Sciences Meeting and Exhibit,”* AIAA, Reno, NV, 2004, pp. 371-380.

[24] SAE International Standards Engineers, “Environmental Control Systems Terminology,” SAE ARP-147E, Warrendale, PA, July 2012.

[25] SAE International Standards Engineers, "Environmental Systems Schematic Symbols,” SAE ARP-780B, Troy, MI, Jan. 2010.

[26] SAE International Standards Engineers, “Engine Bleed Air Systems for Aircraft,” SAE ARP-1796A, Troy, MI, March 2007.

[27] Slingerland, R. and Zandstra S., “Bleed Air versus Electric Power Off-takes from a Turbofan Gas Turbine over the Flight Cycle,” *7th Aviation Technology, Integration and Operations Conference*, AIAA, Belfast, Northern Ireland, 2007.

[28] Moir, I., and Seabridge, A., “Environmental Control Systems,” *Aircraft Systems: Mechanical, Electrical and Avionics Subsystems Integration*, 3rd ed., Wiley, Hoboken, NJ, 2008, pp. 259-296.

[29] Lee, J.J., Lukachko, S.P., Waitz, I.A., and Schafer, A., “Historical and future trends in aircraft performance, cost and emissions,” *Annual Review of Energy and the Environment*, Vol. 26, 2001, pp. 167-200.

[30] Mecham, M., “More Flight Time,” *Aviation Week & Space Technology*, Vol. 162, No. 16, 2005, pp. 60 -60.

[31] Code of Federal Regulations, Title 14, “Airworthiness Standards: Transport Category Airplanes,” FAA Part 25, Appendix C.

[32] Department of Defense Handbook, “Global Climatic Data for Developing Military Products,“ MIL-HDBK-310, Lincoln, MA, 1997

[33] Newman, W. H., Viele M. R., and Hrach, F. J., “Reduced Bleed air Extraction for DC-10 Cabin Air Conditioning,”*16th Joint Propulsion Conference*, *AIAA/SAE/ ASME*, Hartford, CT, 1980, pp. 1197-1204.

[34] Rannenberg, G. C., “Simple/Bootstrap Cooling System for a New Transport Airplane,” *AIAA Aircraft Design and Operations Meeting*, Los Angeles, CA, 1969 pp. 787-793.

[35] Dornheim, M. A., “Electric Cabin: The 787 generates at least four times more electricity than normal. Traditionally bleed-powered systems now use volts,” *Aviation Week & Space Tech.*, Vol. 162, No. 13, 2005, pp. 47-48.

[36] Tegtmeier, L. A., "Honeywell also announced an electric APU, the RE50". *Overhaul & Maintenance*, Vol. IX, No. 10, 2004, p. 11.

[37] Sweetman, B., "Unlaunched A350 Jet Takes Shape Very Publicly," *Aviation Week Show News*, *Paris Air Show*, June, 2005.

[38] Giese, G., "Air Cycle Machine – History and potential applications," Global Energy LLC, Madison, WI, December 2006. [www.globalmicroturbine.com/Site/Applications/Entries/2006/12/11_ACM_Air_Cycle_Machine.html. Accessed 2/25/2013.]

[39] Lipman, T. E., and Delucchi, M. A., "A Retail and Lifecycle Cost Analysis of Hybrid Electric Vehicles," *Transportation Research Part D*: *Transport and Environment*, Vol. 11, No. 2, 2006, pp. 115-132.

[40] Embraer Commercial Aviation, "E-Jets Family – Embraer 175," EMBRAER, Sao Jose Dos Campos – SP Brazil, May 2007. [http://www.embraercommercialjets.com/#/en/products_detail/2. Accessed 3/26/2013]

[41] Kays, W. M., Crawford, M. E. and Weigand W., Convective Heat and Mass Transfer, 4th ed., McGraw Hill, New York, NY, 2005.

[42] Tona, C., Raviolo, P. A., Pellegrini, L. F., and Oliveira, S., "Exergy and Thermoeconomic Analysis of a Turbofan Engine During a Typical Commercial Flight," *Energy International Journal*, Vol. 35, No. 2, 2010, pp. 952-959.

[43] Chepko, A. B., and Weck, O., "A Modeling Framework for Applying Discrete Optimization to System Architecture Selection and Application to In-Situ Resource Utilization," *12th AIAA/ISSMO Multidisciplinary Analysis and Optimization Conference*, Victoria, British Columbia, Canada, 2008

[44] Greenberg, H., "The Nature of Mathematical Programming," Mathematical Programming Glossary, Denver, CO., 2010. [http://glossary.computing.society.informs.org/index.php?page=nature.html]

[45] Vargas, J., Bejan, A., "Integrative thermodynamic Optimization of the Environmental Control System of an Aircraft," *International Journal of Heat and Mass Transfer*, Vol. 44, 2001, pp. 3907-3917.

[46] Kundu, Ajoy. "Aerodynamic Considerations", *Aircraft Design*. 1st ed. Cambridge University Press, Cambridge, 2010. Pp. 259-313.

[47] Brinson, T., Ordonez, J. C., and Luongo, A. C., “Optimization of an Integrated SOFC-Fuel Processing System for Aircraft Propulsion,” *Fifth International Conference on Energy Sustainability*, ASME Washington, DC, 2011

[48] Veres, J. P., “Overview of High-Fidelity Modeling Activities in the Numerical Propulsion System Simulations (NPSS) Project,” NASA TM-2002-211351, June 2002.

[49] GE Aviation, “Business & General Aviation – CF34” General Electric Company, Cincinnati, Oh, May 2010. [http://www.geaviation.com/bga/engines/cf34-10.html]

Appendix A

Cabin Heat Load Calculations (37kFt, 0.85M, 20%Hot Day)

The following constants were used to develop a simplified cabin model:

$$\gamma = 1.40,\ \Re_{air} = 53.35\ \frac{lbf\ ft}{lbm\ R},\ \mathrm{Cp} = \frac{\gamma R}{(\gamma - 1)} \tag{A.01}$$

Where gamma is the heat capacity ratio and R is the universal gas constant for air. Cp is the specific heat of air. The Stefan-Boltzmann constant s is defined as:

$$\sigma = 0.1714 \text{ x } 10^{-8} \frac{BTU}{hr\ ft^2 R^4} \tag{A.02}$$

These calculations assume the cabin dimensions of a typical regional jet with specifications obtained from aircraft brochure[40]. The number of passengers in the study including crew is Pax = 85.

To calculate the solar radiation the following radiation use the following relation from Majumdar, N. C. [3].

$$S = S_e t^m (t_w)^{(W\ m_r)^q} \tag{A.03}$$

Where S_e is the effective radiation intensity above the troposphere given as 95.5% of solar constant S_c:

$$S_e = 95.5\% \cdot S_c \tag{A.04}$$

Where the solar constant is given by:

$$S_c = 1367 \frac{W}{m^2} \tag{A.05}$$

The expression t^m can be obtained by defining t as follows[3]:

$$t = \exp(-a\,H) \tag{A.06}$$

Where *a* is termed the extinction coefficient and H is an equivalent altitude for a homogenous atmosphere and can be approximated by:

$$H = \frac{\mathrm{P_{amb}}}{\rho\,\mathrm{g}} \tag{A.07}$$

Lasty the exponent *m* in equation A.03 is the given by:

$$m = \left(\frac{\mathrm{P_{amb}}}{1000}\right) \cdot \mathrm{m_r} \tag{A.08}$$

Where m_r is the secant of the sun's current zenith angle. The next expression of equation A.03 is the term t_w, this value can be obtained as[3] t_w = 0.8507. The exponents on t_w are; *W*, precipitable water vapor in the atmosphere, and *q*, a precipitation experimental constant[3].

$$W = .16\left(\frac{2\mathrm{x}10^{-7}\exp(0.035*\mathrm{T_{day}})}{1000}\right) \tag{A.09}$$

At this point equation A.03 can be evaluated to find the solar heat flux may be obtained.

To calculate the radiation lost to the sky the following equation is used with the sky temperature approximation[2] as follows:

$$q''_{sky} = \epsilon\sigma\left[{T_{surface}}^4 - {T_{sky}}^4\right] \tag{A.10}$$

Where ϵ is the emmisivity and σ is the Stefan-Boltzmann constant and T_{sky} can be obtained as follows[2]:

$$T_{sky} = T_{amb}[0.711 + 0.0056T_{dp} + 7.3\times10^{-5}{T_{dp}}^2 + 0.013\cos(2\pi t/24)]^{1/4} \tag{A.11}$$

In equation A.11, T_{db} represent the dew point temperature at the given altitude. An initial guess at the surface temperature for equation A.10 can be guessed as the recovery temperature, given by equation 4.12.

As outline in section 4.2.3, and equation 4.13 the total heat transfer across the wall of the aircraft can be approximated as a resistance circuit as depicted in Figure 4.6. The heat transfer can be computed as follows:

$$q_{skin} = \frac{(T_{cabin} - T_{rec})}{R_{equiv}} \tag{A.12}$$

Each resistance represents a heat transfer mechanism. The convection from the cabin conditions to the skin has the equivalent resistance given by:

$$R_{conv_{cabin}} = \frac{1}{h_{cab} A_{hx}} \tag{A.13}$$

Where h_{cab} is the forced convection heat transfer coefficient ant A_{hx} is the total heat transfer area within the cabin. The conduction through the skin, assuming a cylindrical body:

$$R_{cond} = \frac{ln(r_o/r_i)}{2\pi L_{AC} k} \tag{A.14}$$

Where r_o and r_i are the external and internal radii respectively. L_{ac} is the total length of the fuselage and *k* is the thermal conductivity of the aircraft's skin. The convection to atmosphere is:

$$R_{conv_{cabin}} = \frac{1}{h_0 A_{hx}} \tag{A.15}$$

In this case h_o is the heat transfer coefficient external to the cabin. The equivalent resistances for the two radiation mechanisms are:

Radiation to sky:

$$R_{sky} = \frac{(T - T_{rec})}{\epsilon_{alum}\ \sigma\ F_s\ A_{hx}(T^4 - t_{sky}^4)} \tag{A.16}$$

Irradiation from the sun:

$$R_{sky} = \frac{(T_{rec} - T)}{\alpha_{alum}\ F_s\ q_{solar}''\ A_{hx}} \tag{A.16}$$

Where ϵ_{alum} is the emissivity of aluminum and $\alpha_{alum}$is the absorbance of aluminum. F_s is a shape factor to account for the visible surface area of the aircraft. The total thermal resistance across the fuselage is:

$$\mathrm{R}_{equiv} = R_{\mathrm{conv}_{\mathrm{cabin}}} + R_{cond} + \frac{R_{conv} * R_{rad} * R_{solar}}{R_{conv} * R_{rad} * + R_{conv} * R_{solar} + R_{rad} * R_{solar}} \tag{A.17}$$

At this point equation A.12 can be used to calculate the heat flux per unit area of the cabin surface. Because the thermal resistance of radiation is a function of the aircrafts skin surface temperature, an iteration has to be performed in order to obtain the correct heat transfer. The iteration consists of equating the heat transfer across the wall of the fuselage, equation A.12 to the heat transfer from the external wall to ambient. This will ensure that the surface temperature of the fuselage is correct.

In addition to the skin heat transfer, the internal loads have to be accounted for in this analysis. The loads included are the human latent heat, obtained from ASHRAE:

$$\mathrm{q}_{human} = (120\ W)\ \cdot Pax \tag{A.18}$$

To obtain the internal electrical heat load assume a nominal electronics load at cruise of 40kW and an overall efficiency of 80%. Hence the total heat generated is:

$$\mathrm{q}_{electric} = (40\ kW)\ \cdot (1 - 0.8) \tag{A.19}$$

The total heat load now can be fully obtained:

$$\mathrm{q}_{total} = q_{skin} + q_{human} + q_{electronic} \tag{A.20}$$

The mass flow required for this aircraft can be obtained by assuming a flow/passenger requirement[7].

$$\mathrm{Q}_{rec} = 20\ \frac{ft^3}{min} \cdot Pax \tag{A.21}$$

Using the density of air inside the cabin, the mass flow rate is:

$$\dot{m}_{rec} = \mathrm{Q}_{rec}\ \rho_{cab} \tag{A.21}$$

This appendix provided description of the cabin model used to obtain the internal heat load requirements for the air cycle system. This model is crucial in this study because is sets the boundary conditions for all location in the envelope.